A FINITE ELEMENT FUNDAMENTAL TO THIN SHELL THEORY

A thesis submitted for the degree of

Doctor of Philosophy

by

Michael Patrick Mould

Department of Mathematics and Statistics

Brunel University

July 1989

This work is dedicated to my parents

Michael and Angela.

ACKNOWLEDGEMENTS

I would like to take this opportunity to express my appreciation and gratitude to Les Morley, the principal supervisor of my studies, for initiating this project and for his expert guidance, helpful suggestions and, above all, encouragement at all stages of the work presented in this thesis.

I also wish to express my gratitude to Prof. J.R. Whiteman for supervising this project, for his support and patience during my period in continuation status and his help with the error analysis of Chapter 6.

I wish to record my deep appreciation of the financial support provided by the Procurement Executive of the Ministry of Defence with particular thanks to Dr. David Allman of the Royal Aerospace Establishment in his role as project coordinator.

A special thank you is due Florence Dalgleish, my 'second mother', who gave me a home from from home during my time at Brunel.

My thanks are also due to:

the staff of the computer unit of Brunel University for providing the computing facilities;

Program Advisory for the many suggestions which helped ease the process of debugging my computer programs.

M.P.M. July 1989

ABSTRACT

This work is intended to contribute to the search for an explanation of the way a really good finite element should behave during analysis of a general shell problem.

The finite element analysis of thin shells is currently receiving much attention in the international literature. Indeed it seems that in almost every new issue of the engineering journals there is a proposal for a new and more efficient shell element. The reason for this is of course the underlying complexity of the shell problem and, more specifically, the difficulty of taking bending into correct account.

In order to elicit an understanding of the use of the finite element method in shell problems an in-depth study is presented of the behaviour of a vehicle shell finite element. This element is the very simple combined constant membrane stress and constant bending moment flat triangle. The examination of its behaviour reveals that the characteristics of an assembly of these elements are such as to enable recovery, in a remarkable way, of each of the types of deformation identified by the classical first approximation theory. Recovery of rigid body movement, inextensional bending, membrane action and edge effect is achieved to an accuracy consistent with the order of magnitude of inherent errors of the classical theory. Thus, the element is seen to hold a position of fundamental importance with regard to the numerical analysis of thin shells.

Special attention is given to the sensitive low energy bending response. This reveals that there are two quite different roles for the element bending freedoms. One role concerns inextensional bending movements which extend over the whole model. The other role concerns local rotational movements which accompany the curvature changes of inextensional bending and edge effect. Extensive numerical comparisons are made against solutions obtained from the classical theory for shells which are very deep with strongly negative Gaussian curvature and which are considered to provide very severe tests. Investigation of edge effect concerns a cantilevered circular cylinder under edge moment. To complete this examination of bending details are given of a matrix procedure which is intended to assess thin shell finite element models in their response to inextensional bending.

To conclude this work the results of a preliminary study of the mathematical details of convergence of the vehicle element are presented. This investigation is specific to the geometry of a circular cylinder and clamped boundary conditions. It is shown that, despite the highly nonconforming nature of the element, O(h) asymptotic convergence in the energy norm is achieved and in this respect is similar in behaviour to the Clough-Johnson flat plate shell finite element.

CONTENTS

LIST OF PRINCIPAL NOTATION

A Greek index refers to a surface component of a vector or tensor and has range {1,2}, a Latin index refers to a Cartesian component and has range {1,2,3}. The Einstein summation convention is employed whereby a suffix used once ranges over the indices and a suffix which is repeated is summed over the indices

a	determinant of the metric tensor of the undeformed middle surface.
$a_{\alpha\beta}$	covariant components of the first fundamental (metric) tensor of the undeformed middle surface.
$\underline{a}_i$	covariant base vectors of reference coordinate system on the undeformed middle surface.
b	determinant of the second fundamental tensor of the undeformed middle surface.
$b_{\alpha\beta}$	covariant components of the second fundamental tensor of the undeformed middle surface.
$c_{\alpha\beta}$	covariant components of the third fundamental tensor of the undeformed middle surface.
dA	differential element of area of the undeformed middle surface.
dV	differential element of volume of the undeformed shell.
$\underline{e}_i$	orthonormal vectors of a fixed Cartesian coordinate system.
E	Young's modulus.
E^{ijkl}	contravariant tensor of elastic moduli.
$\underline{g}_i$	covariant base vectors of a reference coordinate system in undeformed shell.

g_{ij} covariant components of the metric tensor of reference coordinate system in the undeformed shell.

$\bar{g}_i$ covariant base vectors of a reference coordinate system in the deformed shell.

$\bar{g}_{ij}$ covariant components of the metric tensor of a reference coordinate system in the deformed shell.

H mean curvature of the undeformed middle surface.

$h^{\alpha}_{\alpha'}$ functions of the undeformed middle surface base vectors defined by (2.5.8).

K Gaussian curvature of the undeformed middle surface.

$[K]$ global stiffness matrix.

$[K_\gamma]$ global membrane stiffness matrix.

$[K_\kappa]$ global bending stiffness matrix.

K_ν effective Kirchhoff shear force on the shell boundary, see (3.5.7).

L characteristic wavelength of deformation pattern on the middle surface.

l_i element side length.

M shell middle surface.

$M^{\alpha\beta}$ contravariant components of stress couple tensor.

M_ν effective normal bending moment on the shell boundary, see (3.5.7).

M_τ effective twisting bending moment on the shell boundary, see (3.5.7).

M_{ib} number of global mechanisms in the shell finite element model.

M_l number of local mechanisms in the shell finite element model.

N number of degrees of freedom in the shell finite element model.

N_b number of bending freedoms in the shell finite element model.

N^j element shape functions.

N_m number of membrane freedoms in the shell finite element model.

n_v number of vertices in the shell finite element model.

n_s number of midside nodes in the shell finite element model.

$n_{\Gamma s}$ number of midside nodes on the boundary of the finite element model.

Q^α transverse shear force on shell boundary, see (3.5.7).

R minimum principal radius of curvature.

$\underline{r}$ position vector of a point in the undeformed shell.

$\underline{\bar{r}}$ position vector of a point in the deformed shell.

t shell thickness.

T^{α} contravariant components of effective membrane force on boundary, see (3.5.7).

$\underline{t}_{\alpha}$ unit vectors in directions of the reference coordinate system of the undeformed middle surface.

$\underline{t}_{\alpha'}$ orthonormal vectors on the undeformed middle surface.

$\underline{U}$ vector of global Cartesian displacement components.

$\underline{u}$ vector of displacement components measured in a local curvilinear coordinate system.

$\underline{u}_1$ vector of boundary connectors of a shell finite element model.

$\underline{u}_2$ vector of interior connectors of a shell finite element model.

$\underline{V}$ space of functions containing solution of (6.2.9), see (6.2.6).

$\underline{V}_h$ subspace of $\underline{V}$.

$\dot{\underline{V}}_h$ space of functions containing solution of (6.3.6).

$\tilde{\underline{V}}_h$ space of functions containing solution of (6.4.18).

U strain energy per unit area of the undeformed middle surface.

U_{γ} membrane strain energy per unit area of the undeformed middle surface.

U_{κ} bending strain energy per unit area of the undeformed middle surface.

x^i_j element geometric connectors.

x^i coordinate functions referred to fixed Cartesian coordinate system.

$\underset{\sim}{X}_{hi}$ space of functions defined by (6.3.3) and (6.3.4).

$\tilde{X}_{hi}$ space of functions defined by (6.4.2) and (6.4.3).

$\tilde{\tilde{X}}_{hi}$ space of functions defined by (6.4.12).

$\hat{\Gamma}^{\lambda}_{\alpha\beta}$ Christoffel symbols of the reference coordinate system in space.

γ_{ij} covariant components of the three-dimensional strain tensor.

$\overset{\circ}{\gamma}_{\alpha\beta}$ covariant components of three-dimensional strain tensor evaluated on the middle surface.

Γ middle surface boundary curve.

δ^{α}_{β} Kronecker delta symbol.

$\varepsilon_{\alpha\beta}$ covariant permutation tensor of the undeformed middle surface.

$\kappa_{\alpha\beta}$ covariant components of the shell finite element curvature change.

λ_{γ} eigenvalue of membrane stiffness matrix $[K_{\gamma}]$.

λ_{κ} eigenvalue of bending stiffness matrix $[K_{\kappa}]$.

μ^{β}_{α} tensor relating base vectors at points off the middle surface to base vectors on the middle surface.

μ determinant of μ^{α}_{β} .

ν Poisson's ratio.

$\underline{\nu}$ unit vector normal to undeformed middle surface boundary curve Γ in the tangent plane.

ξ^{i} curvilinear coordinates in the undeformed (and deformed) shell.

Π total potential energy functional.

$\delta\Pi$ first variation of the total potential energy of the shell.

$\rho_{\alpha\beta}$ curvature change tensor.

$\underline{\tau}$ unit vector tangent to to middle surface boundary curve Γ in the tangent plane.

ϕ_{α} rotation of the normal in the ξ^{α}-coordinate directions at the middle surface.

Φ strain energy per unit volume of the undeformed shell.

Ω region of two-dimensional Euclidean space used to define the shell.

$\omega_{\alpha\beta}$ rotation tensor about the normal in the undeformed middle surface.

$()_{||}$ denotes covariant differentiation in space.

$()_{|}$ denotes covariant differentiation on the middle surface.

$()_{,}$ denotes partial differentiation.

$()_{h}$ denotes a quantity defined element by element, see Chapter 6.

$\hat{}$ denotes a quantity associated with a flat element, see Chapter 6.

$\tilde{}$ denotes a quantity associated with a patch element, see Chapter 6.

CHAPTER 1

INTRODUCTION

Thin shells have many useful properties which lend themselves to the efficient construction of modern engineering structures and industrial equipment. When suitably designed, even very thin shells can support large loads, and shells are therefore employed in applications where a combination of light weight and strength is essential, such as in the aerospace industry. In other cases, for instance in petrochemical plants and architectural structures, the combined strength and enclosing properties of shells are utilised, as in the design of pressure vessels, roofs and domes.

Their widespread use has been the stimulus for many researchers in the field of solid mechanics and the search for a general theory with which to describe and analyse the behaviour of thin shell structures under load has resulted in an immense and flourishing literature on the subject. The motivation for this theory derives from two principal sources. Firstly, there is the resulting reduction of a three-dimensional problem to a problem which is characterised by two-dimensional field equations. This dimensional reduction is achieved by introducing weighted averages, across the thickness of the shell, of the problem variables i.e. displacements and stresses. This process hides some of the details of a full three-dimensional analysis but leads to an overall gain in simplicity which in most cases is necessary in order to obtain a solution to a shell problem. Secondly, any shell theory which is to be of practical use must be able to properly account for the detailed state of stress and deformation due to the interaction of both membrane and bending actions. Moreover, it is the struggle to safeguard against bending effects that is one of the most

important problems facing the designer of thin shell structures. Indeed, it is the degree to which bending effects can be eliminated, localised or limited in magnitude that principally determines the stiffness of a shell structure. Thus, the designer must be able to correctly evaluate displacements and stresses in those regions of the shell where bending occurs.

The difficulties associated with bending effects are reflected in the development of shell theory. Historically, the general bending theory was preceded by the so called membrane theory which is considerably simpler and, in certain special cases, can give an adequate description of the state of stress in a shell. The study of the shell problem using this theory neglects all bending moments and transverse shear forces. This assumption is justified when the shell has negligible bending stiffness or when the changes of curvature and twist of the middle surface are negligible. For membrane theory the number of unknowns is equal to the number of equilibrium equations, so that the problem is statically determinate (at least in relation to the balance of forces in an infinitesimal element of the shell). In general, the displacements obtained from solutions of membrane theory may be written as the sum of a particular integral and a solution to the corresponding homogeneous equation system. The particular integral corresponds to membrane action of the shell, albeit in linear combination with displacements due to rigid body movement and bending. The homogeneous solution is identified either with deformations of the shell as a rigid body or as pure bending of the shell. Thus, the solution obtained from membrane theory presents pure bending and rigid body deformations on an equal basis. Physically this means that a freely flexible shell admits the possibility of deforming without offering resistance to such displacements i.e. it can act as a mechanism.

In some problems it may happen that the stress resultants and displacements which are found from membrane theory enable the required boundary conditions to be satisfied at the edge of the shell. In general

this is not possible for a membrane shell since the simplified theory does not allow it to be loaded along its edge by transverse forces or moments and the normal displacement and rotation at its edge may not be restrained. A further source of inconsistency in the membrane theory derives from the fact that the equations that determine the forces in the shell take no account of the compatibility relations of the middle surface strain measures. Thus, although the relative simplicity of the membrane theory makes it appealing as a starting point for the analysis of shell structures, the fact that it is only applicable to a limited class of problem forces the responsible engineer to include a proper account of the effects of bending into the design process.

The origins of the bending theory may be traced to early work on flat plates by Cauchy (1882) and Poisson (1829). In these works the dimensional reduction is based upon a power series expansion of the dependent variables in the coordinate perpendicular to the middle surface of the plate. Later, Kirchhoff (1876) introduced a theory of thin plates, based on the following kinematic assumptions:

- points which lie on one and the same normal to the undeformed middle surface also lie on one and and the same normal to the deformed middle surface;
- the displacements in the direction of the normal to the middle surface are equal for all points on the same normal.

Kirchhoff's theory proves to be very fruitful and is widely used in mechanics and engineering today.

The first attempt to formulate a general bending theory for thin shells is accredited to Aron (1874). A first complete linear theory, based on Kirchhoff's work on plates, is given by Love (1927), and is often referred to as Love's first approximation. Subsequent theoretical efforts have been directed towards improvements of Love's formulation and the associated differential equations. Despite its shortcomings Love's theory

occupied a position of prominence for the best part of a century. The central problems, namely a satisfactory derivation of the constitutive relations, together with an appraisal of their accuracy as compared with the governing three-dimensional equations were not resolved until the early 1960's. It is worth noting that a factor in developing the modern shell theory is the use of the tensor calculus to provide a concise means of expressing properties of the geometry and deformation on an arbitrarily curved surface.

Because of the complexity of the governing equations the available analytical solutions to thin shell problems are limited in scope and generally do not apply to arbitrary middle surface geometries, loading conditions, boundary conditions, or many other aspects of practical design. These complications which attend the solution of problems involving thin shells have, therefore, motivated the development of approximate methods of solution based on techniques of numerical analysis. With the advent of the digital computer the finite element method has come to the fore as an approach to thin shell analysis. Satisfactory results have been obtained when treating thin shells, such as occur in curved aerodynamic surfaces, but results have not met with universal acceptance and there is an awareness that reliable results are not always guaranteed. Difficulties arise in both the shell theory to be used and the discretisation process for developing a finite element model. The two difficulties appear to be mutually exclusive of each other. On the one hand shell theories are characterised by:

- including or excluding strong membrane-bending interaction;
- use of a shallow or deep-shell description of the middle surface geometry;
- including or excluding transverse shears;
- including or excluding large rotation and strain effects.

On the other hand, in finite element models attempts are made to include as general a formulation as possible. These concerns are compounded by significant costs in computing and the absence, until recently, as in Morley and Mould (1987), of any routine means by which to verify finite elements for general shells of arbitrary Gaussian curvature.

It is evident that, as a result of the coupling between membrane and bending actions due to the shell curvature, the physical behaviour of a thin shell is quite unlike that of a flat plate, and this causes great perplexity over their analysis and design. For example, there are often large areas of the shell middle surface where membrane stresses constitute the only design concern and stresses may be calculated purely from equilibrium considerations and the membrane theory. Most shell finite element models attempt to provide for both membrane and bending capability and so are clearly overcomplicated for this to be their sole purpose. Their complexity derives from the fact that unless the shell is adequately constrained (in addition to the rigid body constraints), the displacements from membrane theory are not unique and are quite meaningless, at least for the purposes of stiffness design, despite being capable of generating accurate membrane stresses. Uniqueness of displacement is assured only when the bending actions are also taken into account. Also, knowledge of the performance of finite elements in flat plate problems has only limited use in deciding upon their suitability for use in shell problems. This is especially evident when it is noted that there is no assurance of lowest order convergence like that conferred by the well-known constant strain and constant curvature change criteria.

In the displacement formulation for thin shell finite elements it is a relatively straight forward matter to obtain a satisfactory representation of the membrane stresses. However, it is quite a formidable task to introduce a capability into a finite element shell model which is able to give a proper account of the effects of bending and of inextensional bending in particular. In the absence of this capability the finite element model is overstiff and has given rise, see Morley (1972) and

Stolarski and Belytschko (1982, 1983), in the literature to notions like 'sensitive solution', 'membrane locking' and benefits of 'reduced integration'. Each of these problems are consequences of the fact that it is so easy for the element fibre strains of bending to be overwhelmed by the strains of membrane action. Bending is also central to the continuing controversy over the merits of curved shell finite elements where coupling between membrane and bending is essentially predetermined at element level in comparison with flat elements where coupling occurs only after assembly of the model. In both cases there is also a dependency upon the nature of interelement connection i.e. so that it does not inhibit an otherwise available capability for bending.

The ensuing complications are acceptable, and the higher computing costs justifiable, only when bending is taken into correct account so that there is versatility in responding to all the requirements of bending effects. Decisions based on finite element shell models really require a deeper insight than is presently available into the true role of bending.

In this work a study is made of the behaviour of a very simple six node triangular flat finite element in relation to exact results from thin shell theory and which reveals considerations which are fundamental to all shell finite element formulations. In the absence of simple constant strain patch tests the objective in validation of finite element shell models must be to search for versatility in responding to the different kinds of deformation which are identified by the classical theory, namely:

- rigid body movement where it is required to calculate displacements to the exclusion of membrane strain and curvature change;
- 'inextensional' bending, where it is required to calculate curvature changes (and stress couples) and their displacements to the exclusion of membrane strain;
- 'pure' membrane action, where it is required to calculate stress resultants and membrane strains to the exclusion of bending moments and curvature change;

- edge effect, where it is required to calculate membrane strains stress resultants, curvature changes, stress couples and displacements.

The approximate nature of the classical theory is used to advantage in deciding upon acceptable deviation of numerical solutions from membrane action or from inextensibility of bending. The criteria follow from a fundamental result of Koiter (1959, 1960) which states that "...Love's strain energy expression as the sum of extensional energy and bending energy is a consistent first approximation of the basic assumption of plane stress, and the relative error in this approximation does not exceed t/R or $(t/L)^2$ whichever of these may be critical. In this result t is the thickness of the shell, R is the smallest principal radius of curvature and L is the smallest wavelength of deformation pattern on the middle surface...". This result has seen many important consequences in classical theory and so cannot be ignored in finite element analysis of shells which aims to give numerical solutions of the classical theory.

In Chapters 2 and 3 some of the elements of classical linear thin theory are discussed. The development follows that of Koiter (1959, 1960, 1961, 1966, 1970), Sanders (1959), Naghdi (1963, 1972) and Leonard (1961), and as such is effected in a curvilinear coordinate system on the middle surface using the tools of tensor calculus.

In the design process the engineer must make a selection from available shell finite elements in order to achieve an appropriate accuracy for a given problem. A brief review of the principal types of finite elements that have been proposed for solution of shell problems is given in Chapter 4. This is not intended to be comprehensive but is provided to give a flavour of the approaches that have been developed from the many researches in the field. The need for verifying finite element accuracy is becoming more widely recognised, see Morley and Morris (1978), Morris (1985) and MacNeal and Harder (1985), and it is clear that general procedures for validating shell finite elements are needed to facilitate the designers choice and so provide confidence in the resulting numerical

solutions. In order to part way meet this demand comparison solutions for inextensional bending and membrane actions are presented which can be used to investigate such capability in all types of shell finite element models. Also considered is the solution to the well-known problem of a cantilevered circular cylinder under constant end moment which is subsequently used to investigate the recovery of the displacements and stresses of edge effect.

Use of these comparison solutions in Chapter 5 leads to a detailed examination of mechanisms in the so called transitional and membrane models. The transitional model derives from the bending model by removing the bending rigidity from each finite element in the shell model. The bending freedoms are then clearly identified since the finite element model is then able to behave as a mechanism under bending action. The membrane model then derives from the transitional model by removing the midside rotation connectors. It is then appropriate to compare its behaviour against the classical membrane theory for a real shell. On examination it is found that the membrane model is susceptible to a number of movements which are pure mechanisms and which extend over the whole of the finite element assembly. A fundamental result follows, namely that the number of these mechanisms is related to the number of elements on the finite element model boundary. The transitional model displays these same mechanisms in addition to mechanisms of local rotation at the element sides which find their interpretation in the bending model where they accompany the curvature changes of inextensional bending and of edge effect. Thus, two very different roles are established for bending freedoms in thin shell finite element models.

For the purposes of engineering design the most convincing examination of bending needs to be specific to the finite element bending model. It is essential that it be in accord with results of classical theory for the real shell and be consequent upon the actions of edge effect and inextensional bending. As in classical theory, it is exceptional for inextensional bending to occur other than in the presence of membrane strain and so this requires a definition which is in accordance with

Koiter's fundamental result. The bending model is examined for recovery of 'inextensional' bending action under displacement and rotation prescribed patch test problems. Accuracy of the finite element solution is assessed in the same spirit as in Koiter's development of a consistent first approximation theory. It is found that good recovery is obtained not only of the displacements but also of curvature change and of membrane strain. Also a satisfactory ratio of extensional to bending strain energy is obtained which provides a very convenient global measure of assessment, again in accordance with Koiter's result.

The ability to recover the above curvature changes is indispensable for a satisfactory response of the bending model to local edge effect. Because of axisymmetry it is necessary to consider only one longitudinal strip of elements. Surprisingly good agreement is obtained with the comparison solution for stress resultants and stress couples as well as for displacement. With regard to the controversy over the respective merits of curved and flat elements, it is important to note that the total absence of coupling between bending and membrane action in this model evidently does not constitute a deficiency. The assessment of peak stresses of edge effect derives entirely from consideration of a single flat strip of flat finite elements. To conclude the investigation of bending action a matrix procedure is described which is intended to identify the ability of a shell finite element assembly in response to inextensional bending. The matrix procedure is an elaboration of the well-known principle whereby rigid body movements are revealed from eigenvalue analysis of the stiffness matrix without need for reference to actual comparison solutions. The last two sections of Chapter 5 present results of numerical experiments which investigate the capability of the vehicle element to represent the effects of membrane forces. The first of these establishes that the element is able to recover 'pure' membrane action in the bending model to the effective exclusion of curvature change, in a manner consistent with first approximation theory. The final section presents results of testing the

vehicle element in estimating the initial buckling loads of flat plates and cylindrically curved panels.

It is evident from the numerical results presented in this work that the importance of a curved element geometry does not play as fundamental a role as might be expected from intuition. This is considered further in Chapter 6 where some of the mathematical details of convergence of the flat vehicle element are investigated. Here results are presented for the specific geometry of a circular cylinder and clamped boundary conditions. This work is seen as a first step toward a general analysis able to account for arbitrary middle surface geometry and boundary conditions and provides theoretical results which support those from the numerical experiments considered above.

CHAPTER 2

TENSOR PRELIMINARIES AND NOTATION

2.1 Introduction

Tensor calculus is widely used in the modern treatment of the theory of thin shells, see, for example, Naghdi (1963, 1972), Niordson (1985). This means of formulating the governing equations offers advantages over earlier theories, such as those of Gol'denveizer (1961) and Novozhilov (1959), among which the generality and compact form are to be emphasised.

The aim of this chapter is to summarise some of the ideas and selected results from the tensor calculus and the differential geometry of surfaces and to provide opportunity to introduce the notation used in the derivations given in the sequel. More elaborate accounts of these subjects can be found in, for example, Flügge (1972), Naghdi (1963, 1972), O'Neill (1966).

2.2 Geometry of the middle surface

A commonly used notion of a thin shell is of a body that can be described by two curved surfaces whose distance apart is small compared with their other dimensions. If the shell has no other boundary than these two surfaces then it is said to be closed or complete. If it is not complete then it is assumed that it is bounded by a curve on the middle surface and a normal section along this curve. More precisely, the geometry of a shell may be described in the following manner. Consider a

simply connected surface M in three-dimensional Euclidean space, bounded by a curve Γ, and let it be determined by the parametric representation

$$\underline{r}=\underline{r}(\xi^{\alpha}) \tag{2.2.1}$$

where $\underline{r}$ is the position vector from the origin of a fixed right-handed Cartesian coordinate system and the domain of definition of the parameters ξ^{α} ($\alpha = 1,2$) is a bounded open subset Ω in the ξ^{α}-plane, with boundary $\partial\Omega$, see Fig. 2.1. It is assumed that there is a one-to-one correspondence between the coordinates $(\xi^1,\xi^2) \in \Omega$ and the points of the surface M. Let a unit normal vector be erected at every point of $M \cup \Gamma$ and denote the perpendicular distance of a point on the normal from M by ξ^3, so that $\xi^3 = 0$ is the surface M, and let

$$-\frac{1}{2}t \leq \xi^3 \leq \frac{1}{2}t \tag{2.2.2}$$

where t is, in general, a function of the coordinates ξ^{α} although in the sequel it is taken to be constant. Consider now a closed region in space, the points of which are given by

$$\underline{r}(\xi^{\alpha},\xi^3) = \underline{r}(\xi^{\alpha},0) + \xi^3\underline{a}_3 \ . \tag{2.2.3}$$

.

The three-dimensional body whose particles occupy this region is called the shell, the surface defined by (2.2.1) is called the middle surface and t is called the thickness of the shell.

There are, of course, many ways of constructing coordinate systems on a surface. Therefore, in actual calculation, it is necessary to refer quantities to a fixed Cartesian coordinate system x^i ($i = 1,2,3$) so that the coordinates x^i are independent of the choice of the curvilinear coordinates ξ^i in the shell. Thus the position vector $\underline{r}$ has the alternate representation

$$\underline{r} = x^i \underline{e}_i \tag{2.2.4}$$

where $\underline{e}_i$ are unit vectors in the positive x^i directions.

The covariant base vectors of the middle surface $\xi^3 = 0$ are defined by

$$\underline{a}_\alpha = \underline{r}_{,\alpha} , \tag{2.2.5}$$

where the comma preceding the subscript is used to denote partial differentiation with respect to the surface coordinates. It is assumed that the condition

$$|\underline{a}_1 \times \underline{a}_2| > 0 \tag{2.2.6}$$

is satisfied everywhere on the middle surface.

The scalar product of these surface tangent vectors defines the symmetric covariant metric tensor or first fundamental tensor of the middle surface

$$a_{\alpha\beta} = \underline{a}_\alpha \cdot \underline{a}_\beta . \tag{2.2.7}$$

The symmetric contravariant metric tensor is defined by the equations

$$a^{\alpha\lambda} a_{\lambda\beta} = \delta^\alpha_\beta , \tag{2.2.8}$$

where δ^α_β is the Kronecker symbol. The determinant associated with the metric tensor is denoted by a and is given by

$$a = \det(a_{\alpha\beta}) . \tag{2.2.9}$$

Let ξ^α and $\xi^\alpha+d\xi^\alpha$ be the coordinates of two neighbouring points on the middle surface. The length of the infinitesimal line element connecting these points is determined by

$$d\underline{r}\cdot d\underline{r} = (ds)^2 = a_{\alpha\beta}\, d\xi^\alpha d\xi^\beta \qquad (2.2.10)$$

the right hand side of this equation is known as the first fundamental form of the surface. The element of surface area is then given by

$$dA = \sqrt{a}\; d\xi^1 d\xi^2 \qquad (2.2.11)$$

which, because of the relation

$$|\underline{a}_1 \times \underline{a}_2| = a\ , \qquad (2.2.12)$$

and the assumption expressed by (2.2.6), is a strictly positive quantity everywhere on the middle surface.

Associated tensors are denoted by the same kernel letter, and the raising and lowering of indices is performed by means of the metric tensors $a^{\alpha\beta}$ and $a_{\alpha\beta}$ respectively. The contravariant base vectors of the middle surface are given by

$$\underline{a}^\alpha = a^{\alpha\lambda}\underline{a}_\lambda\ , \qquad (2.2.13)$$

and provide the following scalar products

$$\underline{a}^\alpha\cdot\underline{a}^\beta = a^{\alpha\beta}\ , \qquad \underline{a}^\alpha\cdot\underline{a}_\beta = \delta^\alpha_\beta\ . \qquad (2.2.14)$$

The antisymmetric surface permutation tensors $\varepsilon_{\alpha\beta}$ and $\varepsilon^{\alpha\beta}$ are defined by the non-zero components

$$\varepsilon^{12} = -\varepsilon^{21} = 1/\sqrt{a}, \qquad \varepsilon_{12} = -\varepsilon_{21} = \sqrt{a} \ . \tag{2.2.15}$$

The unit vector normal to the middle surface is defined by means of the cross product of the tangent base vectors

$$\underline{a}^3 = \underline{a}_3 = \frac{1}{2}\varepsilon_{\alpha\beta}\underline{a}^{\alpha} \times \underline{a}^{\beta} \ , \tag{2.2.16}$$

so that the vector triad $\underline{a}_1, \underline{a}_2, \underline{a}_3$, in that order, form a right-handed coordinate system.

The curvature of the middle surface is characterised by the second fundamental form

$$d\underline{r}\cdot d\underline{a}_3 = -b_{\alpha\beta}\, d\xi^{\alpha} d\xi^{\beta} \tag{2.2.17}$$

where the symmetric second fundamental tensor or curvature tensor is defined by

$$b_{\alpha\beta} = \underline{a}_3\cdot\underline{a}_{\alpha,\beta} = -\underline{a}_{3,\beta}\cdot\underline{a}_{\alpha} \ . \tag{2.2.18}$$

The components of the third fundamental tensor $c_{\alpha\beta}$ are identified as the coefficients of the third fundamental form of the middle surface:

$$d\underline{a}_{3,\alpha}\cdot d\underline{a}_{3,\beta} = c_{\alpha\beta}\, d\xi^{\alpha} d\xi^{\beta} \tag{2.2.19}$$

so that

$$c_{\alpha\beta} = \underline{a}_{3,\alpha}\cdot\underline{a}_{3,\beta} = b_{\alpha\lambda}b^{\lambda}_{\beta} = b^{\lambda}_{\alpha}b_{\lambda\beta} \ . \tag{2.2.20}$$

Note that the convention adopted in (2.2.17) is such that for positive curvature of a sphere the positive direction of the normal to the surface is towards its centre.

From the curvature tensor two important scalar quantities can be derived; these are the surface invariants known as the mean and Gaussian curvatures H and K of the middle surface

$$H = \frac{1}{2}b^{\lambda}_{\lambda} , \qquad K = \frac{b}{a} \tag{2.2.21}$$

where b is the determinant of the components of the curvature tensor,

$$b = \det(b_{\alpha\beta}) . \tag{2.2.22}$$

In the following discussion partial derivatives of the base vectors and unit normal are required. These may be expressed as linear combinations of themselves according to the well-known formulae of Gauss

$$\underline{a}_{\alpha,\beta} = \Gamma^{\lambda}_{\alpha\beta}\underline{a}_{\lambda} + b_{\alpha\beta}\underline{a}_{3} , \qquad \underline{a}^{\alpha}_{,\beta} = -\Gamma^{\alpha}_{\beta\lambda}\underline{a}^{\lambda} + b^{\alpha}_{\beta}\underline{a}_{\lambda} , \tag{2.2.23}$$

and Weingarten

$$\underline{a}_{3,\alpha} = -b^{\lambda}_{\alpha}\underline{a}_{\lambda} = -b_{\alpha\lambda}\underline{a}^{\lambda} \tag{2.2.24}$$

where $\Gamma^{\lambda}_{\alpha\beta}$ denotes the Christoffel symbol (of the second kind) of the middle surface. The Christoffel symbols can be expressed in the following manner in terms of the metric tensor

$$\Gamma^{\lambda}_{\alpha\beta} = \frac{1}{2}a^{\lambda\omega}(a_{\beta\omega,\alpha} + a_{\omega\alpha,\beta} - a_{\alpha\beta,\omega}) . \tag{2.2.25}$$

It should be noted that the Christoffel symbols are not, in general, components of a tensor although, as can be seen from (2.2.25), they are symmetric in the indices α and β.

So far the discussion has focused on some of the geometric properties of the two-dimensional middle surface. But the shell is actually a three-dimensional body so that it is also proper to consider quantities

associated with a point off the middle surface and to express these in terms of quantities defined on the middle surface.

Recall that the set of normal coordinates in space is such that the position vector $\underline{r}$ of a point in the shell is given by (2.2.3). Differentiation of this expression, with respect to ξ^α and ξ^3, gives the following expressions for the base vectors in space

$$\underline{g}_\alpha = \underline{a}_\alpha - \xi^3 b_\alpha^\lambda \underline{a}_\lambda = \mu_\alpha^\lambda \underline{a}_\lambda , \qquad \underline{g}_3 = \underline{a}_3 , \tag{2.2.26}$$

where

$$\mu_\alpha^\beta = \delta_\alpha^\beta - \xi^3 b_\alpha^\beta \tag{2.2.27}$$

is a second order tensor, of mixed variance, relating the base vectors at the points $\underline{r}(\xi^\alpha, \xi^3)$ and $\underline{r}(\xi^\alpha, 0)$. The components of the metric tensor in space g_{ij} $(i,j = 1,2,3)$ are given by the scalar products

$$\left.\begin{aligned} g_{\alpha\beta} &= \underline{g}_\alpha \cdot \underline{g}_\beta = a_{\alpha\beta} - 2\xi^3 b_{\alpha\beta} + (\xi^3)^2 c_{\alpha\beta} , \\ g_{\alpha 3} &= \underline{g}_\alpha \cdot \underline{g}_3 = 0 , \\ g_{33} &= \underline{g}_3 \cdot \underline{g}_3 = 1 , \end{aligned}\right\} \tag{2.2.28}$$

with associated contravariant components

$$g^{ik} g_{kj} = \delta_j^i . \tag{2.2.29}$$

These tensors are used to raise and lower indices on space tensors.

The vectors $\underline{g}_i$ satisfy the relation, c.f. (2.2.16),

$$\underline{g}_3 = \frac{1}{2}\bar{\varepsilon}_{\alpha\beta} \underline{g}^\alpha \times \underline{g}^\beta \tag{2.2.30}$$

where

$$\bar{\varepsilon}_{\alpha\beta} = \mu\varepsilon_{\alpha\beta} \tag{2.2.31}$$

and

$$\mu = \det(\mu^{\alpha}_{\beta}) \tag{2.2.32}$$

The derivatives of the base vectors $\mathbf{g}_i$ may be written in terms of the Christoffel symbols in space, c.f. (2.2.23) and (2.2.24),

$$\mathbf{g}_{i,j} = \hat{\Gamma}^{k}_{ij}\mathbf{g}_k , \qquad \mathbf{g}^{i}_{,j} = -\hat{\Gamma}^{i}_{jk}\mathbf{g}_i , \tag{2.2.33}$$

where

$$\hat{\Gamma}^{k}_{ij} = \frac{1}{2}g^{kl}(g_{jl,i} + g_{li,j} - g_{ij,l}) , \tag{2.2.34}$$

so that $\hat{\Gamma}^{k}_{ij}$ is symmetric with respect to the indices i and j, as in (2.2.26). From (2.2.23), (2.2.24) and (2.2.26) it follows that the Christoffel symbol in space with two or three indices 3 vanish and the symbols with one index 3 may be expressed in terms of the second and third fundamental tensors of the middle surface:

$$\left.\begin{aligned} &\hat{\Gamma}^{3}_{33} = \hat{\Gamma}^{\alpha}_{33} = \hat{\Gamma}^{3}_{3\alpha} = \hat{\Gamma}^{3}_{\alpha 3} = 0 , \\ &\hat{\Gamma}^{3}_{\alpha\beta} = \hat{\Gamma}^{3}_{\beta\alpha} = b_{\alpha\beta} - \xi^{3}c_{\alpha\beta} , \\ &\hat{\Gamma}^{\alpha}_{3\beta} = \hat{\Gamma}^{\alpha}_{\beta 3} = -b^{\alpha}_{\beta} + \xi^{3}c_{\alpha\beta} . \end{aligned}\right\} \tag{2.2.35}$$

It follows from (2.2.34) and (2.2.35) that the Christoffel symbols in space with three Greek indices reduce to the values given by (2.2.25) when evaluated on the middle surface, i.e.

$$\hat{\Gamma}^{\lambda}_{\alpha\beta}(\xi\ ,0) = \Gamma^{\lambda}_{\alpha\beta}\ . \tag{2.2.36}$$

The element of volume dV of the shell is defined by the usual vector triple product

$$dV = g_1 \times g_2 \cdot g_3\ d\xi^1 d\xi^2 d\xi^3 = \sqrt{g}\ d\xi^1 d\xi^2 d\xi^3 \tag{2.2.37}$$

where g is the determinant of the space metric, c.f. (2.2.9). Recalling (2.2.27) and (2.2.28) allows (2.2.37) to be written in the form

$$dV = \sqrt{a}\left[1 - 2\xi^3 H + (\xi^3)^2 K\right]\ d\xi^1 d\xi^2 d\xi^3 \tag{2.2.38}$$

where use is made of the identity

$$\det(g_{ij}) = \det(g_{\alpha\beta}) = \mu^2 a \tag{2.2.39}$$

together with

$$\mu = \det(\mu^{\alpha}_{\beta}) = \sqrt{\frac{g}{a}}\left[1 - 2\xi^3 H + (\xi^3)^2 K\right]\ . \tag{2.2.40}$$

2.3 Covariant differentiation

In a curvilinear coordinate system the partial derivatives of a vector do not transform between coordinate systems as tensor quantities. However, there is an operation in the tensor calculus, known as covariant differentiation, that does preserve the tensor character.

Covariant differentiation in space is denoted by an additional subscript preceded by a double vertical line. The rules for covariant space differentiation are given by

$$
\left.
\begin{aligned}
T_{||k} &= T_{,k} \,, \\
T^{i}_{\ ||k} &= T^{i}_{\ ,k} + \hat{\Gamma}^{i}_{lk} T^{l} \,, \\
T_{i||k} &= T_{i,k} - \hat{\Gamma}^{l}_{ik} T_{l} \,, \\
T_{ij||k} &= T^{ij}_{\ \ ,k} - \hat{\Gamma}^{l}_{ik} T_{lj} - \hat{\Gamma}^{l}_{jk} T_{il} \,,
\end{aligned}
\right\} \qquad (2.3.1)
$$

where T is a scalar, T^{i} and T_{i} are the contravariant and covariant components of a space vector, T_{ij} are the covariant components of a second order space tensor and the Christoffel symbols in space are given by (2.2.35). The covariant derivatives of the metric tensor are zero, see Flügge (1972). Moreover, in Euclidean space the order of covariant differentiation is immaterial.

A space vector $\underline{T}$ at a point on the middle surface may alternatively be written as a linear combination of the base vectors and unit normal vector

$$
\underline{T} = T^{\lambda} \underline{a}_{\lambda} + T^{3} \underline{a}_{3} \,, \qquad (2.3.2)
$$

where T^{α} and T^{3} constitute a contravariant space vector. On the other hand T^{α} may be regarded as a contravariant surface vector and T^{3} as a surface invariant. Similar decompositions hold for covariant space vectors and also for space tensors defined on the middle surface. The rules for connecting the covariant spatial derivatives of space vectors and tensors and the covariant surface derivatives of the surface representation of these vectors and tensors are summarised below:

$$
\left.
\begin{aligned}
T^{\alpha}{}_{||\beta} &= T^{\alpha}{}_{,\beta} + \Gamma^{\alpha}_{\lambda\beta}T^{\lambda} + \Gamma^{\alpha}_{3\beta}T^{3} = T^{\alpha}{}_{|\beta} - b^{\alpha}_{\beta}T^{3} \ , \\
T^{3}{}_{||\beta} &= T^{3}{}_{,\beta} + \Gamma^{3}_{\lambda\beta}T^{3} = T^{3}{}_{,\beta} - b_{\beta\lambda}T^{3} \ , \\
T_{\alpha||\beta} &= T_{\alpha,\beta} - \Gamma^{\lambda}_{\alpha\beta}T_{\lambda} - \Gamma^{3}_{\alpha\beta}T_{3} = T_{\alpha|\beta} - b_{\alpha\beta}T_{3} \ , \\
T_{3||\beta} &= T_{3,\beta} - \Gamma^{\lambda}_{3\beta}T_{\lambda} = T_{3|\beta} + b_{\lambda\beta}T^{\lambda} \ , \\
T_{\alpha\beta||\lambda} &= T_{\alpha\beta,\lambda} - \Gamma^{\mu}_{\alpha\lambda}T_{\mu\beta} - \Gamma^{3}_{\alpha\lambda}T_{3\beta} - \Gamma^{\mu}_{\beta\lambda}T_{\alpha\mu} - \Gamma^{3}_{\beta\lambda}T_{\alpha 3} \ , \\
&= T_{\alpha\beta|\lambda} - b_{\alpha\lambda}T_{3\beta} - b_{\beta\lambda}T_{\alpha 3}, \text{ etc.}
\end{aligned}
\right\} \quad (2.3.3)
$$

The geometry of the middle surface is non-Euclidean, so that it is not, in general, possible to interchange the order of repeated covariant surface differentiation, although this is possible for a surface invariant.

2.4 Geometry of the shell boundary

The boundary conditions appropriate for the shell problem are obtained in the next chapter from a consideration of the principle of virtual work and the line integral which results through application of the divergence theorem. In order to put these in a suitable form, the geometry of the boundary curve Γ of the middle surface is described.

At any point of Γ, see Fig. 2.2, there are three mutually perpendicular unit vectors $\underline{\nu}$, $\underline{\tau}$, $\underline{a}_3$, where $\underline{\tau}$ is a tangent vector to Γ and $\underline{\nu}$ is a normal vector to Γ perpendicular to $\underline{a}_3$. The positive sense of $\underline{\tau}$ is taken to be such that $\underline{\nu}$, $\underline{\tau}$, $\underline{a}_3$, in that order, will define a right-handed coordinate system, see Fig. 2.2. It is convenient to define the boundary Γ by $\tau(\xi^{\alpha})$, where τ is the arc length along Γ measured from some invariant point on the curve. The unit vector $\underline{\tau}$ in

the middle surface is expressed in terms of the covariant and contravariant base vectors according to

$$\underline{\tau} = \frac{d\xi^{\lambda}}{d\tau}\,\underline{a}_{\lambda} = \tau^{\lambda}\underline{a}_{\lambda} = \tau_{\lambda}\underline{a}^{\lambda} \ . \tag{2.4.1}$$

Similarly, the unit vector $\underline{\nu}$ may be written

$$\underline{\nu} = \nu_{\lambda}\underline{a}^{\lambda} = \varepsilon^{\lambda\mu}\tau_{\mu}\underline{a}_{\lambda} \ . \tag{2.4.2}$$

The differential element of arc length $d\tau$ along the boundary is related to the differential element $d\xi^{\alpha}$ of the coordinate curves by

$$\underline{\tau}\, d\tau = \underline{a}_{\alpha}\, d\xi^{\alpha} \tag{2.4.3}$$

so that

$$\tau^{\alpha}\, d\tau = d\xi^{\alpha} \tag{2.4.4}$$

Expressions for derivatives of quantities defined along the boundary follow from (2.4.4). Thus the total derivative of a scalar T with respect to the Gaussian coordinates is given by

$$\frac{dT}{\partial\tau} = \tau^{\alpha}\,\frac{\partial T}{\partial\xi^{\alpha}} \ , \tag{2.4.5}$$

and the gradient $T_{,\alpha}$ may be resolved along the directions normal and tangential to the boundary curve according to

$$T_{,\alpha} = \nu_{\alpha}\,\frac{\partial T}{\partial\nu} + \tau_{\alpha}\,\frac{\partial T}{\partial\tau} \ . \tag{2.4.6}$$

Note is made of the divergence theorem on the middle surface for the conversion of surface integrals into line integrals and vice-versa. If

T^{α} is a contravariant surface vector then the divergence theorem may be written

$$\int_{\Omega} T^{\alpha}|_{\alpha} \sqrt{a}\, d\xi^1 d\xi^2 = \int_{\Gamma} T^{\lambda} \nu_{\lambda}\, d\tau \qquad (2.4.7)$$

2.5 Practical components

Although the tensor calculus provides a natural and concise means by which to express the governing equations of a thin shell when referred to an arbitrary curvilinear coordinate system it does give rise to the following practical problem. The covariant and contravariant components of a tensor do not have the same kind of physical significance in a curvilinear coordinate system as they do in a rectangular Cartesian system. In fact they do not generally share common units of measurement, so they do not relate directly with quantities capable of physical measurement and special difficulty arises when the axes are oblique, as is commonly the case in a typical shell problem. This is at odds with the requirements of engineering and finite element analysis where it is required to determine the magnitude of quantities such as displacements, strains and material properties in any specified direction on the shell middle surface.

McConnell (1931) is generally attributed the first satisfactory explanation of the physical components of a tensor. His approach is to consider a tensor field referred to an orthogonal curvilinear coordinate system and to define the physical components at a given point as its components in the rectangular Cartesian system whose axes are parallel to the curvilinear coordinate axes at that point. This definition is adequate so long as the tensor components are defined in an orthogonal coordinate system, however, as mentioned above it is generally desirable in shell problems to have quantities capable of direct physical measurement in an oblique coordinate system. The required extension of McConnell's

definition can be found in the work of Truesdell (1953) where transformation formulae are given for the left and right physical components of tensor fields referred to an oblique curvilinear coordinate system.

The following considers a different approach developed by Morley (1987) to meet present day requirements in engineering and finite element analysis whereby physically measureable quantities are defined which have orthogonal components orientated as required with respect to the tensor coordinates whether these are orthogonal or oblique - these are called practical components.

Recall from (2.2.3) that the position vector $\underline{r}$ of a point on the middle surface is expressed as a function of the curvilinear coordinates ξ^α and is used to define the base vectors $\underline{a}_\alpha$, see (2.2.5). Now define unit vectors $\underline{t}_\alpha$ tangent to the coordinate curves ξ^α by the relations

$$\underline{t}_\alpha = \frac{1}{a_\alpha}\,\underline{a}_\alpha \quad \text{(no sum)} \tag{2.5.1}$$

where

$$a_\alpha = |\underline{a}_\alpha \cdot \underline{a}_\alpha|, \tag{2.5.2}$$

so that these vectors satisfy

$$\underline{t}_1 \cdot \underline{t}_1 = \underline{t}_2 \cdot \underline{t}_2 = 1, \qquad \underline{t}_1 \cdot \underline{t}_2 = \cos\beta\ , \tag{2.5.3}$$

where β is the angle included between the coordinate curves as shown in Fig. 2.3. From this it follows that the components of the metric tensor are given by

$$\left.\begin{aligned} &a_{11} = (a_1)^2\ , \qquad a_{12} = a_{21} = a_1 a_2 \cos\beta\ , \qquad a_{22} = (a_2)^2\ , \\ &a^{11} = a_{22}/a\ , \qquad a^{12} = a^{21} = -a_{12}/a\ , \qquad a^{22} = a_{11}/a \end{aligned}\right\} \tag{2.5.4}$$

where

$$\left.\begin{aligned} a &= \det\,(a_{\alpha\beta}) = (a_1 a_2 \sin\,\beta)^2\ , \\ 1/a &= \det\,(a^{\alpha\beta}) \end{aligned}\right\} \qquad (2.5.5)$$

Let $\underline{t}_{\alpha'}$ denote an orthogonal set of unit vectors, see Fig. 2.3,

where

$$\underline{t}_{\alpha'}\cdot\underline{t}_{\beta'} = \delta_{\alpha'\beta'}\ , \qquad \underline{t}_{\alpha'} = \underline{t}^{\alpha'} \qquad (2.5.6)$$

and

$$\left.\begin{aligned} \underline{t}_1\cdot\underline{t}_1 &= \cos\,\lambda, \qquad \underline{t}_1\cdot\underline{t}_2 = \cos\,(\beta+\lambda)\ , \\ \underline{t}_2\cdot\underline{t}_1 &= \sin\,\lambda, \qquad \underline{t}_2\cdot\underline{t}_2 = \sin\,(\beta+\lambda)\ . \end{aligned}\right\} \qquad (2.5.7)$$

It is possible to resolve the (orthogonal) vectors $\underline{t}_{\alpha'}$ along the directions of the base vectors $\underline{a}_\alpha$ according to

$$\underline{t}_{\alpha'} = h^{\alpha}_{\alpha'}\underline{a}_\alpha\ , \qquad (2.5.8)$$

where

$$\left.\begin{aligned} h^1_{1'} &= \frac{\sin\,(\beta+\lambda)}{a_1\sin\,\beta}\ , \qquad h^2_{1'} = -\frac{\sin\,\lambda}{a_2\sin\,\beta}\ , \\ h^1_{2'} &= -\frac{\cos\,(\beta+\lambda)}{a_1\sin\,\beta}\ , \qquad h^2_{2'} = \frac{\cos\,\lambda}{a_2\sin\,\beta}\ , \end{aligned}\right\} \qquad (2.5.9)$$

Equation (2.5.8) may be inverted to give

$$\underline{a}_\alpha = h^{\alpha'}_{\alpha}\,\underline{t}_{\alpha'}\ , \qquad (2.5.10)$$

where

$$\left.\begin{aligned} h_1^{1'} &= a_1\cos\lambda, \qquad h_1^{2'} = a_1\sin\lambda\ , \\ h_2^{1'} &= a_2\cos(\beta+\lambda), \qquad h_2^{2'} = a_2\sin(\beta+\lambda)\ . \end{aligned}\right\} \tag{2.5.11}$$

It is now shown, by examples, that the h-symbols have the property that products with any surface vector or tensor in any curvilinear coordinate system ξ^α give the orientated physical components referred to orthogonal coordinates. To this end the physical properties of $h^{\alpha}_{\alpha'}$ and $h^{\alpha'}_{\alpha}$ are summarised by

$$\left.\begin{aligned} &h^{\alpha'}_{\alpha}h^{\beta}_{\alpha'} = \delta^{\beta}_{\alpha}\ , \qquad h^{\alpha'}_{\alpha}\ h^{\alpha}_{\beta'} = \delta^{\alpha'}_{\beta'}\ , \\ &h^{\alpha}_{\alpha'}h^{\alpha'}_{\alpha} = \delta^{\alpha}_{\alpha} = \delta^{\alpha'}_{\alpha'} = 2\ , \\ &h^{\alpha}_{\alpha'}a_{\ \alpha\beta} = h^{\alpha'}_{\beta}\ , \qquad h^{\alpha'}_{\alpha}a^{\alpha\beta} = h^{\beta}_{\alpha'}\ , \\ &h^{\alpha}_{\alpha'}h^{\beta}_{\beta'}a_{\alpha\beta} = \delta^{\beta'}_{\alpha'}\ , \qquad h^{\alpha'}_{\alpha}h^{\beta'}_{\beta}a^{\alpha\beta} = \delta^{\alpha'}_{\beta'}\ , \\ &a_{\alpha\beta} = h^{\alpha'}_{\alpha}h^{\alpha'}_{\beta}\ , \qquad a^{\alpha\beta} = h^{\alpha}_{\alpha'}h^{\beta}_{\alpha'} \\ &\sqrt{a} = h_1^{1'}h_2^{2'} - h_2^{1'}h_1^{2'}\ , \qquad 1/\sqrt{a} = h^1_{1'}h^2_{2'} - h^1_{2'}h^2_{1'} \\ &= \tfrac{1}{2}\varepsilon^{\alpha\beta}\ \varepsilon_{\alpha'\beta'}h^{\alpha'}_{\alpha}h^{\beta'}_{\beta}\ , \qquad = \tfrac{1}{2}\varepsilon_{\alpha\beta}\varepsilon^{\alpha'\beta'}h^{\alpha}_{\alpha'}h^{\beta}_{\beta'}\ , \end{aligned}\right\} \tag{2.5.12}$$

where $\varepsilon^{\alpha\beta}$, $\varepsilon_{\alpha'\beta'}$ etc. are the permutation tensors, of the oblique and orthogonal coordinate systems. (Note that in these equations the summation convention for repeated indices with primes has been extended to any position.)

Consider the surface vector $\underline{T}$ given by

$$\underline{T} = T^{\lambda}\underline{a}_{\lambda} + T^{3}\underline{a}_{3} = T_{\lambda}\underline{a}^{\lambda} + T_{3}\underline{a}^{3} \ . \tag{2.5.13}$$

Substitution into these relations from (2.5.10) gives

$$\underline{T} = h^{\alpha'}_{\alpha}T^{\alpha}\underline{t}_{\alpha'} + T^{3}\underline{a}_{3} = h^{\alpha}_{\alpha'}T_{\alpha}\underline{t}_{\alpha'} + T_{3}\underline{a}^{3} \tag{2.5.14}$$

and, remembering that the vectors $\underline{t}_{1'}$, $\underline{t}_{2'}$ and $\underline{a}_{3} = \underline{a}^{3}$ are orthogonal to each other and of unit magnitude, it follows that the quantities

$$T_{\alpha'} = h^{\alpha}_{\alpha'}T_{\alpha} = h^{\alpha'}_{\alpha}T^{\alpha} = T^{\alpha'} \tag{2.5.15}$$

are the components of $\underline{T}$ measured in the directions of the vectors $\underline{t}_{\alpha'}$, which can be orientated as required with respect to the coordinates ξ^{α} by specifying the angle λ. These are called the practical components of the surface vector $\underline{T}$. By definition it follows that $T^{3} = T_{3}$ is identical with its practical component.

In classical physics only scalars and vectors have physical significance and tensor components are determined by equations relating them to measured vector components and scalars. This observation underlies the definition of practical components for tensors of higher order. By way of illustration consider the following tensor equation relating vector components R^{α} and S_{β} :

$$R^{\alpha} = T^{\alpha\beta}S_{\beta} \tag{2.5.16}$$

where $T^{\alpha\beta}$ are identified as the contravariant components of a second order tensor. The practical components of R^{α} and S_{β} are defined as in (2.5.15) giving

$$R^{\alpha} = h^{\alpha}_{\alpha'}R_{\alpha'} \ , \qquad S_{\beta} = h^{\beta'}_{\beta}S_{\beta'} \ , \tag{2.5.17}$$

where $R_{\alpha'}$ and $S_{\beta'}$ are referred to the orthogonal directions of the vectors $\underline{t}_{\alpha'}$. Substituting from (2.5.17) into (2.5.16) and making use of the relations listed in (2.5.12) gives

$$R_{\alpha'} = h_{\alpha}^{\alpha'} h_{\beta}^{\beta'} T^{\alpha\beta} S_{\beta'} \ , \tag{2.5.18}$$

which is the defining relation for the practical components

$$T_{\alpha'\beta'} = h_{\alpha}^{\alpha'} h_{\beta}^{\beta'} T^{\alpha\beta} \ . \tag{2.5.19}$$

Making use of the properties of the h-symbols it follows that

$$\left.\begin{aligned} T_{\alpha'\beta'} &= h_{\alpha'}^{\alpha} h_{\beta'}^{\beta} T_{\alpha\beta} \ , \qquad T_{\alpha\beta} = h_{\alpha}^{\alpha'} h_{\beta}^{\beta'} T_{\alpha'\beta'} \ , \\ &= h_{\alpha'}^{\alpha} h_{\beta}^{\beta'} T_{\alpha}^{\cdot\beta} \ , \qquad T_{\alpha}^{\cdot\beta} = h_{\alpha}^{\alpha'} h_{\beta'}^{\beta} T_{\alpha'\beta'} \ , \\ &= h_{\alpha}^{\alpha'} h_{\beta'}^{\beta} T_{\cdot\beta}^{\alpha} \ , \qquad T_{\cdot\beta}^{\alpha} = h_{\alpha'}^{\alpha} h_{\beta}^{\beta'} T_{\alpha'\beta'} \ , \\ &= h_{\alpha}^{\alpha'} h_{\beta}^{\beta'} T^{\alpha\beta} \ , \qquad T^{\alpha\beta} = h_{\alpha'}^{\alpha} h_{\beta'}^{\beta} T_{\alpha'\beta'} \ , \end{aligned}\right\} \tag{2.5.20}$$

where $T^{\alpha'\beta'} = T_{\alpha'\beta'}$ etc. Practical components of general tensors of all orders follow from similar considerations.

In applications it will be necessary to determine values of the trigonometric functions of the angle λ specific to given directions on the middle surface. To this end let the coordinate $\xi^{2'}$ be aligned along a curve on the middle surface whose points are specified by the position vector

$$\underline{r}(\xi^{\alpha}) = \underline{r}(\xi^{2'}) \ . \tag{2.5.21}$$

The element of arc along this curve is

$$d\tau = a_{2'} d\xi^{2'} \tag{2.5.22}$$

and the unit tangent vector is given by

$$\underline{t}_{2'} = \frac{1}{a_{2'}} \underline{r}_{,2'} = \frac{1}{a_{2'}} \xi^{\alpha}{}_{,2'} \underline{a}_{2} \tag{2.5.23}$$

where

$$(a_{2'})^2 = (\xi^{1}{}_{,2'} a_1)^2 + 2\xi^{1}{}_{,2'} \xi^{2}{}_{,2'} a_1 a_2 \cos\beta + (\xi^{2}{}_{,2'} a_2)^2 . \tag{2.5.24}$$

The required trigonometric relations appropriate to a point $\xi^{2'}$ on the curve follows from the scalar products, see (2.5.7),

$$\left.\begin{aligned} \sin\lambda &= \underline{t}_{2'} \cdot \underline{t}_1 = \frac{1}{a_{2'}} \xi^{1}{}_{,2'} a_1 + \frac{1}{a_1} \xi^{2}{}_{,2'} a_2 \cos\beta , \\ \sin(\beta+\lambda) &= \underline{t}_{2'} \cdot \underline{t}_1 = \frac{1}{a_{2'}} \xi^{1}{}_{,2'} a_1 \cos\beta + \frac{1}{a_1} \xi^{2}{}_{,2'} a_2 , \end{aligned}\right\} \tag{2.5.25}$$

and

$$\left.\begin{aligned} \cos\lambda &= \frac{1}{\sin\beta} (\sin(\beta+\lambda) - \sin\beta\cos\lambda) , \\ \cos(\beta+\lambda) &= \cos\beta\cos\lambda - \sin\beta\sin\lambda . \end{aligned}\right\} \tag{2.5.26}$$

The unit vector tangent to the middle surface and orthogonal to $\underline{t}_{2'}$ is given by

$$\underline{t}_{1'} = \frac{1}{a_{2'}\sin\beta}\left[(\xi^{1}{}_{,2'} a_1\cos\beta + \xi^{2}{}_{,2'} a_2)\underline{t}_1 - (\xi^{1}{}_{,2'} a_1 + \xi^{2}{}_{,2'} a_2\cos\beta)\underline{t}_2\right] \tag{2.5.27}$$

In applications such as finite element analysis it is frequently required to calculate principal values of symmetric tensors e.g. the principal curvatures and principal stresses. The use of the relationships satisfied by the h-symbols provides a concise expression for these values. Principal values of a symmetric tensor $T_{\alpha\beta}$ occur, see Malvern (1969), when

$$T_{1'2'} = h^{\alpha}_{1'} h^{\beta}_{2'} T_{\alpha\beta} = 0 \qquad (2.5.28)$$

Substituting from (2.5.9) and making use of (2.5.4) and (2.5.5) shows that this condition is satisfied when the angle λ is such that

$$\tan 2\lambda = \frac{(2T_{11}\sqrt{a} - T_{11}a_{22}\sin 2\beta)}{(T_{11}a_{22}\cos 2\beta - 2T_{12}a_{12} + T_{22}a_{11})}. \qquad (2.5.29)$$

CHAPTER 3

ELEMENTS OF FIRST APPROXIMATION THIN SHELL THEORY

3.1 Introduction

Shell theory is based on a reduction of the equations of elasticity from three to two dimensions. In this chapter some of the elements of the linear theory of thin shells are briefly recalled, see Koiter (1959, 1960, 1961, 1966, 1970), Sanders (1959), Naghdi (1963, 1972), Leonard (1961). The intention is to indicate the nature and complexity of the shell problem.

To begin, the deformation of the middle surface is considered. The strain measures used to describe a change in configuration are introduced and the compatibility equations relating these quantities are given. Attention is then directed to the statics of the shell. From a three-dimensional state of stress it is possible to derive statically equivalent forces and moments, acting at the middle surface, and to deduce two-dimensional equations of equilibrium, expressed in terms of these integrated quantities. This is followed by a derivation of the boundary conditions appropriate to the two-dimensional equations of equilibrium.

The connection between the kinematics and statics of the middle surface is considered in the section on Love's strain energy expression. Here details are given of Koiter's (1959, 1960) fundamental result concerning the consistency of first approximation shell theories founded on the basic assumption of plane stress. It is noted that the inherent errors of this approximate theory allow for a certain degree of freedom in the definition of the curvature change tensor and also have ramifications in the assessment of numerical solutions to the shell problem.

The remaining sections briefly discuss the static-geometric analogy and the simplified membrane and shallow shell theories.

3.2 Deformation of the middle surface

Consider a point in the shell with Gaussian coordinates ξ^i in the undeformed state and let $\underline{u}$ denote the displacement vector which carries the a material point in the shell to a new position in space in a deformed configuration of the shell. The new position is given by

$$\bar{\underline{r}} = \underline{r} + \underline{u} \ . \tag{3.2.1}$$

It is found that the deformation of the shell can be adequately described by two tensor fields which characterise the stretching and bending of differential line elements.

After the change of position defined by (3.2.1) the distance $d\sigma$ between two neighbouring points of the shell in the initial configuration changes to $d\bar{\sigma}$ in the deformed configuration, where, c.f. (2.2.10),

$$(d\bar{\sigma})^2 = \bar{g}_{ij}\, d\xi^i d\xi^j \tag{3.2.2}$$

and $\bar{g}_{ij}$ is the metric tensor in space of the deformed coordinate system. The quantity

$$(d\bar{\sigma})^2 - (d\sigma)^2 = (\bar{g}_{ij} - g_{ij})\, d\xi^i d\xi^j \tag{3.2.3}$$

is a measure of the change in distance between two neighbouring points in the shell during deformation. The strain tensor γ_{ij} is defined by

$$\gamma_{ij} = \frac{1}{2}(\bar{g}_{ij} - g_{ij}) \ . \tag{3.2.4}$$

The covariant components of the strain tensor may be expressed in terms of the displacement vector as follows. The deformed base vectors are defined as the partial derivatives of (3.2.1) with respect to the Gaussian coordinates:

$$\bar{\underline{g}}_i = \bar{\underline{r}}_{,i} = \underline{g}_{,i} + \underline{u}_{,i} \tag{3.2.5}$$

so that

$$\bar{g}_{ij} = \bar{\underline{g}}_i \cdot \bar{\underline{g}}_j = g_{ij} + \underline{g}_i \cdot \underline{u}_{,j} + \underline{g}_{,j} \cdot \underline{u}_{,i} \tag{3.2.6}$$

and substituting into (3.2.3) gives

$$\gamma_{ij} = \frac{1}{2}(g_i \cdot \underline{u}_{,j} + \underline{g}_j \cdot \underline{u}_{,i} + \underline{u}_{,i} \cdot \underline{u}_{,j}) \ . \tag{3.2.7}$$

Let the displacement vector be decomposed into covariant components according to

$$\underline{u} = u_k \underline{g}^k \ , \tag{3.2.8}$$

and, using the rules for covariant space differentiation, allows the derivatives in (3.2.7) to be written

$$\underline{u}_{,i} = u_{k||i} \underline{g}^k \tag{3.2.9}$$

so that

$$\gamma_{ij} = \frac{1}{2}(u_{i||j} + u_{j||i} + g^{kl} u_{k||i} u_{l||j}) \ . \tag{3.2.10}$$

Now choose as a reference coordinate system that given by (2.2.26), so that the components of the space metric tensor are given by (2.2.28). The basic kinematical assumption of classical Kirchhoff-Love theory is that the

normals to the undeformed middle surface are mapped to normals of the deformed middle surface without any change in length. This assumption requires the components of the spatial metric tensor to be specified by

$$\bar{g}_{\alpha\beta} = \bar{a}_{\alpha\beta} - 2\xi^3\bar{b}_{\alpha\beta} + (\xi^3)^2\bar{c}_{\alpha\beta} , \qquad \bar{g}_{\alpha 3} = 0, \qquad \bar{g}_{33} = 1 , \quad (3.2.11)$$

where $\bar{a}_{\alpha\beta}$, $\bar{b}_{\alpha\beta}$ and $\bar{c}_{\alpha\beta}$ are the first, second and third fundamental forms of the deformed middle surface. The base vectors $\underline{a}_\alpha$ on the deformed middle surface are calculated from (3.2.5) by setting $\xi^3 = 0$, i.e.

$$\underline{\bar{a}}_\alpha = \underline{\bar{r}}_{,\alpha}\big|_{\xi^3 = 0} . \qquad (3.2.12)$$

The components of $\bar{b}_{\alpha\beta}$ and $\bar{c}_{\alpha\beta}$ are determined by relations similar to (2.2.18) and (2.2.20). It follows that the strain tensor of (3.2.3) may therefore be written

$$\gamma_{\alpha\beta} = \frac{1}{2}\left[(\bar{a}_{\alpha\beta} - a_{\alpha\beta}) - 2\xi^3(\bar{b}_{\alpha\beta} - b_{\alpha\beta}) + (\xi^3)^2(\bar{c}_{\alpha\beta} - c_{\alpha\beta})\right] , \quad (3.2.13)$$

so that, neglecting terms in $(\xi^3)^2$, the geometry of the deformed shell is specified to first order by the first and second fundamental tensors of the middle surface. This prompts the following choice for the middle surface strain measures:

$$\overset{\circ}{\gamma}_{\alpha\beta} = \frac{1}{2}(\bar{a}_{\alpha\beta} - a_{\alpha\beta}) , \qquad \overset{\sim}{\rho}_{\alpha\beta} = \bar{b}_{\alpha\beta} - b_{\alpha\beta} , \qquad (3.2.14)$$

where the notation $^\circ$ indicates evaluation on the middle surface.

Clearly the explicit equations for the tensors of membrane strain and curvature change in terms of the displacement components are very complicated. A fundamental assumption of a linear or small strain theory of elasticity is that displacement gradients are small. This allows the

expression for the strain tensor in surfaces parallel to the middle surface to be simplified by neglecting the quadratic terms, so that

$$\gamma_{\alpha\beta} = \frac{1}{2}(u_{\alpha||\beta} + u_{\beta||\alpha}) \cdot \tag{3.2.15}$$

On the middle surface the spatial covariant derivatives may be expressed in terms of surface derivatives by using (2.3.3), so that

$$\overset{\circ}{\gamma}_{\alpha\beta} = \frac{1}{2}(u_{\alpha|\beta} + u_{\beta|\alpha}) - b_{\alpha\beta}u_3 \cdot \tag{3.2.16}$$

The rotation about the normal to the middle surface is described by the antisymmetric tensor

$$\omega_{\alpha\beta} = \frac{1}{2}(u_{\beta||\alpha} - u_{\alpha||\beta}) = \frac{1}{2}(u_{\beta|\alpha} - u_{\alpha|\beta}) = \frac{1}{2}(u_{\alpha,\beta} - u_{\beta,\alpha}) \ , \tag{3.2.17}$$

where again use is made of the relations given in (2.3.3).

The rotation of the normal at the middle surface is defined by the surface vector ϕ_α , given by

$$\phi_\alpha = \omega_{\alpha 3} = \frac{1}{2}(u_{3||\alpha} - u_{\alpha||3}) \ , \tag{3.2.18}$$

but the component of transverse shear is required to vanish in Kirchhoff theory so that

$$\gamma_{\alpha 3} = \frac{1}{2}(u_{\alpha||3} + u_{3||\alpha}) = 0 \ , \tag{3.2.19}$$

and using this to substitute into (3.2.18) gives

$$\phi_\alpha = u_{3||\alpha} \cdot \tag{3.2.20}$$

Use of the rules of equation (2.3.3) relating covariant spatial and surface differentiation gives

$$\phi_\alpha = u_{3|\alpha} + b_\alpha^\lambda u_\lambda = u_{3,\alpha} + b_\alpha^\lambda u_\lambda \ . \qquad (3.2.21)$$

The rotation about the middle surface normal is given by

$$\phi = h_1^\alpha, h_2^\beta, \omega_{\alpha\beta} \ . \qquad (3.2.22)$$

The expression for the curvature change tensor $\rho_{\alpha\beta}$ in terms of the displacement components is, see Koiter (1966), Niordson (1985),

$$\tilde{\rho}_{\alpha\beta} = u_{3|\alpha\beta} - c_{\alpha\beta}u_3 + b_\alpha^\lambda u_{\lambda|\beta} + b_\beta^\lambda u_{\lambda|\alpha} + b_{\alpha|\beta}^\lambda u_\lambda \ . \qquad (3.2.23)$$

It is noted that any independent pair of linear combinations of the tensors (3.2.16) and (3.2.23) constitute an equivalent description of the middle surface. In particular, the following modified tensor of curvature change

$$\rho_{\alpha\beta} = \tilde{\rho}_{\alpha\beta} - \frac{1}{2}(b_\alpha^\lambda \gamma_{\lambda\beta} + b_\beta^\lambda \gamma_{\lambda\alpha}) \qquad (3.2.24)$$

has advantages in general discussions on shell theory, see Budiansky and Sanders (1963).

3.3 Compatibility equations

The local deformation of a shell at a point on the middle surface is completely described by six numbers, three membrane strains and three bending strains. Considered as functions of the coordinates ξ^α they cannot be independent since they determine $\bar{a}_{\alpha\beta}$ and $\bar{b}_{\alpha\beta}$ which are not independent. There must therefore be relations connecting the strain measures. These are the equations of compatibility. In tensor form these may be written, see Koiter (1961, 1966),

$$\left.\begin{aligned} &\varepsilon^{\alpha\lambda}\varepsilon^{\beta\mu}[\gamma_{\alpha\beta|\lambda\mu} + b_{\alpha\beta}\rho_{\lambda\mu}] = 0 \ , \\ &\varepsilon^{\alpha\lambda}\varepsilon^{\beta\mu}\left([\rho_{\lambda\mu} + \tfrac{1}{2}b^{\omega}_{\lambda}\gamma_{\omega\mu} + \tfrac{1}{2}b^{\omega}_{\mu}\gamma_{\omega\lambda}]_{|\beta} + b^{\omega}_{\beta}[\gamma_{\omega\lambda|\mu} + \gamma_{\omega\mu|\lambda} - \gamma_{\lambda\mu|\omega}]\right) = 0 \ , \end{aligned}\right\} \quad (3\ 3.1)$$

where here, and in the sequel, the notation $^{\circ}$ is dropped and it is understood that the membrane strain tensor is evaluated at the middle surface.

3.4 Equilibrium equations

In a shell the system of stresses is described by a stress resultant tensor $N^{\alpha\beta}$ corresponding to tension and shear stresses, a stress couple tensor $M^{\alpha\beta}$ corresponding to bending and twisting moments and a vector Q^{α} of transverse shear forces. As in plates all these forces and moments participate in establishing the equilibrium of the shell but, because of its curvature, they interact with each other in a much more complicated way.

All these resultant stress quantities are related to the three-dimensional stresses throughout the shell as follows. Consider the section through the shell shown in Fig. 3.1. The subelement of height $d\xi^3$ has area

$$d\underline{A} = d\underline{r} \times \underline{g}_3 d\xi^3 = dA_{\lambda}\, \underline{g}^{\lambda} \qquad (3.4.1)$$

where it is noted that the line element vector defining the base of this subelement is given by

$$d\underline{r} = \underline{g}_{\lambda} d\xi^{\lambda} \ . \qquad (3.4.2)$$

and

$$dA_\alpha = \bar{\varepsilon}_{\alpha\lambda} d\xi^\lambda d\xi^3 \ . \tag{3.4.3}$$

Across this subelement a force $d\underline{F}$ is transmitted which can be written in terms of the stress tensor according to

$$\begin{aligned} d\underline{F} &= dF^\lambda \underline{g}_\lambda + dF^3 \underline{g}_3 \\ &= \sigma^{\alpha\lambda} dA_\alpha \underline{g}_\lambda + \sigma^{\alpha 3} dA_\alpha \underline{g}_3 \ . \end{aligned} \tag{3.4.4}$$

The first term represents a force in the tangent plane parallel to the middle surface, while the second represents a force normal to the shell.

These stresses are now used to derive statically equivalent forces and moments acting at the middle surface and then to deduce the two-dimensional equations of equilibrium expressed in terms of these integrated quantities.

Integrating across the shell thickness gives the resultant

$$\int_{-h/2}^{h/2} dF^3 \underline{g}_3 = \underline{a}_3 \int_{-h/2}^{h/2} \sigma^{\alpha 3} dA_\alpha = \underline{a}_3 d\xi^\lambda \int_{-h/2}^{h/2} \sigma^{\alpha 3} \bar{\varepsilon}_{\alpha\lambda} d\xi^3 \tag{3.4.5}$$

and using (2.2.31) to express the permutation tensor $\bar{\varepsilon}_{\alpha\lambda}$ in terms of the permutation tensor $\varepsilon_{\alpha\lambda}$ on the middle surface gives

$$\int_{-h/2}^{h/2} dF^3 \underline{g}_3 = \underline{a}_3 d\xi^\lambda \varepsilon_{\alpha\lambda} \int_{-h/2}^{h/2} \sigma^{\alpha 3} \mu \ d\xi^3 \ . \tag{3.4.6}$$

The vertical force may now be written

$$\int_{-h/2}^{h/2} dF^3 \underline{g}_3 = \varepsilon_{\alpha\lambda} d\xi^\lambda Q^\alpha \underline{a}_3 \ , \tag{3.4.7}$$

where

$$Q^\alpha = \int_{-h/2}^{h/2} \sigma^{\alpha 3} \mu \ d\xi^3 \tag{3.4.8}$$

is the transverse shear force acting on the shell.

Next consider the first term of (3.4.4). This term contains a factor g_λ which depends, through (2.2.26), on ξ^3, so that this equation may be used to express the force in the reference frame defined by $\underline{a}_\alpha$:

$$\int_{-h/2}^{h/2} dF^\lambda \underline{g}_\lambda = \int_{-h/2}^{h/2} \sigma^{\alpha\lambda} \bar{\varepsilon}_{\alpha\mu}\, d\xi^\mu d\xi^3 \underline{g}_\lambda = \varepsilon_{\alpha\mu} d\xi^\mu \underline{a}_\omega \int_{-h/2}^{h/2} \sigma^{\alpha\lambda}\mu\, \mu_\lambda^\omega d\xi^3 \ . \quad (3.4.9)$$

Define the stress resultant tensor by

$$N^{\alpha\beta} = \int_{-h/2}^{h/2} \sigma^{\alpha\lambda}\mu\, \mu_\lambda^\beta d\xi^3 \ , \quad (3.4.10)$$

so that

$$\int_{-h/2}^{h/2} dF^\lambda \underline{g}_\lambda = \varepsilon_{\alpha\lambda} d\xi^\lambda N^{\alpha\mu} \underline{a}_\mu \ . \quad (3.4.11)$$

The force $d\underline{F}$ has a moment arm $\xi^3 \underline{a}_3$ with respect to the centre of the section and hence a moment

$$d\underline{M} = \xi^3 \underline{a}_3 \times \underline{dF} = \xi^3 (\sigma^{\alpha\lambda} \underline{a}_3 \times \underline{g}_\lambda + \sigma^{\alpha 3} \underline{a}_3 \times \underline{g}_3) dA_\alpha \ . \quad (3.4.12)$$

Since $\underline{a}_3 = \underline{g}_3$ the second term on the right hand side is zero and the total moment of forces $d\underline{F}$ in the section element is therefore

$$\int_{-h/2}^{h/2} d\underline{M} = \int_{-h/2}^{h/2} \xi^3 \sigma^{a\lambda} \underline{a}_3 \times \mu_\lambda^\theta \underline{a}_\theta \varepsilon_{\alpha\omega}\mu\, d\xi^\omega d\xi^3 \quad (3.4.13)$$

$$= \varepsilon_{\alpha\lambda} \varepsilon_{\beta\theta} \underline{a}^\theta d\xi^\lambda \int_{-h/2}^{h/2} \xi^3 \sigma^{\alpha\omega} \mu_\omega^\beta \mu\, d\xi^3 \ .$$

Define the stress couple tensor by

$$M^{\alpha\beta} = \int_{-h/2}^{h/2} \xi^3 \sigma^{\alpha\lambda} \mu_\lambda^\beta \mu\, d\xi^3 \ , \quad (3.4.14)$$

so that

$$\int_{-h/2}^{h/2} d\underline{M} = \varepsilon_{\alpha\lambda}\varepsilon_{\beta\mu} d\xi^{\lambda} M^{\alpha\beta}\, \underline{a}^{\mu} \ . \qquad (3.4.15)$$

The stress resultants $N^{\alpha\beta}$, $M^{\alpha\beta}$ and Q^{α} must satisfy certain differential equations which express the equilibrium of the shell element. These equations are obtained from the three-dimensional equations of equilibrium, see Green and Zerna (1954),

$$\sigma^{ij}{}_{||j} + F^{i} = 0 \ , \qquad (3.4.16)$$

$$\varepsilon_{ijk}\sigma^{ij} = 0 \ , \qquad (3.4.17)$$

where F^{i} are the components of volume forces distributed throughout the shell. The idea is to integrate these equations after multiplying through by a suitable factor so that the resulting integrals coincide with those used to define the membrane stress resultant, moment resultant and transverse shear force.

The equations of equilibrium in terms of the above stress resultants, together with the resultants of the externally applied forces f^{i} and moments m^{α}, are, see Naghdi (1963),

$$N^{\lambda\alpha}{}_{|\lambda} - b^{\alpha}_{\lambda}Q^{\lambda} + f^{\alpha} = 0 \ , \qquad (3.4.18)$$

$$Q^{\lambda}{}_{|\lambda} + b_{\lambda\mu}N^{\mu\lambda} + f^{3} = 0 \ , \qquad (3.4.19)$$

$$M^{\lambda\alpha}{}_{|\lambda} - Q^{\alpha} + m^{\alpha} = 0 \ , \qquad (3.4.20)$$

and from (3.4.17)

$$\varepsilon_{\alpha\beta}(N^{\beta\alpha} - b^{\beta}_{\lambda}M^{\lambda\alpha}) = 0 \ , \qquad (3.4.21)$$

which expresses the equilibrium condition of moments about the normal of the middle surface.

The analysis of Section 3.1 shows that six measures of strain are sufficient to describe the deformation of the middle surface. However, it is suggested by (3.4.18), (3.4.19) and (3.4.20) that ten stress measures are involved since $N^{\alpha\beta}$ and $M^{\alpha\beta}$ are not, in general, symmetric. These equations may be simplified by defining the following modified stress resultants

$$\tilde{M}^{\alpha\beta} = \frac{1}{2}(M^{\alpha\beta} + M^{\beta\alpha}), \qquad \tilde{N}^{\alpha\beta} = N^{\alpha\beta} + b^{\beta}_{\lambda}M^{\lambda\alpha}, \tag{3.4.22}$$

which are symmetric, the symmetry of $\tilde{N}^{\alpha\beta}$ follows from (3.4.21), and using (3.2.20) to eliminate the transverse shears the remaining equations of equilibrium now read

$$\left.\begin{aligned} &\tilde{N}^{\alpha\lambda}{}_{|\lambda} - b^{\alpha}_{\mu}{}_{|\lambda}\tilde{M}^{\mu\lambda} - 2b^{\alpha}_{\beta}\tilde{M}^{\beta\lambda}{}_{|\lambda} + r^{\alpha} = 0 , \\ &b_{\lambda\mu}\tilde{N}^{\lambda\mu} - b_{\omega\lambda}b^{\lambda}_{\mu}\tilde{M}^{\omega\mu} + \tilde{M}^{\lambda\mu}{}_{|\lambda\mu} + r^{3} = 0 . \end{aligned}\right\} \tag{3.4.25}$$

where $r^{\alpha} = f^{\alpha} - b^{\alpha}_{\lambda}m^{\lambda}$, $r^{3} = f^{3} + m^{\lambda}{}_{|\lambda}$.

It is later required to introduce a further definition for a modified stress resultant given by

$$\hat{N}^{\alpha\beta} = \tilde{N}^{\alpha\beta} - \frac{1}{2}\,(b^{\alpha}_{\lambda}\tilde{M}^{\lambda\beta} + b^{\beta}_{\lambda}\tilde{M}^{\lambda\alpha}) . \tag{3.4.24}$$

The equations of equilibrium written in terms of $\hat{N}^{\alpha\beta}$ and $\tilde{M}^{\alpha\beta}$ are

$$\left.\begin{aligned} &\hat{N}^{\beta\alpha}{}_{|\beta} - b^{\alpha}_{\lambda}\tilde{M}^{\beta\lambda} - \frac{1}{2}\,(b^{\alpha}_{\lambda}\tilde{M}^{\beta\lambda} - b^{\beta}_{\lambda}\tilde{M}^{\lambda\alpha})_{|\beta} + r^{\alpha} = 0 \\ &\tilde{M}^{\alpha\beta}{}_{|\alpha\beta} - b_{\alpha\beta}\hat{N}^{\alpha\beta} + r^{3} = 0 \end{aligned}\right\} \tag{3.4.25}$$

It is noted that since the above derivation of the equilibrium equations

starts from the three-dimensional equations for a volume element of a shell they do not involve any approximations.

3.5 Boundary conditions

By means of a direct calculation, see Niordson (1985), it is possible to show that the familiar three-dimensional internal work expression

$$\frac{1}{2}\int \sigma^{ij}\gamma_{ij}\, dV \tag{3.5.1}$$

reduces exactly to the following integral over the shell middle surface

$$\int_{\Omega} (\tilde{N}^{\alpha\beta}\gamma_{\alpha\beta} + \tilde{M}^{\alpha\beta}\tilde{\rho}_{\alpha\beta})\ \sqrt{a}\ d\xi^1 d\xi^2 \tag{3.5.2}$$

when the deformations are constrained by the Kirchhoff assumptions. This result is independent of the stress distribution throughout the shell.

The principal of virtual work may be written

$$\begin{aligned}\delta V = &\int_{\Omega} (\tilde{N}^{\alpha\beta}\delta\gamma_{\alpha\beta} + \tilde{M}^{\alpha\beta}\delta\tilde{\rho}_{\alpha\beta})\ \sqrt{a}\ d\xi^1 d\xi^2 \\ &- \int_{\Omega} \bar{f}^{i}\delta u_i\ \sqrt{a}\ d\xi^1 d\xi^2 \\ &- \int_{\Gamma_t} (\bar{N}^{\alpha}\delta u_{\alpha} + \bar{Q}\delta u_3 + \bar{M}^{\alpha}\delta\phi_{\alpha})\ d\tau \\ &= 0\end{aligned} \tag{3.5.3}$$

where the overbar notation indicates a prescribed value of applied traction in the domain Ω and on the part of the boundary curve Γ_t where tractions are imposed. Substituting into (3.5.3) using (3.2.16) and (3.2.23) and applying the divergence theorem gives a surface integral, from

which the equilibrium equations of (3.4.25) are recovered, and a contour integral along the edge of the middle surface

$$\int_\Gamma \left((\tilde{N}^{\beta\alpha} + 2b_\gamma^\alpha \tilde{M}^{\beta\gamma}) \nu_\beta \delta u_\alpha + \tilde{M}^{\beta\alpha} \nu_\beta \delta u_{3,\alpha} - \tilde{M}^{\beta\alpha}{}_{|\beta} \nu_\alpha \delta u_3 \right) d\tau \tag{3.5.4}$$

$$- \int_{\Gamma_t} \left(\bar{N}^\alpha \delta u_\alpha + \bar{Q} \delta u_3 + (\bar{M}_\nu \nu_\beta + \bar{M}_\tau \tau_\beta) a^{\alpha\beta} \delta\phi_\alpha \right) d\tau$$

where $\bar{M}_\nu$ and $\bar{M}_\tau$ are applied edge bending and twisting moments, and ν_α, τ_α are defined by (2.4.1) and (2.4.2). Using (2.4.6) the partial derivatives of δu_3 may be written

$$\delta u_{3,\alpha} = \nu_\alpha \frac{\partial \delta u_3}{\partial \nu} + \tau_\alpha \frac{\partial \delta u_3}{\partial \tau} , \tag{3.5.5}$$

so that a further integration by parts reduces the first term of (3.5.4) to

$$\int_\Gamma \left((\tilde{N}^{\beta\alpha} + 2b_\gamma^\alpha \tilde{M}^{\beta\gamma}) \nu_\beta \delta u_\alpha + \tilde{M}^{\beta\alpha} \nu_\beta \nu_\alpha \frac{\partial \delta u_3}{\partial \nu} \right.$$

$$\left. - [\tilde{M}^{\beta\alpha}{}_{|\beta} \nu_\alpha + \frac{\partial}{\partial \tau} (\tilde{M}^{\alpha\beta} \nu_\alpha \tau_\beta)] \delta u_3 \right) d\tau \tag{3.5.6}$$

$$+ \tilde{M}^{\alpha\beta} \nu_\alpha \tau_\beta \delta u_3 \Big|_+^- .$$

The boundary conditions follow by considering arbitrary variations of δu_i and $\partial(\delta u_3)/\partial \nu$ along the edge curve:

$$\left.
\begin{aligned}
T^\alpha &= (\tilde{N}^{\beta\alpha} + 2b_\lambda^\alpha \tilde{M}^{\beta\lambda}) \nu_\beta = \bar{N}^\alpha + a^{\lambda\beta} b_\lambda^\alpha (\bar{M}_\nu \nu_\beta + \bar{M}_\tau \tau_\beta) = \bar{T}^\alpha , \\
K_\nu &= \tilde{M}^{\alpha\beta}{}_{|\alpha} \nu_\beta + \frac{\partial}{\partial \tau} (\tilde{M}^{\alpha\beta} \nu_\alpha \tau_\beta) = \bar{Q} + \frac{\partial \bar{M}_\tau}{\partial \tau} = \bar{K}_\nu , \\
M_\nu &= \tilde{M}^{\alpha\beta} \nu_\alpha \nu_\beta = \bar{M}_\nu ,
\end{aligned}
\right\} \tag{3.5.7}$$

and at a corner point

$$M_\tau\Big|_+^- = \tilde{M}^{\alpha\beta}\nu_\alpha\tau_\beta\Big|_+^- = \bar{M}_\tau \ , \tag{3.5.8}$$

where T^α, K_ν, M_ν, M_τ are the effective membrane force, Kirchhoff shear force and normal and twisting bending moments at the middle surface boundary.

The equilibrium equations together with the above boundary conditions provide the means to formulate a well-posed mathematical problem. In principle there are two different lines that could be followed.

On the one hand, the displacements u_i can be selected as unknowns. The membrane strains and curvature changes may be expressed in terms of u. Next the constitutive equations may be used to give stress and moment resultants in terms of u_i and finally the equations of equilibrium yield three partial differential equations for the three unknowns. The equations are of second order in u_α and of fourth order in u_3. There are precisely four boundary conditions of either kinematic or static type. From (3.5.4) and (3.5.7) it is possible to prescribe

$$\left.\begin{aligned} &\text{either } T^\alpha \text{ or } u_\alpha \ , \\ &\text{and either } K_\nu \text{ or } u_3 \ , \\ &\text{and either } M_\nu \text{ or } \frac{\partial u_3}{\partial \nu} \ , \end{aligned}\right\} \tag{3.5.9}$$

at the boundary.

The second way to formulate a well-posed problem is to take the six strain measures as unknowns. Use of the constitutive relations and equilibrium equations gives partial differential equations for three of the unknowns. The equations of compatibility give another three differential equations enabling all six strain measures to be determined.

3.6 Love's strain energy expression

In an elastic shell the work done by the applied loads is stored in the shell as an internal energy, usually called the elastic strain energy. For the development of a first approximation shell theory a simple expression for the strain energy may be obtained on the basis of the following assumptions introduced by Koiter (1959, 1960):

- the geometry of the shell is such that the ratio of its thickness to the smallest principal radius of curvature is negligible compared with unity i.e. $t/R \ll 1$;
- the strains are small everywhere in the shell;
- the state of stress is approximately plane so that the effect of transverse normal stress may be neglected.

Further, it is assumed that the material of the shell is homogeneous and isotropic so that the strain energy per unit volume of the undeformed body may be represented by a quadratic function of the strain components according to Hooke's law.

The strain energy density of the undeformed shell may be written, see Green and Zerna (1954),

$$\Phi = \frac{1}{2}E^{ijkl}\gamma_{ij}\gamma_{kl} = \frac{1}{2}\sigma^{ij}\gamma_{ij} \qquad (3.6.1)$$

and, making use of the assumption of plane stress, this may be simplified to

$$\Phi = \frac{1}{2}E^{\alpha\beta\lambda\mu}\gamma_{\alpha\beta}\gamma_{\lambda\mu} \ , \qquad (3.6.2)$$

where E^{ijkl} is the contravariant tensor of elastic moduli, defined by

$$E^{ijkl} = \frac{E}{1 - \nu^2}\left[\nu g^{ij}g^{kl} + \frac{1 - \nu}{2}(g^{ik}g^{jl} + g^{il}g^{jk})\right] , \qquad (3.6.3)$$

where g^{ij} is the contravariant metric tensor in space, E is Young's modulus, and ν is Poisson's ratio. The relationship between the stresses σ^{ij} and the corresponding strains is

$$\sigma^{\alpha\beta} = E^{\alpha\beta\lambda\mu}\gamma_{\lambda\mu} , \qquad \sigma^{\alpha 3} = \sigma^{3\alpha} = \sigma^{33} = 0 . \qquad (3.6.4)$$

For the approximation of plane stress the transverse shear strains are zero, consistent with the Kirchhoff theory, so that the transverse normal strains may be written in terms of the strain in surfaces parallel to the middle surface according to

$$\gamma_{33} = -\frac{\nu}{1 - \nu}\gamma^{\lambda}_{\lambda} . \qquad (3.6.5)$$

The strain energy per unit area of the undeformed middle surface is obtained by multiplying (3.6.2) by the differential element of volume, see (2.2.38), and then integrating through the thickness of the shell

$$U = \int_{-h/2}^{h/2} \Phi \sqrt{a}\ [1 - 2\xi^3 H + (\xi^3)^2 K]\ d\xi^3 . \qquad (3.6.6)$$

Assuming the strain energy density Φ to be a smooth function of the Gaussian coordinates provides for the Taylor series expansion with respect to the coordinate ξ^3

$$\Phi(\xi^\alpha, \xi^3) = \Phi(\xi^\alpha, 0) + \xi^3 \Phi_{|\,|3}(\xi^\alpha, 0) + \ldots \qquad (3.6.7)$$

Recall that the shell is assumed to be composed of homogeneous material so that the covariant derivatives of the tensor of elastic moduli with respect to ξ^3 are all zero, this allows the above expression to be written

$$\Phi(\xi^{\alpha},\xi^{3}) = \frac{1}{2}\overset{\circ}{E}{}^{\alpha\beta\lambda\mu}\left[\overset{\circ}{\gamma}_{\alpha\beta} + \xi^{3}\overset{\circ}{\gamma}_{\alpha\beta||3} + \cdots\right]\left[\overset{\circ}{\gamma}_{\lambda\mu} + \xi^{3}\overset{\circ}{\gamma}_{\lambda\mu||3} + \cdots\right] . \quad (3.6.8)$$

Now substitute into (3.6.6) integrate with respect to ξ^3 and retaining only the first two terms gives

$$U = \frac{t}{2}\overset{\circ}{E}{}^{\alpha\beta\lambda\mu}\overset{\circ}{\gamma}_{\alpha\beta}\overset{\circ}{\gamma}_{\lambda\mu} + \frac{t^3}{24}\overset{\circ}{E}{}^{\alpha\beta\lambda\mu}\overset{\circ}{\gamma}_{\alpha\beta||3}\overset{\circ}{\gamma}_{\lambda\mu||3} , \quad (3.6.9)$$

which is Love's approximate strain energy expression. The first term represents the extensional strain energy U_γ due to the middle surface strains $\overset{\circ}{\gamma}_{\alpha\beta}$, and the second term represents the bending strain energy U_K due to the change of curvature of the middle surface.

Let γ denote the absolute value of the largest extension of the middle surface, K the largest physical change of curvature and L the smallest 'wavelength of the deformation pattern' on the middle surface so that

$$\left|\frac{d\gamma}{d\sigma}\right| = O\left(\frac{\gamma}{L}\right), \qquad \left|\frac{dK}{d\sigma}\right| = O\left(\frac{K}{L}\right) , \quad (3.6.10)$$

where $d\sigma$ is the element of arc on the middle surface. Koiter (1959, 1960) shows that the relative error in neglecting the higher order terms of (3.6.8) does not exceed the order of magnitude

$$\frac{t}{R} , \qquad \left(\frac{t}{L}\right)^2 . \quad (3.6.11)$$

In other words, Love's strain energy expression is justified as a consistent first approximation on the basic assumption of plane stress, and has an accuracy limited by the order of magnitude estimates given in (3.6.11).

Koiter's (1970) arguments show further that the transverse shear stresses obtained from equilibrium conditions are in general of order t/L times the bending stresses and their omission from the strain energy

implies a relative error of order $(t/L)^2$. The transverse normal stress is, in general, of order t/R or $(t/L)^2$ times the direct or bending stresses so omission of its contribution in the strain energy involves relative errors of the same order of magnitude.

This fundamental result has many important consequences in classical theory. Of importance for practical applications of the theory is the fact that it is possible to add to the expressions for the physical components of the changes of curvature terms of the type γ/R multiplied by a non-dimensional factor of order unity. This allows for possible simplification of the tensor of change of curvature by addition of suitable terms of this type. In particular, mention is made of one more equivalent definition for the curvature change tensor, see Koiter (1966),

$$\rho^{*}_{\alpha\beta} = \sqrt{\frac{\bar{a}}{a}}\, \bar{b}_{\alpha\beta} - b_{\alpha\beta} \,. \qquad (3.6.12)$$

3.7 The static-geometric analogy

The literature on the linear theory of shells refers to an interesting and useful analogy between the homogeneous equilibrium equations in terms of stress and moment resultants and the compatibility conditions in terms of membrane and bending strains. This is the static-geometric analogy of Gol'denveizer (1961) and Lurie (1961). Its importance lies in the fact that it leads in a natural way to the introduction of stress-functions.

The exact correspondence between the static and kinematic equations is, however, exhibited only when a special choice is made from among the alternative but equivalent forms of the stress resultant tensor and curvature change tensor. The detailed study of Budiansky and Sanders (1961) shows that a static-geometric analogy can be constructed in terms of the tensors $\hat{N}^{\alpha\beta}$, $\tilde{M}^{\alpha\beta}$, $\gamma_{\alpha\beta}$ and $\rho_{\alpha\beta}$.

It is convenient to define the new quantities

$$\hat{\gamma}^{\alpha\beta} = -\varepsilon^{\alpha\lambda}\varepsilon^{\beta\mu}\gamma_{\lambda\mu} , \qquad \hat{\rho}^{\alpha\beta} = -\varepsilon^{\alpha\lambda}\varepsilon^{\beta\mu}\rho_{\lambda\mu} . \tag{3.7.1}$$

Inserting these definitions into the equations of compatibility, see (3.3.1), gives, after some algebra,

$$\hat{\rho}^{\lambda\alpha}{}_{|\lambda} + b_{\mu}^{\alpha}\hat{\gamma}^{\lambda\mu}{}_{|\lambda} + \frac{1}{2}(b_{\mu}^{\alpha}\hat{\gamma}^{\lambda\mu} - b_{\mu}^{\lambda}\hat{\gamma}^{\alpha\mu})_{|\lambda} = 0 \tag{3.7.2}$$

$$\hat{\gamma}^{\alpha\beta}{}_{|\alpha\beta} + b_{\alpha\beta}\hat{\rho}^{\alpha\beta} = 0 \tag{3.7.3}$$

These are precisely of the same form as the equations of equilibrium given in (3.4.25) for the homogeneous case $r^i = 0$.

The static-geometric analogy has the following useful consequence. Since the equations of compatibility are identically satisfied whenever the strain tensor $\gamma_{\alpha\beta}$ and curvature change tensor $\rho_{\alpha\beta}$ are derived from a set of arbitrarily selected displacements u_α and u_3 , the stress resultant tensor and stress couple resultant tensor must be derivable from a vector and a scalar function so that the homogeneous equations of equilibrium are satisfied.

The explicit expressions for $\gamma_{\alpha\beta}$ and $\rho_{\alpha\beta}$ in terms of the middle surface displacements are given by (3.2.16) and (3.2.24) so that

$$\begin{aligned}\hat{\rho}^{\alpha\beta} = -\varepsilon^{\alpha\lambda}\varepsilon^{\beta\mu}[&u^3{}_{|\lambda\mu} + \frac{1}{4}\, b_{\lambda}^{\omega}(3u_{\omega|\mu} - u_{\mu|\omega}) \\ &+ \frac{1}{4}\, b_{\mu}^{\omega}(3u_{\mu|\omega} - u_{\omega|\mu}) + u^{\omega}b_{\lambda\mu|\omega}]\end{aligned} \tag{3.7.4}$$

$$\hat{\gamma}^{\alpha\beta} = \varepsilon^{\alpha\lambda}\varepsilon^{\beta\mu}[\frac{1}{2}\,(u_{\lambda|\mu} + u_{\mu|\lambda}) - b_{\lambda\mu}u^3] \tag{3.7.5}$$

Now let $\chi_\alpha(\xi^\alpha)$ be an arbitrary vector function and χ_3 be an arbitrary scalar function. If the stress resultant tensor and couple resultant tensor are defined by

$$\hat{N}^{\alpha\beta} = -\varepsilon^{\alpha\lambda}\varepsilon^{\beta\mu}[\chi_{3|\lambda\mu} + \tfrac{1}{4}b_{\lambda}^{\omega}(3\chi_{\omega|\mu} - \chi_{\mu|\omega})$$

$$+ \tfrac{1}{4}b_{\mu}^{\omega}(3\chi_{\mu|\omega} - \chi_{\omega|\mu}) + \chi^{\omega}b_{\lambda\mu|\omega}] \qquad (3.7.6)$$

$$\tilde{M}^{\alpha\beta} = \varepsilon^{\alpha\lambda}\varepsilon^{\beta\mu}[\tfrac{1}{2}(\chi_{\lambda|\mu} + \chi_{\mu|\lambda}) - b_{\lambda\mu}\chi_3] \qquad (3.7.7)$$

then these static measures will satisfy the equations of equilibrium irrespective of the choice of χ_α and χ_3 .

The solution of a real shell problem in terms of stress functions proceeds by using (3.7.6) and (3.7.7) to find the stress resultant tensor and stress couple resultant. Then the constitutive relations and the compatibility conditions are used to obtain a system of three partial differential equations for the three unknown functions χ_α and χ_3. In finite element analysis, however, it is necessary to know the displacements and rotations of the middle surface so that formidable difficulties are encountered with the present means of solution. It is quite impracticable, except for surfaces of simple geometry, to integrate strain-displacement relations when the strains are obtained from stress functions.

3.8 The membrane state

For shells the membrane state is an approximation that has been found useful in many cases of practical interest. Putting $M^{\alpha\beta} \equiv 0$ in (3.4.25) gives the following system,

$$\left.\begin{aligned} N^{\alpha\beta}{}_{|\alpha} + f^{\alpha} = 0 \ , \\ -b_{\alpha\beta}N^{\alpha\beta} + f^{3} = 0 \ , \end{aligned}\right\} \qquad (3.8.1)$$

which consists of three equations for the three unknown components $N^{\alpha\beta}$ which are consequently statically determined.

In cases of practical interest the justification of the use of these equations can only be established a posteriori by the following procedure:

(1) $N^{\alpha\beta}$ are determined from (3.8.1).

(2) The strain tensor $\gamma_{\alpha\beta}$ is found from Hooke's law.

(3) The displacements u_i are found by integrating (3.2.16).

(4) $\rho_{\alpha\beta}$ is determined from (3.2.24) and $M^{\alpha\beta}$ from Hooke's law.

(5) The terms neglected from the equilibrium equations are calculated and their contribution to the order of magnitude estimates given by (3.6.11).

3.9 Shallow shell theory

In some applications it is possible to define a plane which is nearly parallel to the middle surface. If this is used as a reference plane and two components of the position vector are chosen to be parallel to the plane and the third perpendicular, then the height of the middle surface above the plane is given by

$$x^3 = x^3(x^1,x^2) \ . \tag{3.9.1}$$

The shallow shell theory makes two simplifying hypotheses. The first is a geometric assumption,

$$x^3{}_{,\alpha} << 1 \ , \tag{3.9.2}$$

i.e. the surface slopes with respect to the reference plane are negligible.

The second is a kinematic approximation which assumes that the in-plane displacements are small in relation to the normal component. Thus, the rotations become

$$\phi_\alpha = u_{3,\alpha}, \tag{3.9.3}$$

and the membrane strain and curvature change tensors are given by

$$\gamma_{\alpha\beta} = \frac{1}{2}(u_{\alpha,\beta} + u_{\beta,\alpha}) - x^3{}_{,\alpha\beta}u_3 \quad , \tag{3.9.4}$$

$$\rho_{\alpha\beta} = u_{3,\alpha\beta} \, . \tag{3.9.5}$$

CHAPTER 4

PATCH TEST SOLUTIONS FOR SHELL ELEMENTS

4.1 Introduction

Confidence in the use of the finite element method in shell problems should rest upon satisfaction of certain sufficiency tests which are derived as solutions to the classical theory. However, a major shortcoming which has impaired the development of shell elements is that they are not always tested against a set of problems which fully examine the capabilities required in a really good shell element. Study of the governing equations considered in Chapter 3 shows that there are four characteristic solution types corresponding to rigid body, inextensional bending, membrane and edge effects. Thus, in patch test evaluation of a candidate shell element the philosophy centres on the requirement that each of these four effects must be properly represented and able to be recovered by the finite element model to within the accuracy afforded by first approximation theory. Inadequacies of a candidate shell element in this spectrum of attributes must be seen as a severe handicap to its use in solving practical shell problems.

It is widely accepted that confidence is secure in the validation of elements for flat plate problems but it is hardly the case with respect to curved shells. A particular handicap is that the well-known patch tests requiring recovery of rigid body modes and a set of three linearly independent constant membrane strains and/or three linearly independent constant curvature changes, see Zienkiewicz (1973), are no longer available. Instead resort has to be made to membrane strain and curvature changes which are only approximately constant to within the accuracy

afforded by shell theory, see Morley (1972) and Morley and Morris (1978). To compound this difficulty a problem exists when testing and using shell elements with respect to the widely differing energy levels of membrane and bending. Because shells are much stiffer in membrane action than in bending, the stiffness matrix will have a high condition number which may lead to numerical problems of ill-conditioning. Rigid body modes contribute zero strain energy while the membrane/bending energies differ by a large factor of the order $(R/t)^2$. Of course, the singularities due to the zero energy rigid body movements may be removed by prescribing the rigid body hold but there is no corresponding control available to deal with the low energy contribution from bending actions. Note that the static-geometric analogy shows that a similar ill-conditioning of the stiffness matrix is to be expected in equilibrium elements but with a reversal of the roles of membrane and bending modes. Studies of some basic computational difficulties of numerical stability and the condition number of stiffness matrices in shell problems are given in the work of Fried (1971, 1975).

Bearing in mind the above difficulties it is not surprising to find that several alternative approaches have been proposed to the direct use of deep shell theory in developing shell finite elements. The following briefly considers some of the many contributions which endeavour to obtain numerical solutions to the shell problem using the finite element method.

There are four options that have emerged in shell element formulation:

- a flat element approximating the actual shell curvature and formulated using plate theory;
- a curved element reproducing the actual shell curvature and formulated by shell theory;
- a curved element approximating the actual shell curvature and formulated by shell theory;
- a solid or degenerated solid element.

The first option is the earliest and simplest type of finite element used in solving shell problems. The actual curved middle surface is approximated by a faceted assembly of flat elements. Because the element is flat there is no coupling between the membrane stiffness and bending stiffness at element level, this occurs only on assembly of the individual element matrices. Thus it is possible to adopt a standard plane stress element to represent the membrane stiffness of the shell together with a standard plate bending element to represent its bending stiffness.

Although flat rectangular and quadrilateral elements are restricted in their use (because all four nodes should be in the same plane) these were the first successful shell elements to be programmed and were used in arch dam design and for the analysis of cylindrical shell roofs, see Zienkiewicz and Cheung (1965) and Zienkiewicz (1965).

It is clear that if the geometry of a doubly curved shell is to be approximated by flat elements then it is only triangular elements that are really acceptable. The two earliest triangular elements are due to Zienkiewicz et al (1968) and Clough and Johnson (1968). Both groups of authors employ the constant strain triangle for membrane stresses together with their own plate bending elements, see Bazeley et al (1965) and Clough and Tocher (1965). Use of the constant moment element in shell analysis is reported by Herrmann and Campbell (1967) and by Dawe (1972).

The advantage of employing an assembly of flat elements to represent a shell structure lies primarily in their simplicity and ease of formulation. In addition, they easily handle rigid body movements without incurring any error. For practical purposes the flat element approximation permits an easy coupling with edge and rib members, a facility sometimes not present in curved element formulations. On the other hand it must be borne in mind that because of the geometrical approximation of the curved shell considerable errors are likely to be incurred for coarse meshes. Another difficulty is that most shell elements have just two rotational degrees of freedom per node in the local element coordinate system. The in-plane or drilling rotation is missing, see Allman (1988a, 1988b, 1988c). This can

result in a singularity of the stiffness matrix on transformation to the global coordinate system if the elements meeting at a node are coplanar. It is also to be noted that due to the different orders of polynomials used to describe the element displacement fields in plane stress and plate bending elements, the displacements will not be compatible along element edges as adjacent elements are not, in general, coplanar.

In the case of curved elements the complexity of the actual shell geometry and the use of shell theory can lead to very complex formulations with consequent high computational costs. Major difficulties are encountered in the formulation of these elements as a result of inadequacies in representing rigid body modes and ineffective representation of the coupling between membrane and bending responses at element level. Aspects of the representation of rigid body movement in curved shell finite elements has been considered by many authors, including Ashwell and Sabir (1971), Mebane and Stricklin (1971), Fonder and Clough (1973), Fried (1975), Morley (1972) and Dawe (1974). The basic problem is that if the displacement components are chosen to be those tangential and normal to the element middle surface then the rigid body movement of the element cannot be exactly represented by the usual polynomial shape functions since they are properly represented by transcendental functions of the surface coordinates. The term 'membrane locking' is coined by Stolarski and Belytschko (1982, 1983) to describe the second problem. They show that it is derived from an inadequate representation of inextensional deformations. Due to the curvature of the element a bending deformation is accompanied by stretching of its middle surface and so membrane energy is generated, effectively increasing the bending stiffness, and this can cause a bending dominated response to be replaced by a spurious membrane dominated response.

One of the first curved elements is due to Grafton and Strome (1963). They describe an element which is a simple conical frustum intended for use in analysing pressure vessels under axisymmetrical loading. The

displacements of the shell are approximated using the radial and axial components and the rotation at each nodal point.

Olsen and Lindberg (1968) formulate a stiffness matrix for a four noded cylindrical shell element. An incomplete quartic (12 term) polynomial is used to describe the radial displacement, while the in-plane displacements are described by an incomplete cubic (9 terms). The element connectors at each node are the displacement values together with first derivatives giving a total of 36 degrees of freedom. By finding eigenvalues of free vibration of the unconstrained stiffness matrix the authors found that only the rigid body translations in the circumferential and longitudinal directions are represented exactly, the remaining modes are represented only approximately.

Bogner et al (1967) construct a cylindrical element in curvilinear coordinates. This element employs a sixteen degree of freedom bicubic Hermite polynomial for each of the displacement components resulting in a 48x48 stiffness matrix. Cantin and Clough (1968) report on a related element, which uses the same bicubic representation of the radial displacement but employs bilinear polynomials for the in-plane displacements. It has 6 degrees of freedom at each node, function values of each displacement, together with first derivatives and mixed second derivative of the radial displacement, giving a 24x24 stiffness matrix. Cantin and Clough observe that the polynomial shape functions employed to represent the element displacements cannot reproduce the rigid body modes of the curved element. In order to correct this they suggest that trigonometric functions be included in the displacement representation. Displacement compatibility is satisfied only at nodal points. A simplified form of Cantin and Clough's element, which reduces the size of the element stiffness matrix to 20x20, is given by Sabir and Lock (1972).

A doubly curved shell element based on shallow shell theory is given by Connor and Brebbia (1967). The in-plane displacements are represented by bilinear polynomials whereas the normal displacement is represented by the same twelve term polynomial used by Olsen and Lindberg (1968). The

displacements are compatible along the element boundaries but compatibility of normal displacement slope is not satisfied. The displacement expansions are, in general, unable to represent all the rigid body movements.

Henshell et al (1971) construct a cylindrical hybrid shell element from the principal of minimum complementary energy by assuming a fourteen term optimum stress function within the element. Bilinear polynomials are used for the in-plane displacements and a version of the Birkhoff-Garabedian (1960) polynomial, modified so as to include rigid body modes, is used for the normal displacement.

As in flat plate analysis, both single field and subdivided approaches have been used in the construction of curved triangular elements.

The displacement field proposed by Bazeley et al (1965) for flat plates is adopted by Strickland and Loden (1968) in a formulation of a doubly curved triangular shell element using shallow shell theory. This field, which describes the radial displacements, is accompanied by linear polynomials for the tangential displacements.

Bonnes et al (1968) subdivided a curved triangular element into subregions. Applying Reissner's (1960) shallow shell theory, the radial and tangential displacement fields are described by cubic polynomials in each subregion. The resulting formulation has 36 degrees of freedom per element, 9 degrees of freedom at each vertex, the displacement components and the two first derivatives of each component, and three degrees of freedom at the midside positions, the derivatives of displacements in the outwards normal direction. Neither interelement compatibility nor rigid body movement requirements are met.

A similar approach is taken by Sander and Idelsohn (1982) who derive a family of curved triangular and quadrilateral elements based on deep shell theory. The elements are subdivided into three or four regions in each of which the tangential displacements are represented by linear, quadratic or cubic polynomials while the normal displacement in each case is taken as a cubic polynomial.

Several authors have constructed elements which provide for strict interelement compatibility of displacement fields and exact representation of rigid body modes. These elements are embedded in deep shell theory and employ high order polynomials in their formulation. The SHEBA element of Argyris and Scharpf (1968), the element of Dupuis and Goël (1970) and the element of Dawe (1975) are examples of such refined elements. The SHEBA element employs an isoparametric quintic polynomial representation for all the displacement components giving an element with 63 degrees of freedom comprising the displacement with first and second derivative at each vertex together with normal derivatives at the midside nodes. Cartesian displacement connectors are used to construct the stiffness matrix so that the element is able to exactly represent rigid body modes. The work of Dupuis and Goël is based on a shell theory written in terms of a Cartesian coordinate system where the equations are expressed in relation to the height of the middle surface above a reference plane. The displacement patterns employed are high order rational or quintic polynomials giving rise to elements with 27 or 56 degrees of freedom. Dawe (1975) develops a conforming triangular element using a constrained quintic polynomial to represent each displacement component. It has the same vertex connectors as the SHEBA element but the normal derivative is constrained to be of cubic variation so that the element has a 54 degrees of freedom.

An element related to that of Dawe, formulated using shallow shell theory, is given in the work of Cowper et al (1968, 1970). This also uses a constrained quintic polynomial to represent the normal displacement component but employs cubics to describe the in-plane displacements giving a total of 36 degrees of freedom.

The fact that second order derivatives are used by such elements leads to difficulties in taking account of the boundary conditions and to difficulties where there are abrupt changes of curvature. Moreover, analytical functions describing the middle surface geometry are necessary. Consequently, this type of element is useful only in the hands of an expert if they are to be used for application to general shell problems, and

therefore their range of application within a commercial finite element package is rather limited.

The compatibility conditions required by the principle of minimum potential potential energy demand continuity of the normal displacement slope across interelement boundaries for a shell element based on Kirchhoff theory. Difficulties in forming a fully conforming Kirchhoff theory shell element with simple connectors have prompted the development of elements based on theories which relax the Kirchhoff assumptions.

In one approach the displacements of the middle surface and rotations of the normals are each independently assumed. Melosh (1966) employed this for plate bending problems and Utku (1967) applied it to shallow shell elements. However, all of these elements inherit problems of excessive shear stiffness for coarse meshes and slow convergence.

To overcome such problems of an otherwise attractive approach, the imposition of the Kirchhoff hypothesis at a discrete number of points in the element was proposed and used by Wempner et al (1968). This scheme has become known as 'discrete Kirchhoff theory' (DKT). Several examples of application of this approach appear in the literature. Wempner et al describe a rectangular shell element. Although the formulation is for general shells the applications were limited to flat plates and cylindrical shells. Dhatt (1970) gives a triangular shell element based on shallow shell theory. All displacement components are described by cubic polynomials giving 27 degrees of freedom. Batoz and Dhatt (1972) present a related element which employs linear polynomials for the in-plane displacements which are coupled with the transverse displacements in order to satisfy the rigid body modes for shallow shells. Murthy and Gallagher (1986) present a curved shell element with 27 degrees of freedom, 9 at each vertex. The degrees of freedom are the tangential and normal displacement components and their first derivatives with respect to the curvilinear coordinates of the middle surface. The strain energy density is calculated using the linear shear theory described by Wempner et al (1968). The strain displacement relations are initially defined in terms of

displacements and rotations referred to local coordinates on the middle surface and are subsequently transformed to global coordinates enabling an isoparametric representation of the middle surface displacements and exact recovery of rigid body movements.

The fourth alternative route to shell element construction was introduced by Ahmad et al (1968), based on the isoparametric formulation of three-dimensional solid elements. At first sight it seems that the use of solid elements could be used directly for shell problems by reducing their dimension in the direction of the shell thickness and imposing kinematic and stress constraints consistent with Kirchhoff theory. However, unless special care is taken the performance of this type of element deteriorates rapidly as the shell becomes thinner. In particular such shell models tend to be overstiff due to shear and membrane locking, see Parisch (1979), Hughes and Liu (1981), Stolarski and Belytschko (1982, 1983). These undesirable effects reflect the difficulty solid elements have in representing zero in-plane and transverse shear strain states without disrupting bending behaviour. These problems have been alleviated in many cases by use of reduced or selective integration schemes, see Pawsey and Clough (1971) and Zienkiewicz et al (1971). Such effects are particularly prevalent when coarse meshes are used to model high stress gradients or when highly distorted elements are present in the mesh. However, reduced integration does not guarantee a problem free element. An immediate problem is that it reduces the rank of the stiffness matrix and so may result in the development of spurious kinematic modes, see Hughes et al (1977), Belytschko et al (1984, 1985). Also reduced integration is accompanied by a deterioration of membrane-bending coupling which is a central characteristic advanced in favour of these elements.

Two such elements which have come to the fore in recent years are the Semiloof element of Irons (1976) and the QUAD4 element of MacNeal (1978). The first element is similar to the element of Ahmad et al but provides for only one normal rotation at the so-called Loof nodes at each side, thus resulting in 32 degrees of freedom for the element. The discrete Kirchhoff

hypothesis is introduced at the Loof nodes and a reduced integration technique is applied. The second element is a 4-node quadrilateral which is basically a thick shell element where the shear stiffness is improved by applying a reduced integration technique and secondly by adapting the shear modulus according to the actual shell thickness.

4.2 Inextensional bending solutions

Fundamental to any candidate finite element for shell analysis is the need to provide a facility to adequately model the deformations consequent upon bending action. The consequences of any shortcoming in this respect are severe when finite elements are used to analyse a shell which undergoes inextensional bending because it is so easy for even a small membrane strain to cause the membrane energy to overshadow the bending energy. This underlines the difficulty that the displacements of inextensional bending need to be accurate solutions to the governing equations. Indeed it is only rarely that attempts have been made to solve these equations other than for shells with a simple circular cylindrical or hemispherical middle surface, see e.g. Krauss (1967), Flügge (1973). This lack of access to accurate solutions to more general shell shapes has proved a great handicap in finite element assessment.

In determining the displacement field corresponding to an inextensional bending action it is necessary to integrate three homogeneous partial differential equations which have, in general, non-constant coefficients. Emphasis in the classical theory of shells is concerned with the derivation of relations and governing equations in terms of displacement components which are tangential and normal to the middle surface. However, with the finite element method in mind, the solutions given in the sequel are formulated in terms of displacement components referred to a fixed orthogonal Cartesian coordinate system. The middle surface geometry is defined by quadratic or cubic polynomials whose

coefficients are determined by specifying the orthogonal Cartesian components at points on the middle surface and/or at the boundary. This specification allows easy control of Gaussian curvature and depth of shell and so provides a very wide spectrum of shell geometry.

The membrane strain tensor is given by

$$\gamma_{\alpha\beta} = \frac{1}{2}(U^{\alpha}{}_{,\beta} + U^{\beta}{}_{,\alpha} + x^{3}{}_{,\alpha}U^{3}{}_{,\beta} + U^{3}{}_{,\alpha}x^{3}{}_{,\beta}) \ . \qquad (4.2.1)$$

The rotation vector ϕ_{α} of the normal in the directions x^{α} on the deformed middle surface is defined by

$$\phi_{\alpha} = -\frac{1}{\sqrt{a}}(U^{3}{}_{,\alpha} - x^{3}{}_{,\lambda}U^{\lambda}{}_{,\alpha}) \ , \qquad (4.2.2)$$

and the rotation about the normal of the undeformed surface is given by

$$\phi = \frac{1}{2\sqrt{a}}(U^{1}{}_{,2} - U^{2}{}_{,1} + x^{3}{}_{,1}U^{3}{}_{,2} - x^{3}{}_{,2}U^{3}{}_{,1}) \ . \qquad (4.2.3)$$

Advantage is taken of the arguments of Koiter (1966) concerning the equivalence of definition of the curvature change tensor. In particular the modified definition (3.6.12) provides considerable simplification and provides, under the assumption of small strains and rotations

$$\rho^{*}_{\alpha\beta} = -\frac{1}{\sqrt{a}}(U^{3}{}_{,\alpha\beta} - x^{3}{}_{,1}U^{1}{}_{,\alpha\beta} - x^{3}{}_{,2}U^{2}{}_{,\alpha\beta} + x^{3}{}_{,\alpha\beta}U^{1}{}_{,1} + x^{3}{}_{,\alpha\beta}U^{2}{}_{,2}) \ . \qquad (4.2.4)$$

Note that when the displacements of an arbitrary rigid body movement

$$\left.\begin{aligned} U^{1} &= \alpha_{1} + \alpha_{2}x^{2} - \alpha_{5}x^{3} \ , \\ U^{2} &= \alpha_{3} - \alpha_{2}x^{1} - \alpha_{6}x^{3} \ , \\ U^{3} &= \alpha_{4} + \alpha_{5}x^{1} + \alpha_{6}x^{2} \ , \end{aligned}\right\} \qquad (4.2.5)$$

where $\alpha_1,\ldots,\alpha_6$ are constants, are substituted into (4.2.1) and (4.2.4) then the components of the membrane strain and curvature change tensors are zero as required.

Consideration is now given to the inextensional bending of surfaces with explicit polynomial representation, see Morley (1982, 1983a, 1984) and Mould (1989),

$$x^3 = \sum_{i=1}^{p+1} \sum_{j=1}^{i} a_{k(i,j)} (x^1)^{i-j} (x^2)^{j-1} \qquad (4.2.6)$$

where the degree of polynomial is $p \geq 2$, and $a_{k(i,j)}$ are constants with

$$k(i,j) = \tfrac{1}{2}i(i-1) + j \ . \qquad (4.2.7)$$

The components of the linearised membrane strain tensor, see (3.2.16) and (4.2.1), satisfy the first of the differential equations (3.3.1) of compatibility

$$\varepsilon^{\alpha\lambda}\varepsilon^{\beta\mu}\gamma_{\alpha\beta,\lambda\mu} = -\varepsilon^{\alpha\lambda}\varepsilon^{\beta\mu}x^3{}_{,\alpha\beta}U^3{}_{,\lambda\mu} \ . \qquad (4.2.8)$$

The differential operator implicit in this equation occurs frequently in plate and shell theory and is known as Pucher's (1934, 1938) operator. For inextensional bending solutions the strain components

$$\gamma_{\alpha\beta} = 0 \ . \qquad (4.2.9)$$

Evidently, solutions for U^3 of the homogeneous equations

$$\varepsilon^{\alpha\lambda}\varepsilon^{\beta\mu}x^3{}_{,\alpha\beta}U^3{}_{,\lambda\mu} = 0 \qquad (4.2.10)$$

determine inextensional bending deformations of the shell surface defined by (4.2.6). Integration of (4.2.10) determines the remaining displacement components as

$$\left.\begin{aligned} U^1 &= -\int_0^{x^1} x^3{}_{,1}U^3{}_{,1}\,dx^1 + F(x^2)\ , \\ U^2 &= -\int_0^{x^2} x^3{}_{,2}U^3{}_{,2}\,dx^2 + G(x^1)\ , \end{aligned}\right\} \qquad (4.2.11)$$

where the functions $F(x^2)$ and $G(x^1)$ are obtained from the relations

$$\left.\begin{aligned} F_{,2} &= \Big[2x^3{}_{,12}U^3 - \frac{\partial}{\partial x^1}\int_0^{x^2} x^3{}_{,22}U^3\,dx^2 - (x^3{}_{,1}U^3)_{,2} - G_{,1} \\ &\qquad - \frac{\partial}{\partial x^1}(x^3{}_{,2}U^3)\Big|_{x^2=0}\Big]\Big|_{x^1=0} \\ G_{,1} &= \Big[2x^3{}_{,12}U^3 - \frac{\partial}{\partial x^2}\int_0^{x^1} x^3{}_{,11}U^3\,dx^1 - (x^3{}_{,2}U^3)_{,1} - F_{,2} \\ &\qquad - \frac{\partial}{\partial x^2}(x^3{}_{,1}U^3)\Big|_{x^1=0}\Big]\Big|_{x^2=0} \end{aligned}\right\} \qquad (4.2.12)$$

which are found by considering the equation $\gamma_{12} = 0$ along the coordinate lines $x^1 = 0$ and $x^2 = 0$.

With the finite element method in mind solutions of (4.2.10) are now sought in the form of a polynomial series

$$U^3 = \beta_0 + \beta_1 x^1 + \beta_2 x^2 + \sum_{i=3}^{q+1}\sum_{j=1}^{i} c_{1(i,j)}(x^1)^{i-j}(x^2)^{j-1}\ , \qquad (4.2.13)$$

where the degree of the polynommial $q \geq 2$ and where β_0, β_1, β_2 and $c_{1(i,j)}$ are constants with

$$1(i,j) = \tfrac{1}{2}i(i-1) + j - 3\ . \qquad (4.2.14)$$

Examine, first, the role of the linear terms of (4.2.13). It is easily seen that they make no contribution to (4.2.10) and their substitution, together with (4.2.6), into (4.2.11) and (4.2.12) yields

$$U^1 = -\beta_1\left[a_2x^1 + a_4(x^1)^2 + a_5x^1x^2 + a_7(x^1)^3 + a_8(x^1)^2x^2 + a_9x^1(x^2)^2\right] + F(x^2) \tag{4.2.15}$$

$$U^2 = -\beta_2\left[a_3x^1 + a_5x^1x^2 + a_6(x^2)^2 + a_8(x^1)^2x^2 + a_9x^1(x^2)^2 + a_{10}(x^2)^3\right] + G(x^1)$$

and

$$F(x^2) = -(a_3\beta_1 + a_2\beta_2 + G_{,1}\big|_{x^1=0})x^2 - \beta_1a_6(x^2)^2 - \beta_1a_{10}(x^2)^3 + C_F \tag{4.2.16}$$

$$G(x^1) = -(a_3\beta_1 + a_2\beta_2 + F_{,2}\big|_{x^2=0})x^1 - \beta_2a_4(x^1)^2 - \beta_2a_7(x^2)^3 + C_G$$

where $G_{,1}\big|_{x^1=0}$, $F_{,2}\big|_{x^2=0}$, C_F and C_G are unknown constants. Recalling (4.2.5) and using (4.2.6) to substitute for x^3 shows that (4.2.15) and (4.2.16) are, in fact, the explicit expressions for the U^1 and U^2 displacement components of an arbitrary rigid body movement, and provide the following correspondence between constants:

$$\left.\begin{aligned} F_{,2}\big|_{x^2=0} &= -\alpha_2 - \alpha_6a_2\,, & \beta_0 &= \alpha_4\,,\\ G_{,1}\big|_{x^1=0} &= \alpha_2 - \alpha_5a_3\,, & \beta_1 &= \alpha_5\,,\\ C_F &= \alpha_1 - \alpha_5a_3\,,\\ C_G &= \alpha_3 - \alpha_6a_1\,. \end{aligned}\right\} \tag{4.2.17}$$

Now consider the determination of the remaining coefficients of (4.2.13) i.e. those corresponding to the quadratic and higher order polynomial terms. Substitution of (4.2.6) and (4.2.13) into (4.2.10) gives

$$\underline{p}^T[A]\underline{c} = 0\,, \tag{4.2.18}$$

where

$$\underline{P}^T = [1,\ x^1,\ x^2,\ldots,\ (x)^{p-1}] \qquad (4.2.19)$$

is a vector of polynomial terms,

$$\underline{c}^T = [c_1,\ c_2,\ldots,\ c_{½(q+4)(q-1)}] \qquad (4.2.20)$$

and the elements of the matrix [A] are linear combinations of the constants $a_{k(i,j)}$. If (4.2.18) is to hold for a general point on the shell middle surface then

$$[A]\underline{c} = \underline{0}\ . \qquad (4.2.21)$$

This is a homogeneous system of $½(p + q - 3)(p + q - 2)$ equations involving $½(q + 4)(q - 1)$ unknowns. Thus, existence of a vector $\underline{c}$ satisfying (4.2.21) generally requires

$$(q + 4)(q - 1) > (q + p - 3)(q + p - 2)\ , \qquad (4.2.22)$$

from which it is concluded that, in general, the highest order polynomial representation of the middle surface which admits exact inextensional bending solutions of the form described by (4.2.11)-(4.2.13) has $p = 3$. The Fortran computer program described by Mould (1989) considers the case $p = 3$ i.e. a cubic parametric representation. The coefficients $c_{1(i,j)}$ of (4.2.13) are obtained by solving the eigenvalue problem

$$[A]^T[A]\underline{c} = \underline{0}\ . \qquad (4.2.23)$$

The elements of an eigenvector corresponding to a zero eigenvalue determine the required constants.

4.3 Edge effect problem

Flügge's (1973) equations are widely accepted as the standard of comparison for circular cylindrical shells but, keeping within the context of classical first approximation theory, the following makes use of the much simpler but equally accurate Morley-Koiter equations, see Koiter (1968), Morley (1959).

Let the middle surface be described by coordinates of principal curvature (ξ^1, ξ^2) where ξ^1 is the arc-length along a generator and ξ^2 the arc-length in the circumferential direction, perpendicular to the generator. The parametric equations of the middle surface are

$$x^1 = \xi^1 , \qquad x^2 = R \sin \frac{\xi^2}{R} , \qquad x^3 = R \cos \frac{\xi^2}{R} . \tag{4.3.1}$$

The components of the metric tensor are

$$a_{11} = a_{22} = 1 , \qquad a_{12} = a_{21} = 0 , \tag{4.3.2}$$

and

$$b_{11} = b_{12} = b_{21} = 0 , \qquad b_{22} = \frac{1}{R} . \tag{4.3.3}$$

Since the coordinates are Cartesian, all Christoffel symbols vanish and covariant derivatives reduce to partial derivatives.

The axisymmetric homogeneous form of the governing equilibrium equations for displacement components u_1 along a generator and u_3 along an outwards radial direction are

$$\left.\begin{aligned} u_{1,11} + \frac{\nu}{R} u_{3,1} &= 0 \\ \frac{\nu}{R} u_{1,1} + \frac{k}{R^2}\left(R^2 \frac{d^2}{d(\xi^1)^2} + 1\right)^2 u_3 + \frac{u_3}{R^2} &= 0 \end{aligned}\right\} \tag{4.3.4}$$

where the non-dimensional parameter k is defined by

$$k = \frac{1}{12}\left(\frac{t}{R}\right)^2 . \tag{4.3.5}$$

Consistent with these equations are the (modified) components of stress resultant

$$\left.\begin{aligned} N_{11} &= \frac{Et}{1-\nu^2}\left(u_{1,1} + \nu\frac{u_3}{R}\right) , \\ N_{22} &= \frac{Et}{1-\nu^2}\left\{\frac{u_3}{R} + \nu u_{1,1} + (1-\nu)k\left(u_{1,1} + Ru_{3,11}\right)\right\} , \end{aligned}\right\} \tag{4.3.6}$$

and (modified) components of stress couple

$$\left.\begin{aligned} M_{11} &= -D\left(u_{3,11} + \frac{u_3}{R^2}\right) , \\ M_{22} &= -D\left(\nu u_{3,11} - \frac{1-\nu}{R}u_{1,1} + \frac{u_3}{R^2}\right) , \end{aligned}\right\} \tag{4.3.9}$$

where D is the flexural rigidity,

$$D = \frac{Et^3}{12(1-\nu^2)} . \tag{4.3.8}$$

The associated (modified) transverse shear force is

$$Q = \frac{1}{R} M_{11,1} . \tag{4.3.9}$$

The governing equations (4.3.4) give

$$\left\{\frac{k}{1-\nu^2}\frac{d}{d\xi^1}\left(R^2\frac{d^2}{d(\xi^1)^2} + 1\right)^2 + \frac{d}{d\xi^1}\right\}u_3 = 0 , \tag{4.3.10}$$

which leads to the solution, on omitting terms of relative order $(t/R)^2$,

$$
\left.
\begin{aligned}
u_3 &= A_0 + \left(A_1 \sin \frac{\rho\xi^1\lambda_1}{R} + A_2 \cos \frac{\rho\xi^1\lambda_1}{R}\right) \exp\left(\frac{\rho\xi^1\lambda_2}{R}\right) \\
&\quad + \left(A_3 \sin \frac{\rho\xi^1\lambda_1}{R} + A_4 \cos \frac{\rho\xi^1\lambda_1}{R}\right) \exp\left(\frac{\rho\xi^1\lambda_2}{R}\right) , \\
u_{1,1} &= -\frac{\nu u_3}{R} ,
\end{aligned}
\right\} \qquad (4.3.11)
$$

with

$$
\rho^4 = 3(1 - \nu^2)\left(\frac{R}{t}\right)^2 , \qquad \lambda_1 = 1 + \frac{1}{4\rho^2} , \qquad \lambda_2 = 1 - \frac{1}{4\rho^2} . \qquad (4.3.12)
$$

The six constants $A_0,\ldots,A_6$ occurring in equation (4.3.11) are determined so as to satisfy the following boundary conditions

$$
\left.
\begin{aligned}
M_{11} &= \bar{M} , \qquad N_{11} = Q_1 = 0 , \qquad \text{at } \xi^1 = 0, \\
u_1 &= u_3 = u_{3,1} = 0 , \qquad \text{at } \xi^1 = 1 ,
\end{aligned}
\right\} \qquad (4.3.13)
$$

where l is the length of the cylinder.

4.4 Membrane solutions

Recall the discussion of Gol'denveizer's static-geometric analogy given in Section 3.7. This shows that the analysis and solutions given in Section 4.2 for the exact displacements of inextensional bending are directly related to the exact stress functions of homogeneous membrane actions. However, in finite element evaluation it is necessary to know the displacements and rotations of the shell middle surface. It is impractical, except for simple geometries like that of circular cylinders, to exactly integrate strain-displacement relations when strains arise from stress functions through constitutive equations. For this reason

Morley (1983b) considers the class of shells having quadratic parametric representation and derives approximate solutions using the theorem of minimum potential energy.

The Cartesian components of displacement of a point on the middle surface are expressed as quartic polynomials in the surface coordinates

$$\begin{bmatrix} U^1 \\ U^2 \\ U^3 \end{bmatrix} = \begin{bmatrix} \underline{a}^T \\ \underline{b}^T \\ \underline{c}^T \end{bmatrix} \underline{\xi} \tag{4.4.1}$$

where

$$\underline{\xi}^T = (1, \xi^1, \xi^2, (\xi^1)^2, \ldots, (\xi^2)^4), \qquad \underline{\xi} \in R^{15\times 1} \tag{4.4.2}$$

and $\underline{a}$, $\underline{b}$, $\underline{c} \in R^{15\times 1}$ are constant vectors to be determined.

The principle of minimum potential energy for homogeneous membrane actions in an isotropic material requires

$$\delta U_\gamma + \delta U_\kappa - V(N', \delta\underline{u}') = 0 \tag{4.4.3}$$

where the membrane and bending strain energies are given in terms of the practical components of membrane strain and curvature change according to

$$U_\gamma = \int_\Omega \frac{6D}{h^2}\left\{\gamma^2_{1',1'} + \gamma^2_{2',2'} + 2\gamma^2_{1',2'} - 2\nu\left(\gamma^2_{1',2'} - \gamma^2_{1',1'}\gamma^2_{2',2'}\right)\right\} a_1 a_2 \, d\xi^1 d\xi^2 \tag{4.4.4}$$

$$U_\kappa = \int_\Omega \frac{D}{2}\left\{\kappa^2_{1',1'} + \kappa^2_{2',2'} + 2\kappa^2_{1',2'} - 2\nu\left(\kappa^2_{1',2'} - \kappa^2_{1',1'}\kappa^2_{2',2'}\right)\right\} a_1 a_2 \, d\xi^1 d\xi^2 \tag{4.4.5}$$

and the potential energy due to applied tractions is given by

$$V(N', \delta\underline{u}') = \int_\Gamma \left(\bar{N}_{1',1'}\delta u_{1'} + \bar{N}_{1',2'}\delta u_{2'}\right) a_{2'} d\xi^{2'}, \tag{4.4.6}$$

with D the flexural rigidity given by (4.3.8). The membrane strains $\gamma_{\alpha'\beta'}$ and curvature changes $\kappa_{\alpha'\beta'}$ are calculated from the expressions (4.2.1) and (4.2.4) using the assumed displacements of (4.4.1) together with the definition of practical components given by (2.5.20) and an arbitrary, but constant, value of λ. Displacements at the shell boundary are calculated from (4.4.1) using the relations

$$u_{\alpha'} = U^i \underline{e}_i \cdot \underline{t}_{\alpha'} \quad , \tag{4.4.7}$$

where the angle λ, see Fig. 2.3, is chosen to orient the vector $\underline{t}_{2'}$ along the shell boundary Γ in the positive sense. The boundary tractions $\bar{N}_{1'1'}$, $\bar{N}_{2'2'}$ in (4.4.6) are determined, for these same values of λ, from the exact stress functions derived, using the static-geometric analogy, from the exact displacements of inextensional bending given in Section 4.2. Substituting into (4.4.3) gives a (positive definite) linear system from which the unknown vectors $\underline{a}$, $\underline{b}$, $\underline{c}$ and hence displacements U^i are determined.

CHAPTER 5

THE CONSTANT STRESS SHELL FINITE ELEMENT

5.1 Introduction

The purpose of this chapter is to describe the analysis of thin shell structures when the constant bending moment element of Morley (1971) is used in conjunction with the constant membrane stress element of Turner et al (1956). The results presented in the sequel reveal that the characteristics of an assembly of this simple flat element are such as to enable recovery, in a remarkable way, of each of the types of deformation identified by the classical first approximation theory of continuously curved shells. Thus, the element is seen to hold a position of central importance with regard to the numerical analysis of thin shells.

Recall that it is the consequences of bending which have been the most troublesome in the construction of shell finite element models. More specifically, a shell finite element model must be capable of recovering bending strains without them being overwhelmed by spurious membrane strains. It is the intention to investigate this particular aspect of bending action through use of the exact comparison solutions described earlier in Chapter 4. It emerges that there are two quite different roles for the element bending freedoms. One concerns inextensional bending movements which extend over the whole finite element model. The other role concerns local rotational movements which accompany the curvature changes of inextensional bending and of edge effect.

The vehicle finite element considered in this work has an interesting history which is now briefly recalled. Constant moment bending elements were initially suggested by Hellan (1967) and by Herrmann (1968) based on

mixed formulations. In more detail, Herrmann's solution proceeds by way of the Reissner mixed variational principle in conjunction with a linearly varying normal displacement field. This formulation makes use of constant bending moments within the element and enforces continuity of the practical component $M_{1'1'}$ along adjacent element edges. Subsequently, Allman (1971) points out that Herrmann's technique is equivalent to an application of the complementary energy principle with the linear deflection field acting as Lagrangian multiplier terms which ensure equilibrium of the normal forces at nodal points. The work of Morley (1971) shows that the displacement model developed from the potential energy principle is exactly equivalent to the pure equilibrium model whilst being more suited to incorporation into general purpose displacement oriented computer programs. The development of the mixed formulation for application in shell problems is given by Hermann and Campbell (1967) who incorporate the constant stress triangle to represent membrane behaviour, an equivalent displacement formulation is given by Dawe (1972). Here it is preferred to make use of a tensor formulation as in Morley and Mould (1987) and to develop the shell element by way of a generalised principle.

5.2 Element matrices

The element has twelve degrees of freedom and is shown in Fig. 5.1 arbitrarily orientated with respect to a fixed global Cartesian coordinate system x^1, x^2, x^3. The vector $\underline{U}$ representing the displacement of points on the element middle surface may be written in the alternative forms

$$\left.\begin{aligned} \underline{U} &= U^i \underline{e}_i \\ &= u^i \underline{a}_i \ , \end{aligned}\right\} \qquad (5.2.1)$$

where U^i are the global Cartesian displacement components, u^α are the contravariant components of in-plane displacements in the oblique ξ^α-coordinate system, see Fig. 5.1, and u^3 is the displacement normal to the element middle surface.

Vertices of the element are numbered 1,2,3 with geometric connectors x^i_j so that the position vector of a point on the middle surface of an element is given by

$$\underline{r} = x^i \underline{e}_i \ , \tag{5.2.2}$$

where the element geometry is defined in terms of the surface coordinate system according to

$$x^i = x^i_j N^j \ , \qquad i,j = 1,2,3 \tag{5.2.3}$$

and the shape functions N^j are given by

$$N^1 = \xi^1 \ , \qquad N^2 = \xi^2 \ , \qquad N^3 = 1 - \xi^1 - \xi^2 \ . \tag{5.2.4}$$

Local tangent base vectors in the ξ^α directions are introduced by differentiation of (5.2.2), so that

$$\underline{a}_\alpha = \underline{r}_{,\alpha} = x^i{}_{,\alpha} \underline{e}_i \tag{5.2.5}$$

where

$$x^i{}_{,1} = x^i_1 - x^i_3 \ , \qquad x^i{}_{,2} = x^i_2 - x^i_3 \ . \tag{5.2.6}$$

The element middle surface unit normal vector is obtained from the vector product

$$\underline{a}_3 = \frac{\underline{a}_1 \times \underline{a}_2}{|\underline{a}_1 \times \underline{a}_2|} = a^i_3 \, \underline{e}_i \ , \tag{5.2.7}$$

so that

$$\left.\begin{aligned} a_3^1 &= \frac{1}{2A}\,(x^2{}_{,1}\; x^3{}_{,2} - x^2{}_{,2}\; x^3{}_{,1})\ , \\ a_3^2 &= \frac{1}{2A}\,(x^3{}_{,1}\; x^1{}_{,2} - x^3{}_{,2}\; x^1{}_{,1})\ , \\ a_3^3 &= \frac{1}{2A}\,(x^1{}_{,1}\; x^2{}_{,2} - x^2{}_{,2}\; x^1{}_{,1})\ . \end{aligned}\right\} \qquad (5.2.8)$$

The metric tensor $a_{\alpha\beta}$ is given by

$$a_{\alpha\beta} = \underline{a}_\alpha \cdot \underline{a}_\beta \qquad (5.2.9)$$

so that

$$a_{11} = (l_2)^2, \qquad a_{22} = (l_1)^2, \qquad a_{12} = a_{21} = \frac{1}{2}l_{12}\ , \qquad (5.2.10)$$

where the element side lengths are expressed in terms of geometric connectors by

$$\left.\begin{aligned} (l_1)^2 &= (x_2^i - x_3^i)(x_2^i - x_3^i)\ , \\ (l_2)^2 &= (x_3^i - x_1^i)(x_3^i - x_1^i)\ , \\ (l_3)^2 &= (x_1^i - x_2^i)(x_1^i - x_2^i)\ , \\ l_{12} &= (l_1)^2 + (l_2)^2 - (l_3)^2\ , \\ l_{23} &= (l_2)^2 + (l_3)^2 - (l_1)^2\ , \\ l_{31} &= (l_3)^2 + (l_1)^2 - (l_2)^2\ . \end{aligned}\right\} \qquad (5.2.11)$$

The area A of the triangular element and determinant a of the metric tensor are given by

$$16A^2 = a = l_{12}l_{23} + l_{23}l_{31} + l_{31}l_{12} , \tag{5.2.12}$$

so that the contravariant components of the metric tensor are determined as

$$\left.\begin{aligned} a^{11} = a_{22}/a = (l_1/2A)^2 , \qquad a^{22} = a_{11}/a = (l_2/2A)^2 , \\ a^{12} = a^{21} = -a_{12}/a = -l_{12}/(8A^2) \end{aligned}\right\} \tag{5.2.13}$$

The displacement components in the local oblique and global coordinate systems are related by the transformation formulae

$$\left.\begin{aligned} u_\alpha = \underline{U} \cdot \underline{a}_\alpha = U^i(\underline{e}_i \cdot \underline{a}_\alpha) = U^i\, x^i{}_{,\alpha} , \\ U^3 = U_3 = \underline{U} \cdot \underline{a}_3 = \underline{U} \cdot \underline{a}^3 = U^i\, a^3_i , \end{aligned}\right\} \tag{5.2.14}$$

where u_α is the covariant component of in plane displacement in the oblique ξ^α-coordinate system and x^i and $x^i{}_{,\alpha}$ are given above by (5.2.3) and (5.2.6).

Let the displacements U^i of the element middle surface be expressed by the quadratic polynomial

$$U^i = U^i_j N^j + \psi_j \left\{ N^j - (N^j)^2 \right\} a^i_3 \tag{5.2.15}$$

so that the in-plane and normal displacements are given by

$$u^\alpha = u^\alpha_j N^j , \tag{5.2.16}$$

$$u^3 = u^3_j N^j + \psi_j \left\{ N^j - (N^j)^2 \right\} , \tag{5.2.17}$$

where the displacement connector u_j^i is the magnitude of u^i at node j, see Fig. 5.1. The constants ψ_j are to be determined so that there is continuity of the practical component of rotation ϕ_1, at the element midside nodes 4,5 and 6, see Fig. 5.1.

The membrane strain tensor $\gamma_{\alpha\beta}$ is defined by

$$\gamma_{\alpha\beta} = \frac{1}{2}\left(x^i{}_{,\alpha} U^i{}_{,\beta} + x^i{}_{,\beta} U^i{}_{,\alpha}\right) \tag{5.2.18}$$

where derivatives are taken with respect to the oblique ξ^α-coordinate system, shown in Fig. 5.1. The components of this symmetric tensor are

$$\left.\begin{aligned} \gamma_{11} &= (l_2)^2 \varepsilon_2 \ , \qquad \gamma_{22} = (l_1)^2 \varepsilon_1 \\ \gamma_{12} &= \frac{1}{2}\left((l_1)^2 \varepsilon_1 + (l_2)^2 \varepsilon_2 - (l_3)^2 \varepsilon_3\right) \end{aligned}\right\} \tag{5.2.19}$$

with

$$\left.\begin{aligned} \varepsilon_1 &= \frac{1}{(l_1)^2}(x_2^i - x_3^i)(U_2^i - U_3^i) \ , \\ \varepsilon_2 &= \frac{1}{(l_2)^2}(x_3^i - x_1^i)(U_3^i - U_1^i) \ , \\ \varepsilon_3 &= \frac{1}{(l_3)^2}(x_1^i - x_2^i)(U_1^i - U_2^i) \ . \end{aligned}\right\} \tag{5.2.20}$$

The rotation vector ϕ_α is defined by

$$\phi_\alpha = -\underline{U}_{,\alpha} \cdot \underline{a}_3 = -\underline{U}^i{}_{,\alpha}\, a_i^3 \tag{5.2.21}$$

so that

$$\left.\begin{aligned} \phi_1 &= -a_3^i(U_1^i - U_3^i) - \left(\psi_1(1 - 2N^1) - \psi_3(1 - 2N^3)\right) \ , \\ \phi_2 &= -a_3^i(U_2^i - U_3^i) - \left(\psi_2(1 - 2N^2) - \psi_3(1 - 2N^3)\right) \ . \end{aligned}\right\} \tag{5.2.22}$$

The symmetric curvature change tensor $\kappa_{\alpha\beta}$ is defined by

$$\kappa_{\alpha\beta} = -U^i{}_{,\alpha\beta} a_3^i \tag{5.2.23}$$

where the components are

$$\kappa_{11} = 2(\psi_1 + \psi_3) , \qquad \kappa_{12} = 2\psi_3 , \qquad \kappa_{22} = 2(\psi_2 + \psi_3) . \tag{5.2.24}$$

All these tensors are referred to the oblique ξ^α-coordinate system, their practical components referred to selected orthogonal directions $\xi^{\alpha'}$ are given by

$$\gamma_{\alpha'\beta'} = h^\alpha_{\alpha'} h^\beta_{\beta'} \gamma_{\alpha\beta} , \tag{5.2.25}$$

$$\phi_{\alpha'} = h^\alpha_{\alpha'} \phi_\alpha , \tag{5.2.26}$$

$$\kappa_{\alpha'\beta'} = h^\alpha_{\alpha'} h^\beta_{\beta'} \kappa_{\alpha\beta} . \tag{5.2.27}$$

The coordinate $\xi^{1'}$ is chosen to define the outwards pointing in-plane normal and $\xi^{2'}$ is tangential to the element side. For this convention the h-symbols may be calculated using (2.5.23)-(2.5.27) and have components for sides 1,2 and 3 as given in Table 5.1.

The constants ψ_j of (5.2.15) can now be expressed in terms of displacement and rotation connectors. For this purpose it is convenient to introduce the notation

$$\phi_{1',j} \equiv \phi_{1'} \quad \text{at midside node } j \ (j=1,2,3) , \tag{5.2.28}$$

so that the element midside rotation connectors are as shown in Fig. 5.1. Equating (5.2.26) at the midside positions of sides 1,2 and 3 in turn gives the following expressions

$$\left.\begin{aligned}
\Psi_1 &= \tfrac{1}{2}\left(2A\phi_{1,4} - l_1 u_1^3 + (l_{12}/2l_1)u_2^3 + (l_{31}/2l_1)u_3^3 \right) , \\
\Psi_2 &= \tfrac{1}{2}\left(2A\phi_{1,5} - l_2 u_2^3 + (l_{23}/2l_2)u_3^3 + (l_{12}/2l_2)u_1^3 \right) , \\
\Psi_3 &= \tfrac{1}{2}\left(2A\phi_{1,6} - l_3 u_3^3 + (l_{31}/2l_3)u_1^3 + (l_{23}/2l_3)u_2^3 \right) .
\end{aligned}\right\} \qquad (5.2.29)$$

Having obtained expressions for the element membrane strains and curvature changes in terms of the 12 global connectors U_j^i $(i,j = 1,2,3)$ $\phi_{1,j}$ $(j = 4,5,6)$ it is the intention to establish matrix expressions for the element stiffness matrix and load vector due to any applied boundary tractions. This is achieved through use of a variational principle.

As is well-known the construction of a fully compatible displacement model involves many difficulties, and has led to various finite element models based on variational principles other than the principle of minimum potential energy. In order to overcome these difficulties many authors have proposed generalised displacement methods which allow for relaxed smoothness of displacement fields, see Pian and Tong (1969). In preparation for the finite element analysis attention is given to the variational formulation of the vehicle finite element using a generalised principle which provides the governing differential equations for the stretching and bending of flat plates as its Euler equations, together with their natural boundary conditions. Specialisation of this functional for a single element provides a route to the element stiffness matrix.

In the case of a compatible model, a functional Π for the stretching and bending of a thin plate is given by Washizu (1982):

$$\begin{aligned}
\Pi = \int_\Omega \tfrac{1}{2}\Big[E^{\alpha\beta\lambda\mu}\gamma_{\alpha\beta}\gamma_{\lambda\mu} + \frac{h^2}{12}E^{\alpha\beta\lambda\mu}\kappa_{\alpha\beta}\kappa_{\lambda\mu} - f^i u_i \Big] \sqrt{a}\, d\xi^1\, d\xi^2 \\
- \int_\Gamma \left[\bar{N}_{1,\alpha'}u_{\alpha'} + \bar{M}_{1,\alpha'}\phi_{\alpha'} + \bar{Q}_1 u_3\right] d\xi^{2'} ,
\end{aligned} \qquad (5.2.30)$$

where $\bar{N}_{1'\alpha'}$, $\bar{M}_{1'\alpha'}$, $\bar{Q}_{1'}$ are prescribed membrane forces, bending moments and transverse shear force on the plate boundary, see (3.5.7). In the above expression $\gamma_{\alpha\beta}$, $\kappa_{\alpha\beta}$ satisfy the subsidiary conditions of (5.2.18), (5.2.23) and it is required that the displacements u_i satisfy the following:

$$\left.\begin{array}{l} \cdot\ u_\alpha \text{ is continuous in } \Omega_e \text{ and on } \Gamma_e\ ; \\ \cdot\ u_3 \text{ and its first derivatives are continuous in } \Omega_e \text{ and} \\ \quad \text{on } \Gamma_e\ , \text{ and has piecewise continuous derivatives of} \\ \quad \text{second order in the entire region of the plate;} \\ \cdot\ u_\alpha = \bar{u}_\alpha \text{ on } \Gamma_k\ ; \\ \cdot\ u_3 = \bar{u}_3, \qquad \phi_{1'} = \bar{\phi}_{1'} \text{ on } \Gamma_k\ . \end{array}\right\} \quad (5.2.31)$$

The overbar notation indicates a prescribed value and Γ_k indicates the part of the boundary where kinematic boundary conditions are prescribed.

Note that the components of the unit in-plane outwards pointing normal ν_β are related to the h-symbols by the requirement that the typical identity holds:

$$\int_\Gamma N^{\alpha\beta} u_\alpha \nu_\beta d\tau = \int_\Gamma N_{1'\alpha'} u_{\alpha'} d\xi^{2'} \quad (5.2.32)$$

where $N_{1'\alpha'}$, $u_{\alpha'}$ are the practical components given by

$$N_{1'\alpha'} = h^{1'}_{\lambda} h^{\alpha'}_{\alpha} N^{\alpha\lambda}\ , \qquad u_{\alpha'} = h^{\lambda}_{\alpha'} u_\lambda\ , \quad (5.2.33)$$

so

$$N_{1'\alpha'} u_{\alpha'} = h^{1'}_{\lambda} h^{\alpha'}_{\alpha} N^{\lambda\alpha} h^{\mu}_{\alpha'} u_\mu = N^{\alpha\lambda} u_\alpha \nu_\lambda \quad (5.2.34)$$

and recalling (2.5.12) it follows that

$$\nu_\beta = h^{1'}_{\beta}\ . \quad (5.2.35)$$

For the vehicle element the normal displacement component is defined in terms of a quadratic polynomial with vertex and midside connectors. It follows that the element normal displacement is discontinuous along edges shared by adjacent elements. The continuity requirements demanded by a strict application of the functional Π may be relaxed and the subsidiary conditions may be put into the framework of the variational principle by use of Lagrange multipliers.

Following the ideas of Washizu (1982), introduce Lagrange multipliers $N^{\alpha\beta}$, $M^{\alpha\beta}$ and $N_{1'\alpha'}$, $M_{1'\alpha'}$ defined in Ω_e and on Γ_k, respectively. Also define line distributions $\tilde{u}_{i'}$, $\tilde{\phi}_{\alpha'}$ of displacement and rotation between adjacent elements in order to link the respective connectors along element edges. The generalised functional appropriate to a typical element in the global assembly may be expressed as

$$\Pi_g = \int_{\Omega_e} \frac{1}{2}\Big[E^{\alpha\beta\lambda\mu}\gamma_{\alpha\beta}\gamma_{\lambda\mu} + \frac{h^2}{12}E^{\alpha\beta\lambda\mu}\kappa_{\alpha\beta}\kappa_{\lambda\mu} - f^i u_i\Big]\sqrt{a}\, d\xi^1 d\xi^2$$

$$- \int_{\Omega_e}\Big[\gamma_{\alpha\beta} - \frac{1}{2}(u_{\alpha,\beta} + u_{\beta,\alpha})\Big]N^{\alpha\beta}\sqrt{a}\, d\xi^1 d\xi^2$$

$$- \int_{\Omega_e}\Big[\kappa_{\alpha\beta} + u_{3,\alpha\beta}\Big]M^{\alpha\beta}\sqrt{a}\, d\xi^1 d\xi^2 \qquad (5.2.36)$$

$$- \int_{\Gamma_{k_e}}\Big[N_{1'\alpha'}(u_{\alpha'} - \tilde{u}_{\alpha'}) + M_{1'\alpha'}(\phi_{\alpha'} - \tilde{\phi}_{\alpha'}) + Q_{1'}(u_3 - \tilde{u}_3)\Big]d\xi^{2'}$$

$$- \int_{\Gamma_{t_e}}\Big[\bar{N}_{1'\alpha'}u_{\alpha'} + \bar{M}_{1'\alpha'}\phi_{\alpha'} + \bar{Q}_{1'}u_3\Big]d\xi^{2'}$$

The independent quantities subject to variation are $\gamma_{\alpha\beta}$, $\kappa_{\alpha\beta}$; u_i; $N^{\alpha\beta}$, $M^{\alpha\beta}$; $N_{1'\alpha'}$, $M_{1'\alpha'}$ with no subsidiary conditions.

The first variation of this functional provides all the fundamental equations which underlie the displacement formulation of the element:

$$\delta\Pi_g = \int_{\Omega_e} \left[(E^{\alpha\beta\lambda\mu}\gamma_{\lambda\mu} - N^{\alpha\beta})\delta\gamma_{\alpha\beta} + (\frac{h^2}{12}E^{\alpha\beta\lambda\mu}\kappa_{\lambda\mu} - M^{\alpha\beta})\delta\kappa_{\alpha} \right] \sqrt{a}\, d\xi^1 d\xi^2$$

$$- \int_{\Omega_e} \left[\left(N^{\alpha\beta}{}_{,\beta} + f^{\alpha}\right)\delta\gamma_{\alpha\beta} + \left(M^{\alpha\beta}{}_{,\alpha\beta} + f^{3}\right)\delta\kappa_{\alpha\beta} \right] \sqrt{a}\, d\xi^1 d\xi^2$$

$$- \int_{\Omega_e} \left[\left(\gamma_{\alpha\beta} - \tfrac{1}{2}(u_{\alpha,\beta} + u_{\beta,\alpha})\right)\delta N^{\alpha\beta} + \left(\kappa_{\alpha\beta} + u_{3,\alpha\beta}\right)\delta M^{\alpha\beta} \right] \sqrt{a}\, d\xi^1 d\xi^2 \quad (5.2.37)$$

$$- \int_{\Gamma_{k_e}} \left[(u_{\alpha'} - \tilde{u}_{\alpha'})\delta N_{1'\alpha'} + (\phi_{\alpha'} - \tilde{\phi}_{\alpha'})\delta M_{1'\alpha'} + (u_3 - \tilde{u}_3)\delta Q_{1'} \right] d\xi^{2'}$$

$$- \int_{\Gamma_{t_e}} \left[(\bar{N}_{1'\alpha'} - N_{1'\alpha'})\delta u_{\alpha'} + (\bar{M}_{1'\alpha'} - M_{1'\alpha'})\delta\phi_{\alpha'} + (\bar{Q}_{1'} - Q_{1'})\delta u_3 \right] d\xi^{2'} .$$

Recalling the intended connection quantities of the constant stress element immediately allows simplification of the functional Π_g by satisfying the following assumptions:

$$\left.\begin{aligned}
&N^{\alpha\beta} = E^{\alpha\beta\lambda\mu}\gamma_{\lambda\mu}\,,\ M^{\alpha\beta} = \frac{h^2}{12}E^{\alpha\beta\lambda\mu}\kappa_{\lambda\mu} \quad \text{in } \Omega_e\,,\\
&\gamma_{\alpha\beta} = \tfrac{1}{2}(u_{\alpha,\beta} + u_{\beta,\alpha}),\ \kappa_{\alpha\beta} = -u_{3,\alpha\beta} \quad \text{in } \Omega_e\,,\\
&u_\alpha \text{ linear in } \xi^\alpha\,,\ u_3 \text{ quadratic in } \xi^\alpha \text{ in } \Omega_e\,,\\
&u_\alpha = \tilde{u}_\alpha \text{ on } \Gamma_{k_e}\,,\\
&u_3 = \tilde{u}_3 \text{ at nodes on } \Gamma_{k_e},\ \phi_{1'} = \tilde{\phi}_{1'} \text{ at miside nodes on } \Gamma_{k_e}\,,
\end{aligned}\right\} \quad (5.2.38)$$

Consequently the generalised potential energy functional Π_g of (5.2.36) reduces to

$$\Pi_g = \sum_e \int_{\Omega_e} \left[\tfrac{1}{2}N^{\alpha\beta}\gamma_{\alpha\beta} + \tfrac{1}{2}M^{\alpha\beta}\kappa_{\alpha\beta} - f^i u_i \right] \sqrt{a}\, d\xi^1 d\xi^2$$

$$- \sum_e \int_{\Gamma_{t_e}} \left[\bar{N}_{1'\alpha'}u_{\alpha'} + \bar{M}_{1'\alpha'}\phi_{\alpha'} \right] d\xi^{2'} . \quad (5.2.39)$$

Substituting into (5.2.39) from the above expressions and following the usual procedure allows the total potential energy to be expressed as

$$\Pi_g = \sum_e \left(\tfrac{1}{2}\underline{U}^T[k]\underline{U} - \underline{U}^T\underline{f} \right) \quad (5.2.40)$$

where $[k] \in R^{12\times12}$ is an element stiffness matrix, $\underline{f} \in R^{12\times1}$ is a generalised loads vector which may contain contributions from edge tractions applied to the shell if the element boundary coincides with that of the shell, and

$$\underline{U}^T = [U_1^1,\ U_1^2,\ U_1^3,\ U_2^1,\ \ldots,\ \phi_{1,4},\ \phi_{1,5},\ \phi_{1,6}] \qquad (5.2.41)$$

is a vector consisting of the element global degrees of freedom. It is clear from the form of (5.2.39) that the matrix $[k]$ is built up by a sequence of matrix multiplications and integrations, in fact

$$[k] = \int_{\Omega_e} [B]^T[D][B]\sqrt{a}\ d\xi^1 d\xi^2 = A[B]^T[D][B]\ . \qquad (5.2.42)$$

The strain displacement matrix $[B] \in R^{6\times12}$ is found in explicit form from (5.2.25)-(5.2.27) and the elasticity matrix $[D] \in R^{6\times6}$, for the case of an isotropic material, is given by

$$[D] = \begin{bmatrix} 3\times3 & 3\times3 \\ [D_0] & [0\ ] \\ & \\ 3\times3 & \frac{h^2}{12}\ 3\times3 \\ [0\ ] & [D_0] \end{bmatrix} \qquad (5.2.43)$$

where

$$[D_0] = \frac{Et}{1-\nu^2}\begin{bmatrix} 1 & \nu & 0 \\ \nu & 1 & 0 \\ 0 & 0 & 2(1-\nu) \end{bmatrix}\ . \qquad (5.2.44)$$

5.3 Mechanisms of membrane and transitional models

In keeping with the terminology of classical shell theory, an assembly of these constant stress and constant bending moment finite elements is

called the bending model. The bending model is intended to represent all the characteristic behaviours of a real shell which may have any depth and Gaussian curvature. For the immediate discussion the example real shell and 16 finite elements of a bending model are chosen, see Fig. 5.2, to project onto the ξ^α-plane as an arrangement of equilateral triangles. It is required that the adjacent elements are geometrically continuous and, for the present purpose, that the elements meeting at a common vertex are not all coplanar. For definiteness, the finite element geometric connectors x^i_j are assumed to coincide with the corresponding x^i coordinates of the real shell.

Recall that the element has three degrees of freedom at each vertex and one degree of freedom at each midside node. Thus, the bending model has a total of N degrees of freedom,

$$N = 3n_v + n_s \tag{5.3.1}$$

where n_v is the number of vertex nodes and n_s is the number of midside nodes. As an example, the model in Fig. 5.2 has $n_v = 15$, $n_s = 30$ giving $N = 75$. It is useful to also note the topological relationship

$$3n_v = n_s + n_{\Gamma s} - 3n_\Gamma + 6 \tag{5.3.2}$$

where $n_{\Gamma s}$ is the number of midside nodes on the boundary and n_Γ is the number of boundaries as in a multiply connected shell. The model in Fig. 5.2 has $n_{\Gamma s} = 12$, $n_\Gamma = 1$.

The bending freedoms of the bending model are exposed by isolating the membrane strains through reduction to:

(i) a transitional model where all finite elements are assumed to have vanishing flexural rigidity and where $\psi_j = 0$ in (5.2.15)

(ii) a membrane model where, in addition to (i), the midside connectors ϕ_1, are removed.

Initially all models are assumed to be completely free from constraint.

The membrane model (ii) may be regarded as an assembly of flat triangular elements freely hinged along adjacent edges or, equivalently, as a framework of bars with frictionless universal couplings at the joints. Maxwell's rule for frameworks then shows that the membrane model has freedom for M_{ib} mechanisms where

$$M_{ib} = 3n_v - n_s - 6 = n_{\Gamma s} - 3n_\Gamma \tag{5.3.3}$$

where n_v may be interpreted as the number of joints and n_s the number of bars. In particular the model in Fig. 5.2 has $M_{ib} = 9$ mechanisms. Characteristically, these mechanisms involve nonlocal movements and the notation M_{ib} is chosen because these mechanisms are to shown to have the capacity to simulate the real shell displacements of inextensional bending. The second member of (5.3.3) shows that M_{ib} is independent of the interior arrangement of the finite element mesh. In particular, there are no mechanisms (and therefore no inextensional bending modes) in membrane models of closed shells, like a sphere, since $n_{\Gamma s}$ and n_Γ are both identically zero giving $M_{ib} = 0$.

The transitional model (i) has additional freedoms for M_l mechanisms:

$$M_l = n_s \tag{5.3.4}$$

which are to be identified as mechanisms of local rotation at element sides as occur in element bending.

Returning to the bending model, the number N_b of bending freedoms is equal to the total number of mechanisms in the transitional model,

$$N_b = M_{ib} + M_l = 3n_v - 6 \qquad (5.3.5)$$

and leaves N_m membrane freedoms available where

$$N_m = N - N_b - 6 = n_s = M_l \ . \qquad (5.3.6)$$

It is emphasised that the above formulae refer to shell models that are free from constraints. It is possible, for example, to apply a number of constraints such that M_{ib} is reduced by the same number. Also note, for example, that the three component elements shown compounded in Fig. 5.3 contribute no more to M_{ib} than a single element which is not compounded.

In the preceding chapter a detailed description is given of the exact displacement solutions for real shells undergoing inextensional bending and membrane actions. These solutions are used to examine the displacements exhibited by the nonlocal mechanisms in the transitional and membrane models.

In the comparison examples it is assumed that the real shell surface projects onto the x^α-plane as an equilateral triangle, as shown in Fig 5.2, with side length 2 units and with the three vertices resting on the x^α-plane. In the first sequence of examples, the x^3 coordinate is expressed by the quadratic polynomial

$$6x^3 = -3 + 3(x^1 - 1)^2 + 6\sqrt{3}x^2 - 5(x^2)^2 \ , \qquad (5.3.7)$$

which gives a surface symmetrical about $x^1 = 1$ with principal radii of curvature 1.206 and -1.262 at the centroidal position $x^1 = 1$, $x^2 = 1/\sqrt{3}$ of its projection. Thus, the shell is very deep with strongly negative Gaussian curvature and a perspective view is shown in Fig. 5.4. Connectors U^3 on the boundary of the finite element model (e.g. at the 12 boundary

vertex nodes in Fig. 5.2) are assigned with the same values as calculated for the real shell. Similarly, three U^{α} connectors are assigned so as to fix a rigid body movement in the x^{α}-plane. This is sufficient to constrain the mechanisms in the membrane model and so a patch test is constructed with a specific inextensional bending movement imposed by the kinematic boundary conditions. Values for the constants $c_1, c_2, c_3, \ldots$, see (4.2.20), defining the exact comparison solution are given in Table 5.2 and solution values of the U^i connectors at the centroidal position in finite element membrane models are shown in Table 5.3 along with the comparison real shell values; note that these membrane model solutions are independent of the elastic constants and shell thickness. Remarkably, the table shows that exact agreement is obtained for the membrane models when $q = 2,3$ and this holds true for all U^3 connectors. The underlying mathematics of this phenomenon is yet to be understood but it appears to require a projected mesh that is regular but not necessarily equilateral. The table also shows that typical engineering accuracy (errors of less than 5%) prevails for the higher degree polynomials $q = 4,5$; this level of accuracy is regarded as particularly noteworthy since U^3 does not attain its most significant value at the centroidal position (see Table 5.3). Values of the U^{α} connectors are also good approximations.

Note that the membrane model provides no information whatsoever on the curvature changes κ_{ib} and all membrane strains γ_{ib} are identically zero.

For the second sequence of patch tests, the x^3 coordinate is expressed by the cubic polynomial

$$4x^3 = 1 + (x^1 - 1)^2 + (3 + \tfrac{4}{3}\sqrt{3})x^2 + (x^2)^2 - (x^2)^3 \qquad (5.3.8)$$

which gives a more complicated surface again symmetrical about $x^1 = 1$ but with principal radii of curvature 1.512 and -2.547 at the centroidal position. The shell is also very deep with strongly negative Gaussian curvature. Values for the constants which determine the comparison

solution are given in Table 5.4. The patch tests for the membrane models give solution values for the U^3 connector at the centroidal position and these are listed in Table 5.5 along with those for the real shell. Exact agreement is obtained when $q = 3$ and, again, this holds true at all U^3 connectors. Again engineering accuracy prevails for the higher degree polynomials $q = 4,5$.

The evidence is clear that the M_{ib} mechanisms of nonlocal movement in membrane and in transitional models of the constant strain and constant bending finite element have a remarkable capacity to simulate the displacements of inextensional bending while the M_1 mechanisms of local rotation at element midside nodes find their interpretation in the bending model where they accompany the curvature changes both of inextensional bending and of local edge effect. These elementary considerations provide a rationale for shell element design and validation as well as prompting new thoughts on mathematical abstraction. For example the numbers M_{ib} and M_1 (see (5.3.3) and (5.3.4)) may be taken as target numbers for shell models assembled from any kind of finite element. It is important to note that while all bending models are reducible to transitional models (which may or may not possess mechanisms), it is only the exceptional finite element which allows the further reduction to membrane model and this diminishes the central premise advanced in favour of curved shell finite elements.

5.4 The bending model

For the purposes of engineering design, the most convincing examination of bending needs to be specific to the finite element bending model, be in accord with the results of the classical theory of the real shell and be consequent upon the actions of edge effect as well as of inextensional bending.

It is pertinent to recall the discussion of shell theory presented in Chapters 2 and 3, in particular Love's first approximation for the strain energy U as the sum of the extensional energy U_γ and the bending energy U_κ ,

$$U = U_\gamma + U_\kappa \ . \tag{5.4.1}$$

It is a fundamental result of shell theory that the relative error in this approximation does not exceed t/R or $(t/L)^2$, where t is the shell thickness, R is the smallest principal radius of curvature, and L is the smallest wavelength of deformation pattern. The fact that Love's expression contains these inherent errors has far reaching consequences for it is pointless to strive for greater relative accuracy in the components of extensional and flexural strain energies than the amounts just mentioned. This means that there can be an unlimited number of first approximation shell theories, their differences are manifest of terms having order of magnitude equal to those inherently neglected due to the plane stress or equivalent Kirchhoff assumptions.

The curvature changes κ_{ib} of inextensional bending give rise to stress couples which usually require membrane stress resultants in order to maintain a state of homogeneous equilibrium. Consequently, it is exceptional for 'inextensional' bending to occur under first approximation theory other than in the presence of membrane strain γ_{ib} . It is therefore necessary to define what is meant by 'inextensional' bending. Evidently this requires the membrane strain γ_{ib} to be relatively insignificant,

$$\gamma_{ib} = O(\frac{t}{R}.\frac{1}{2}t\kappa_{ib}) \ , \tag{5.4.2}$$

as in the above sense. Note that inextensional bending is a nonlocal phenomenon and for the relative error $(t/L)^2$ to become critical it is necessary that $L < L_e$, where

$$L_e = O(\sqrt{Rt}) \ , \tag{5.4.3}$$

which measures the so called zone of diffusion of edge effect.

Equivalently, inextensional bending may be defined to occur under first approximation shell theory whenever

$$U_\gamma / U_K = O(t/R)^2 . \tag{5.4.4}$$

Although this condition is a logical consequence of (5.4.2) a more straightforward and less stringent criterion may be set by simply requiring the total membrane strain energy to be relatively insignificant in comparison with the total bending strain energy according to the basic estimate of accuracy of classical theory, i.e.

$$U_\gamma / U_K = O(t/R) \ . \tag{5.4.5}$$

The so called real shell inextensional bending solutions clearly do not precisely relate with any properly constituted first approximation theory where the reference middle surface is capable of extension and is free from surface forces. Nevertheless, in view of the above criteria, these are acceptable approximations within the limitations of the theory.

As with the membrane and transitional models the bending model is assessed through patch tests, with prescribed kinematic boundary conditions, for capacity to simulate 'inextensional' bending under first approximation shell theory. First, attention is given to the shell whose reference middle surface is given by the quadratic parametric representation of (5.3.7). Displacement connectors U^3 and rotation connectors on the boundary of the model (e.g. at the 12 boundary vertex nodes and 12 boundary midside positions in Fig. 5.2) are assigned with the same values as calculated from the exact 'inextensional' bending solutions. On fixing the rigid body movements in the x^α-plane, a patch test is

presented which is solved in the usual way with the following values taken for the constants

$$E = 10^7 , \qquad \nu = 0.3 , \qquad t = 0.01 , \tag{5.4.6}$$

where E is Young's modulus, ν is Poisson's ratio, and where the value selected for the shell thickness t is appropriate to a moderately thin shell with $R/t = 120$ at the centroidal position. Solution values for the U^3 connector at the centroidal position are shown in Table 5.3 for bending models. These values, as well as those for the other displacement connectors, differ only slightly from those calculated for the membrane model so that good accuracy is maintained in comparison with the real shell.

A more searching examination is given in Table 5.6 where the global strain energies U_γ and U_κ are listed as well as the most significant principal values of curvature change κ_{ib} and membrane strain γ_{ib} in the finite element which encloses the centroidal position of the bending models. The quadratic reference surface of this shell, (5.3.7), gives

$$\frac{t}{R} = 0.83\times10^{-2} , \qquad \left(\frac{t}{R}\right)^2 = 0.69\times10^{-4} , \qquad \frac{(t)^2}{2R} = 0.41\times10^{-4} , \tag{5.4.7}$$

at the centroidal position and

$$\frac{t}{R} = 0.17\times10^{-1} , \qquad \left(\frac{t}{R}\right)^2 = 0.28\times10^{-3} , \qquad \frac{(t)^2}{2R} = 0.83\times10^{-4} , \tag{5.4.8}$$

at a less critical position where the principal radii of curvature are 0.602 and -1.002. The values of γ_{ib} are seen to fulfil the criterion of (5.4.2) which provides a local definition for inextensional bending. In the global sense, 'inextensional' bending is defined by (5.4.5) which confines the order of magnitude of the strain energy ratio U_γ/U_κ according to the demands of first approximation theory. The last column of Table 5.6 lists calculated values of U_γ/U_κ and these are seen to fulfil

the criterion of (5.4.5). This is further emphasised in Fig. 5.5 which shows the effect of mesh refinement on the value of the ratio of strain energies. The values of curvature change κ_{ib} of 'inextensional' bending at the centroidal position, although not the most significant, compare remarkably well with those for the real shell, especially in view of the piecewise constant representation employed.

The more complicated reference surface for the second sequence of patch tests is given by the cubic representation of (5.3.8), where

$$\frac{t}{R} = 0.66\times10^{-2} , \qquad \left(\frac{t}{R}\right)^2 = 0.44\times10^{-4} , \qquad \frac{(t)^2}{2R} = 0.33\times10^{-4} , \quad (5.4.9)$$

at the centroidal position and

$$\frac{t}{R} = 0.21\times10^{-2} , \qquad \left(\frac{t}{R}\right)^2 = 0.44\times10^{-4} , \qquad \frac{(t)^2}{2R} = 0.10\times10^{-3} , \quad (5.4.10)$$

at a less critical position where the principal radii of curvature are 0.478 and -2.005. The finite element calculations are carried out in a similar manner as described above with values for the U^i connectors at the centroidal position listed in Table 5.5. In Table 5.8, the global U_γ and U_κ are listed as well as the most significant principal values of curvature changes κ_{ib} and membrane strain γ_{ib} in the finite element enclosing the centroidal position.

The values of γ_{ib} fulfil the local measure in (5.4.2) for the relative magnitude of membrane strain and curvature change. With the exception of the coarse mesh of 16 elements for $q = 4,5$, the listed values of U_γ/U_κ fulfil the measure in (5.4.5). Further results are given in Fig. 5.6 which shows a plot of the value U_γ/U_κ against increasing mesh refinement.

The extensive and detailed series of patch tests described above provide for a significant and demanding assessment of this particular finite element shell model. They support the view that bending models assembled from the flat triangular constant bending moment and constant

membrane stress finite element have a capacity to simulate certain modes of 'inextensional' bending of the corresponding real shell under first approximation theory. However, it is to be noted that these tests are in no way definitive and are in conspicuous contrast with those for flat plates, see Zienkiewicz (1973), dominated by the precision of the constant curvature change criteria and the consequent assurance of lowest order convergence. This contrast prompts questions concerning shell models constructed from other elements, in particular those having doubly curved geometry. For instance, it is conceivable that such models could respond favourably to certain patch tests yet remain essentially unable to simulate other modes of 'inextensional' bending even with mesh refinement. This notion is provoked by the investigation described earlier in this chapter which reveals that the nonlocal mechanistic response of the membrane model to the displacements of inextensional bending with the number M_{ib} of these mechanisms increasing directly with the number of elements at the boundary. Thus, for example, $M_{ib} = 6,9,15,18$ respectively for the 9,16,36,49 finite element assemblies. It is to be recognised that while patch testing can provide for a substantial assessment, it is usually limited for practical reasons yet it remains advisable to test for ability to simulate additional inextensional bending modes with mesh refinement. The matrix procedure described in the sequel is intended to be helpful in this respect.

It is appropriate to mention that recovery of 'inextensional' bending is notoriously sensitive to error in the prescription of boundary conditions. Thus, immediate uncertainty arises whenever the geometry of the finite element model is different from that of the comparison real shell. This is further aggravated by the element trial functions which degrade the quality of displacement and rotation representation. Indeed examination of the results given in Tables 5.2-5.7 are noticeably subject to these sensitivities most particularly because the locations of the midside positions are not coincident for the real shell and bending models so that an estimated value for each rotation connector must be used. This

prompts the following caution: it is inadvisable to overprescribe the boundary conditions for this type of 'inextensional' bending patch test.

5.5 Edge effect problem

Ability to recover the curvature changes of 'inextensional' bending is an indispensable prerequisite for a satisfactory response of the bending model to local edge effect. This phenomenon is even more disadvantaged than 'inextensional' bending because access to comparison solutions in classical theory for real shells is now limited to the circular cylinder.

The capacity for the constant membrane stress and constant bending moment finite element bending model in simulating the above edge effect is examined by modelling the circumference of a circular cylinder with flat longitudinal uniform strips. By applying the appropriate conditions of axisymmetry at the longitudinal boundaries it is necessary to consider just one of these flat strips. Each of these is such that there is a more refined gradation of the finite element mesh (so that the element dimensions have the same order of magnitude as the thickness) in the subregion adjacent to the applied edge moment $\bar{M}$ as shown in Fig. 5.7.

A graphical comparison of the finite element results against those of the real cylinder are presented in Fig. 5.8 and are seen to provide a respectable recovery of the real shell solution. More precise results are listed in Table 5.8 where the peak radial deflection u^3 is estimated to within 10% for the coarsest mesh with closer agreement on mesh refinement. Good agreement for the most significant stress resultant $N_{\theta\theta}$ and stress couple M_{xx} $(=\bar{M})$ is achieved at the centroid of the first element. The fibre stress of bending $6M_{xx}/t^2 = 0.240\times10^6$ is here more than twice the membrane fibre stress $N_{\theta\theta}/t = 0.115\times10^6$ while the ratio U_γ/U_K of global strain energies, see (5.4.5), is of order unity.

An important observation follows with regard to the controversy over the merits of flat plate and curved shell finite elements. There are

frequent criticisms concerning the use of flat plate elements with regard to a supposed deficiency namely, the absence of coupling between bending and membrane actions within the individual elements. The above assessment of edge effect, which derives entirely from considerations of a single flat strip of flat finite elements, shows that these disparagements are without foundation.

5.6 Assessment of inextensional bending by a matrix procedure

To conclude the invesigation of bending action the rudiments of a matrix procedure are introduced. Although specific to the particular element described above it holds good promise of further development to facilitate the diagnosis of shell finite element assemblies suffering from deficiency in response to inextensional bending. The matrix procedure is an elaboration upon the well-known principle whereby presumed rigid body movements are revealed from eigenvalue analysis of the stiffness matrix without need for reference to actual comparison solutions.

The stiffness matrix of extensional deformation is straightforward to obtain, it is simply the stiffness matrix of the transitional model where the bending freedoms are made known by the number of extra zero eigenvalues over and above those corresponding to the rigid body movements. Each associated eigenvector should then be obtained in some linear combination of the specific vectors of rigid body, inextensional bending and local rotational movement.

It is convenient to work in terms of a specific example, so attention is focused on the simple 6 finite element shell model which projects onto the x^{α}-plane as an equilateral hexagon as shown in Fig. 5.9. The numerical results are specific to the quadratic reference surface of (5.3.7) and values for the constants E, ν and t are given in (5.4.6).

The model has $n_v = 7$, $n_s = 12$, $n_{\Gamma s} = 6$, $n_{\Gamma} = 1$ and when these values are substituted into (5.3.1)-(5.3.6) they give

$$N = 33, \qquad M_{ib} = 3, \qquad M_l = 12, \qquad N_b = 15, \qquad N_m = 12 \ . \qquad (5.6.1)$$

Clearly an immediate purpose of the assessment is to rederive these values of M_{ib}, M_l, N_b and N_m for they are generally unknown in advance.

Recall that the global stiffness matrix $[K]$ may be written as the sum of the extensional $[K_\gamma]$ and flexural $[K_K]$ stiffness matrices,

$$[K] = [K_\gamma] + [K_K] \ , \qquad [K_\gamma], [K_K] \in R^{33\times 33} \ . \qquad (5.6.2)$$

The assessment begins by testing for the existence of mechanisms in the transitional model where each finite element is assumed to have zero flexural rigidity. Any absence of suitable numbers and kinds of mechanism is taken to indicate that it is unlikely to have a satisfactory response to the actions of 'inextensional' bending and edge effect when $[K_K]$ is non zero as in the actual bending model. Let λ_γ denote the eigenvalue of $[K_\gamma]$, the stiffness matrix of the transitional model, where

$$[K_\gamma]\underline{u} = \lambda_\gamma \underline{u} \ , \qquad \underline{u}^T\underline{u} = 1, \qquad \underline{u} \in R^{N\times 1} \qquad (5.6.3)$$

where $\underline{u}$ denotes a vector of global connection quantities. The eigenvalues λ_γ are assumed to be arranged into ascending order of magnitude. Select the first n eigenvectors (n as yet unknown) which correspond to mechanisms and rigid body movements and arrange them into the columns of a matrix

$$[A] \in R^{33\times n} \ , \qquad n < 33 \qquad (5.6.4)$$

so that a linear combination of these eigenvectors may be written

$$\underline{u} = [A]\underline{d} \ , \qquad \underline{d} \in R^{n\times 1} \ , \qquad (5.6.5)$$

where $\underline{d}$ is an arbitrary vector of constants. Since the bending rigidity has been removed it follows that the associated eigenvalues of λ_γ should be zero if the eigenvectors, i.e. the columns of [A], are to qualify as describing mechanisms and rigid body movements. In any event, the nth eigenvalue should be small enough to satisfy a measure of negligibility such as

$$\lambda_\gamma^{(n)}/\lambda_\gamma^{(n+1)} \leq t/R , \qquad n > 6 \tag{5.6.6}$$

as in (5.4.4) and (5.4.5). Every eigenvector in [A] should then describe the rigid body movements and nonlocal and local mechanisms in some combination. It is now necessary to identify the different kinds of movements.

For the finite element model of Fig. 5.9 it is found from (5.6.3) that there are $n = 21$ eigenvectors with $\lambda_\gamma = 0$ where $\lambda_\gamma^{(22)} = 0.67\times10^4$ so that in (5.6.4)

$$[A] \in R^{33\times21} . \tag{5.6.7}$$

In (5.6.5), let

$$\underline{d} = [D]\underline{d}' , \qquad [D] \in R , \qquad \underline{d}' \in R \tag{5.6.8}$$

where $\underline{d}'$ is another arbitrary vector of constants and [D] is the matrix of eigenvectors satisfying the eigenvalue problem

$$[A]^T[K_K][A]\underline{d}' = \mu\underline{d}' . \tag{5.6.9}$$

The model in Fig. 5.9 gives the required 6 eigenvectors with $\mu = 0$ so that the first six columns in [A'] ,

$$[A'] = [A][D], \qquad [A'] \in R^{33\times 21} \tag{5.6.10}$$

are vectors of rigid body movement.

Now, omit the first six columns of $[A']$ and then the primes so that $n = 15$ and

$$[A] \in R^{33\times 15}, \qquad \underline{d} \in R^{15\times 1}. \tag{5.6.11}$$

It is good practice to normalise the columns of this new matrix $[A]$ and it remains to distinguish between the nonlocal and local mechanisms. Note that it has already been established that

$$N_b = 15, \qquad N_m = N - N_b - 6 = 12. \tag{5.6.12}$$

Let $[A]$ be tested in the first instance for single connector (i.e. local) mechanisms, in other words test whether there exists one or more vectors $\underline{d}$ such that

$$[A]\underline{d} = (\delta_{1k}, \delta_{2k}, \ldots, \delta_{33k})^T \tag{5.6.13}$$

where δ_{ij} is the Kronecker delta and where the suffix k picks out the single connector which is responsible for the mechanism. In the Appendix it is seen on writing

$$\underline{u} = [A]([A]^T[A])^{-1}[A]^T\underline{u}^*, \qquad \underline{u}^* \in R^{33\times 1} \tag{5.6.14}$$

where $\underline{u}^*$ is a dummy global connections vector, that the symmetric matrix

$$[A]([A]^T[A])^{-1}[A]^T \tag{5.6.15}$$

is unique with respect to any substitution of [A] with [A][D] , where [D] is arbitrary and of full rank. Moreover, the matrix in (5.6.5) reveals each single connector mechanism by its zero column and row with unit coefficient at the diagonal position. The model in Fig. 5.9 gives 12 such single connector mechanisms which reconcile with the 12 mid-side rotation connectors giving

$$M_l = 12, \qquad M_{ib} = N_b - M_l = 3 \tag{5.6.16}$$

Subsequent removal of the contributions of these 12 single connector mechanisms from [A] then permits reduction by standard means to the $M_{ib} = 3$ linearly independent columns which describe nonlocal mechanisms orthogonalised with respect to the local mechanisms. The identification of a local mechanism which involves more than one connector requires a different procedure whose development is left for future research.

The remaining 12 eigenvectors arising out of the solution to this eigenproblem for $[K_\gamma]$ in (5.6.3) are associated with eigenvalues which range over $0.67\times10^4 \leq \lambda_\gamma \leq 0.42\times10^6$. These eigenvectors give connector values of pure membrane action in the transitional model. Note, however that such connector values are not unique. This is because the pure membrane stresses remain unchanged when their eigenvectors of connector values are supplemented by any combination of the other 21 eigenvectors associated with $\lambda_\gamma = 0$, i.e. associated with rigid body movements and nonlocal and local mechanisms. This lack of uniqueness is a clear reflection of classical membrane shell theory where the stresses derive solely from considerations of equilibrium.

Satisfactory existence of presumed rigid body movements and of local and nonlocal mechanisms signals that it is worth giving attention to the bending model where the quality of the nonlocal mechanisms can be assessed in their interpretation as movements of 'inextensional' bending. The objective here is at first sight somewhat surprising. It is to perform a routine series of patch tests for inextensional bending which determine the

strain energy ratios U_γ/U_K of (5.4.5) simply from examination of the global stiffness matrices $[K_\gamma]$ and $[K_K]$ and without any reference to the exact solutions for the real shell.

A preliminary step is to condense out all the interior connectors and so it is convenient to write the strain energy U as

$$U = \frac{1}{2}\underline{u}^T[K]\underline{u} = \frac{1}{2}(\underline{u}_1^T\ \underline{u}_2^T)\begin{bmatrix}[K_{11}] & [K_{12}]\\ [K_{21}] & [K_{22}]\end{bmatrix}\begin{Bmatrix}\underline{u}_1\\ \underline{u}_2\end{Bmatrix} \qquad (5.6.17)$$

where vector $\underline{u}_1$ denotes the n_1 boundary connectors and $\underline{u}_2$ denotes the n_2 interior connectors so that

$$[K_{11}] \in R^{n_1 \times n_1}, \qquad [K_{12}] \in R^{n_1 \times n_2}, \qquad [K_{22}] \in R^{n_2 \times n_2}. \qquad (5.6.18)$$

The strain energies U_γ and U_K may be expressed similarly. In Fig. 5.9 the model gives $n_1 = 24$, $n_2 = 9$ so that

$$\underline{u}_1 \in R^{24\times 1}, \qquad \underline{u}_2 \in R^{9\times 1}. \qquad (5.6.19)$$

By the usual means,

$$\underline{u}_2 = -[K_{22}]^{-1}[K_{21}]\ \underline{u}_1, \qquad (5.6.20)$$

so that this $\underline{u}_2$ is the solution vector for all patch tests with prescribed boundary connectors $\underline{u}_1$ under the condition of homogeneous equilibrium in the interior of the shell model.

The next step is to seek the appropriate number of vectors $\underline{u}$ which describe 'inextensional' bending to the satisfactory exclusion of membrane strain. Noting that (5.6.20) gives

$$\underline{u} = \begin{pmatrix}[I]\\ -[K_{22}]^{-1}[K_{21}]\end{pmatrix}\underline{u}_1 \qquad (5.6.21)$$

with $[I] \in R^{24\times24}$ the identity matrix, it is suitable to consider the symmetric eigenproblem

$$[K'_\gamma]\underline{u}_1 = \lambda'_\gamma\underline{u}_1 \ , \qquad \underline{u}_1^T\underline{u}_1 = 1 \ , \qquad [K'_\gamma] \in R^{24\times24} \ , \quad \underline{u}_1 \in R^{24\times1} \tag{5.6.22}$$

where

$$\left.\begin{aligned} [K'_\gamma] &= [K_{\gamma 11}] - [K_{12}][K_{22}]^{-1}[K_{\gamma 21}] - [K_{\gamma 12}][K_{22}]^{-1}[K_{21}] \\ &\quad + [K_{12}][K_{22}]^{-1}[K_{\gamma 22}][K_{22}]^{-1}[K_{21}] \ , \\ [K'_K] &= [K_{K11}] - [K_{12}][K_{22}]^{-1}[K_{K21}] - [K_{K12}][K_{22}]^{-1}[K_{21}] \\ &\quad + [K_{12}][K_{22}]^{-1}[K_{K22}][K_{22}]^{-1}[K_{21}] \ , \end{aligned}\right\} \tag{5.6.23}$$

with

$$\left.\begin{aligned} U_\gamma &= \tfrac{1}{2}\underline{u}^T[K_\gamma]\underline{u} = \tfrac{1}{2}\underline{u}_1[K'_\gamma]\underline{u}_1 \ , \\ U_K &= \tfrac{1}{2}\underline{u}^T[K_K]\underline{u} = \tfrac{1}{2}\underline{u}_1[K'_K]\underline{u}_1 \ , \end{aligned}\right\} \tag{5.6.24}$$

where $[K_K]$ is recorded here in readiness for later use. The eigenvalues λ'_γ of (5.6.22) give

$$\lambda'_\gamma = 2U_\gamma \tag{5.6.25}$$

and their values are listed in Table 5.9 where the presence of more than six λ'_γ which are identically zero is to be welcomed but experience with more complicated bending models indicates that the number of these zeros is not easily predictable and hence is not particularly meaningful.

Investigation of the transitional model has shown that their should be $M_{ib} = 3$ inextensional bending movements. If similar movements exist in

the bending model, then their vectors must be contained somewhere within the first few eigenvectors of (5.6.22) where the extensional strain energy U_γ is suitably small. In the light of the values listed in Table 5.9 it is entirely appropriate to consider for this purpose the first 15 eigenvectors where the eigenvalues satisfy the measure of (5.6.6) with $t/R = 0.27\times10^{-3}$,

$$\lambda'^{(15)}_\gamma/\lambda'^{(16)}_\gamma = 0.32\times10^{-5}, \qquad \lambda'^{(16)}_\gamma/\lambda'^{(17)}_\gamma = 0.16 \ . \tag{5.6.26}$$

Let these 15 eigenvectors be denoted by $[A]$, where

$$[A] \in R^{24\times15} \ . \tag{5.6.27}$$

It is now the purpose to determine whether in $[A]$ there is some linear combination of the vectors which are capable of describing:

- six rigid body movements which can be fixed on prescribing three U^3 with three U^1, U^2 connectors in $\underline{u}_1$,
- three 'inextensional' bending movements which can be fixed on prescribing the remaining three U^3 connectors in $\underline{u}_1$ in addition to the connectors already prescribed above.

(5.6.28)

Similarly as in (5.6.9) and (5.6.10) it is simple to rearrange the columns of matrix $[A]$ so that its first six columns are vectors of presumed rigid body movement. Now rearrange the rows of matrix $[A]$ so that they correspond with (5.6.28) and hence provide the partition

$$\overset{24\times15}{[A]} = \begin{bmatrix} \overset{6\times6}{[A_{11}]} & \overset{6\times9}{[A_{12}]} \\ \overset{3\times6}{[A_{21}]} & \overset{3\times9}{[A_{22}]} \\ \overset{15\times6}{[A_{31}]} & \overset{15\times9}{[A_{32}]} \end{bmatrix} , \tag{5.6.29}$$

where it is good practice to ensure that the columns are normalised. For a sensible choice of connectors which fix the rigid body movements, as in (5.6.28), the matrix $[A_{11}]$ should be non-singular with well conditioned inverse; hence the reduction

$$\begin{bmatrix} 6\times6 & 6\times9 \\ [A_{11}] & [A_{12}] \\ \\ 3\times6 & 3\times9 \\ [A_{21}] & [A_{22}] \\ \\ 15\times6 & 15\times9 \\ [A_{31}] & [A_{32}] \end{bmatrix} \Rightarrow \begin{bmatrix} 6\times6 & 6\times9 \\ [I_6] & [0] \\ \\ 3\times6 & 3\times9 \\ [A'_{21}] & [A'_{22}] \\ \\ 15\times6 & 15\times9 \\ [A'_{31}] & [A'_{32}] \end{bmatrix}, \tag{5.6.30}$$

where $[I_6] \in R^{6\times6}$ is the identity matrix and

$$\left.\begin{aligned} [A'_{21}] &= [A_{21}][A_{11}]^{-1}, \quad [A'_{22}] = [A_{22}] - [A_{21}][A_{11}]^{-1}[A_{12}], \\ [A'_{31}] &= [A_{31}][A_{11}]^{-1}, \quad [A'_{32}] = [A_{32}] - [A_{31}][A_{11}]^{-1}[A_{12}], \end{aligned}\right\} \tag{5.6.31}$$

If the three inextensional bending movements are present, then the matrix

$$[A'_{22}][A'_{22}]^T = \left([A_{22}] - [A_{21}][A_{11}]^{-1}[A_{12}]\right)\left([A_{22}] - [A_{21}][A_{11}]^{-1}[A_{12}]\right)^T \tag{5.6.32}$$

should also be non-singular with well-conditioned inverse leading to the final reduction

$$\begin{bmatrix} 6\times6 & 6\times9 \\ [I_6] & [0] \\ \\ 3\times6 & 3\times9 \\ [A'_{21}] & [A'_{22}] \\ \\ 15\times6 & 15\times9 \\ [A'_{31}] & [A'_{32}] \end{bmatrix} \Rightarrow \begin{bmatrix} 6\times6 & 6\times3 \\ [I_6] & [0] \\ \\ 3\times6 & 3\times3 \\ [A'_{21}] & [I_3] \\ \\ 15\times6 & 15\times3 \\ [A'_{31}] & [A''_{32}] \end{bmatrix}, \tag{5.6.33}$$

where $[I_3] \in R^{3\times3}$ is the identity matrix and

$$[A'_{32}] = [A'_{32}][A'_{22}]^T\left([A'_{22}][A'_{22}]^T\right)^{-1} \quad . \qquad (5.6.34)$$

Each of the last three columns at the right-hand side of (5.6.33) should then describe an inextensional bending movement albeit with the likelihood of exaggerated curvature changes.

The actual calculations provide condition number C_E ,

$$C_E = ||[A'_{22}][A'_{22}]^T||_E||\left([A'_{22}][A'_{22}]^T\right)^{-1}||_E = 13.2 \qquad (5.6.25)$$

where suffix E denotes the Euclidean norm and this value is considered acceptable. Values of U_γ/U_K are listed in Table 5.10 and these are seen to be in accordance with the requirement of (5.4.5). Note that a more refined analysis where the U_K in Table 5.10 are minimised, leads here only to very small adjustments in the ratios U_γ/U_K .

5.7 Membrane action

In this section results are presented of numerical experiments which investigate the ability of the vehicle elements to recover the remaining characteristic mode of deformation i.e. membrane action.

It is appropriate to note that the quality of membrane strain γ_m in a 'pure' membrane action in the bending model, relative to effective exclusion of curvature change κ_m , is measured in classical first approximation shell theory by

$$\frac{1}{2}t\kappa_m = O((t/R)\gamma_m), \qquad \text{i.e. } \kappa_m = O(\gamma_m/R) \ , \qquad (5.7.1)$$

(c.f. (5.4.2)). It therefore follows that 'pure' membrane action may be defined to occur under the classical theory whenever

$$U_K/U_\gamma = O(t/R) \ , \qquad (5.7.2)$$

(c.f. (5.4.5)). In a similar manner to the investigation of bending action the shell finite element model is assessed through patch tests, with prescribed kinematic boundary conditions, now for capacity to simulate 'pure' membrane action under first approximation theory. As for the previous patch test comparison examples it is assumed that the real shell surface projects onto the x^α-plane as an equilateral triangle with side length 2 units and with three vertices resting on the x^α-plane. The x^3 coordinate is given by the quadratic polynomial

$$30x^3 = -3 + 3(x^1 - 1)^2 + 6\sqrt{3}x^2 - 5(x^2)^2 \ , \qquad (5.7.3)$$

which gives a surface symmetrical about $x^1 = 1$ with principal radii of curvature 3.107 and -5.059 at the centroidal position $x_1 = 1$, $x^2 = 1/\sqrt{3}$ of its projection. Thus the shell is deep with strongly negative Gaussian curvature. Displacement connectors U^i and rotation connectors ϕ_1, on the boundary of the finite element model are assigned with the same values as determined by the solutions described in Section 4.4 for the real shell. Similarly, three U^α connectors are assigned so as to fix a rigid body movement in the x^α-plane.

Values for the constant vectors $\underline{a}$, $\underline{b}$, $\underline{c}$, see (4.4.1), defining the comparison solution are given in Table 5.11. Values obtained from the approximate solution of the U^i connectors at the centroid position in the finite element models assembled for a range of successive mesh refinements are shown in Table 5.12 along with comparison real shell values. Values for the constants E and ν are as in (5.4.6) and and the shell thickness is now $t = 0.05$. The results of further calculations are given in Table 5.13 where global strain energies U_γ and U_K are listed together with the most significant principal values of membrane strain γ_m and curvature change κ_m in the finité element which encloses the centroidal

position of the given finite element models. The reference surface of this shell gives

$$\frac{t}{R} = 0.16 , \qquad \left(\frac{t}{R}\right)^2 = 0.24\times10^{-1} , \qquad \frac{(t)^2}{2R} = 0.39\times10^{-2} , \quad (5.7.4)$$

at the centroidal position. The tables show that engineering accuracy is achieved and the values of κ_m are seen to fulfil the criteria of (5.7.1) which, along with (5.7.4), provides a definition of membrane action. Also, in the global sense, 'pure' membrane action of the finite element model is demonstrated in that the ratio U_κ/U_γ is seen to be in accordance with the order of magnitude, see (5.7.2), demanded by first approximation theory. The values of the membrane stress resultants of 'pure' membrane action at the centroidal position also compare favourably with those for the real shell.

5.8 Linear stability problems

The design of thin walled structural components which are to be subject to significant compressive or shearing loads in their plane usually involves an estimate of their lowest buckling load. Buckling occurs when when a structure converts membrane strain energy into strain energy of bending. A thin walled structure having low bending stiffness but high membrane stiffness may fail dramatically because large bending deformations develop during buckling.

In order to study buckling using the finite element method a matrix is needed that accounts for the change in potential energy associated with rotation of line elements under load. This matrix, which is denoted $[k_\sigma]$, is called the geometric stiffness or initial stress stiffness matrix, and accounts for the effect of existing membrane forces on the bending stiffness.

The following analysis follows that of a classical linear buckling problem and is therefore subject to the following restrictions. Forces applied to the structure are fixed in magnitude, global direction and point of application on the structure. Buckling displacements and rotations are small, membrane stresses remain constant at the instant of buckling and the problem is linear in the displacement variables.

The restriction to linear problems implies that stresses used to form $[k_\sigma]$ can be found by a standard linear analysis. A further independent analysis is then performed to find the displacements of buckling. In this class of buckling problem the distribution of stress is unaltered and the analysis proceeds to find the intensity which produces instability.

A geometric stiffness matrix is derived by adding higher order terms to the strain-displacement relations and is described as consistent, see Cook (1981), if it is built using the same shape functions used to build the conventional stiffness matrix. An assumed displacement field is rarely competent enough to model the actual structural deformations, whether the problem is static deflection or buckling, and it is interesting to consider the effect of using different displacement fields.

Before buckling occurs it is assumed that the structure is subject to a system of two-dimensional stresses comprising a membrane state of unit intensity. At some multiple λ of this membrane state buckling is assumed to occur. The principle of stationary potential energy for the buckling problem takes the form, see Washizu (1982),

$$\delta\Pi = 0 \qquad (5.8.1)$$

where

$$\Pi = \frac{1}{2}\int_\Omega \frac{h^2}{12} E^{\alpha\beta\lambda\mu}\kappa_{\alpha\beta}\kappa_{\lambda\mu}\sqrt{a}\, d\xi^1 d\xi^2 + \frac{1}{2}\lambda\int_\Omega \overset{\circ}{N}{}^{\alpha\beta} u_{3,\alpha} u_{3,\beta}\sqrt{a}\, d\xi^1 d\xi^2 \ . \qquad (5.8.2)$$

For use with the vehicle element this functional must be modified so as to allow for a discontinuous deflection field. Use of Lagrange multipliers in a similar manner to that in Section 5.2 gives

$$\Pi = \frac{1}{2}\sum_{e}\left\{\int_{\Omega_e}\frac{h^2}{12}E^{\alpha\beta\lambda\mu}\kappa_{\alpha\beta}\kappa_{\lambda\mu}\sqrt{a}\,d\xi^1 d\xi^2 + \underline{\frac{1}{2}\lambda\int_{\Omega_e}\overset{\circ}{N}{}^{\alpha\beta}u_{3,\alpha}u_{3,\beta}\sqrt{a}\,d\xi^1 d\xi^2}\right\} \tag{5.8.3}$$

$$- \sum_{e}\underline{\int_{\Gamma_e}\lambda(u_3 - \tilde{u}_3)\overset{\circ}{N}_{1',\lambda'}u_{3,\lambda'}\,d\xi^{2'}}\ ,$$

where $\overset{\circ}{N}{}^{\alpha\beta}$ are initial in-plane stress resultants, λ is the multiplying factor of the in-plane stress resultants necessary to achieve initial buckling and $\tilde{u}_3$ is the line distribution of normal displacement on Γ_e common to adjacent elements.

Now seek matrix expressions for the terms in the above variational equation. The first variation of the boundary integral is given by

$$\delta\Pi_{\Gamma e} = \int_{\Gamma e}\left(\overset{\circ}{N}_{1',1'}\frac{\partial\delta u_3}{\partial\xi^{1'}} + \overset{\circ}{N}_{1',2'}\frac{\partial\delta u_3}{\partial\xi^{2'}}\right)(u_3 - \tilde{u}_3)$$

$$+ \int_{\Gamma e}\left(\overset{\circ}{N}_{1',1'}\frac{\partial u_3}{\partial\xi^{1'}} + \overset{\circ}{N}_{1',2'}\frac{\partial u_3}{\partial\xi^{2'}}\right)\delta(u_3 - \tilde{u}_3)\,d\xi^{2'} \tag{5.8.4}$$

$$= \delta\underline{w}[F]^T\int_{\Gamma e}\left([\Sigma_\alpha]^T[H]^T\overset{\circ}{\underline{N}}\,\tilde{\underline{\Sigma}}^T + \tilde{\underline{\Sigma}}\,\overset{\circ}{\underline{N}}[H][\Sigma_\alpha]\right)d\xi^{2'}[F]\underline{w}$$

where

$$\underline{w}^T = [u_1^3,\ u_2^3,\ u_3^3,\ \phi_{1',4},\ \phi_{1',5},\ \phi_{1',6}] \tag{5.8.5}$$

$$[F] = \begin{bmatrix} 1 & 0 & 0 & 0 & 0 & 0 \\ 0 & 1 & 0 & 0 & 0 & 0 \\ 0 & 0 & 1 & 0 & 0 & 0 \\ -1 & l_{12}/2(l_1)^2 & l_{31}/2(l_1)^2 & 2A/l_1 & 0 & 0 \\ l_{12}/2(l_2)^2 & -1 & l_{23}/2(l_2)^2 & 0 & 2A/l_2 & 0 \\ l_{31}/2(l_3)^2 & l_{23}/2(l_3)^2 & -1 & 0 & 0 & 2A/l_3 \end{bmatrix} \tag{5.8.6}$$

$$[\Sigma_\alpha] = \begin{bmatrix} 1 & 0 & -1 & 1+2\xi^1+2\xi^2 & 1-2\xi^1 & 0 \\ 0 & 1 & -1 & 1+2\xi^1+2\xi^2 & 0 & 1-2\xi^2 \end{bmatrix}, \tag{5.8.7}$$

$$\underline{\tilde{\Sigma}} = [\ 0\ 0\ 0\ (1-\xi^1-\xi^2)(\xi^1+\xi^2)\ \ \xi^1(1-\xi^1)\ \ \xi^2(1-\xi^2)\ ]\ . \tag{5.8.8}$$

$$[H] = \begin{bmatrix} h^1_{1',i} & h^2_{2',i} \\ h^1_{2',i} & h^2_{2',i} \end{bmatrix}, \tag{5.8.9}$$

where $i = 1,2,3$ as appropriate to the element side.

From the above it is seen that the boundary integral involves an integrand which is cubic in the coordinates ξ^α. In the numerical calculations a second order Gauss-Legendre integration rule is chosen, which is able to exactly integrate a cubic polynomial.

Transforming to global coordinates gives

$$\delta\Pi_{\Gamma e} = \delta\underline{U}[T]^T[F]\int_{\Gamma e}\left([\Sigma_\alpha]^T[H]^T\underline{\overset{\circ}{N}}\ \underline{\tilde{\Sigma}}^T + \underline{\tilde{\Sigma}}\ \underline{\overset{\circ}{N}}[H][\Sigma_\alpha]\right) d\xi^{2'}[F][T]\underline{U}\ , \tag{5.8.10}$$

where the matrix $[T] \in R^{6\times 12}$ is used to relate $\underline{w}$ to the global connection vector of (5.2.41).

The remaining contribution to the element geometric matrix derives from the second area integral in (5.8.3). This is denoted by

$$\delta\Pi_\Omega = \delta\underline{U}^T[T][F]\int_\Omega [\Sigma_\alpha]^T[H]^T[\overset{\circ}{N}][H][\Sigma_\alpha]\ \sqrt{a}\ d\xi^1 d\xi^2\ [F][T]\underline{U} \tag{5.8.11}$$

where the matrix of initial in-plane stresses is given by

$$[\overset{\circ}{N}] = \begin{bmatrix} \overset{\circ}{N}_{1'1'} & \overset{\circ}{N}_{1'2'} \\ \overset{\circ}{N}_{1'2'} & \overset{\circ}{N}_{2'2'} \end{bmatrix} \tag{5.8.12}$$

Having established matrix expressions for $\delta\Pi_\Omega$ and $\delta\Pi_\Gamma$ it is now straightforward to identify the resulting form of the element geometric matrix

$$[k_\sigma] = [T]^T[F]\Big\{ \int_{\Omega_e} [\Sigma_\alpha]^T[H]^T[N][H][\Sigma\,]\ \sqrt{a}\ d\xi\ d\xi + \int_{\Gamma e} \Big([\Sigma_\alpha]^T[H]\underline{N}\ \underline{\tilde{\Sigma}}^T + \underline{\tilde{\Sigma}}\ \underline{N}^T[H]^T[\Sigma_\alpha]\Big)\ d\xi^{2'}\Big\}[F][T] \tag{5.8.13}$$

Assembly of each of the element matrices $[k]$ and $[k_\sigma]$ gives the global matrices $[K]$ and $[K_\sigma]$ where the global matrix is based on an arbitrary reference intensity of membrane stress resultants. The modified potential energy principle gives, after a first variation,

$$\delta\underline{U}^T\Big([K] + \lambda[K_\sigma]\Big)\underline{U} = 0\ . \tag{5.8.14}$$

This is a generalised eigenvalue equation for the linear stability problem. The critical buckling load is associated with the lowest magnitude eigenvalue of (5.8.14). The computed eigenvalue will be negative if membrane forces are taken as positive in tension. A negative eigenvalue also indicates a reversed direction of shear loading. The corresponding eigenvectors identify the buckled shape, but not its magnitude.

The results of a number of simple examples are given in Tables 5.14 and 5.15 for an isotropic flat plate and a cylindrically curved panel subject to various uniform in-plane loading conditions. The kinematic boundary conditions for the buckling problem are assumed to correspond to either simply supported or clamped edges and the finite element solutions are compared with classical solutions given by Timoshenko and Gere (1961). The examples are calculated using a range of mesh refinements over the whole mesh or, by use of symmetry, from the corresponding mesh over a quarter of the plate or panel. In all examples, the constants E, h and ν are given as in (5.4.6).

The three sets of results labelled A,B,C listed for each combination of boundary and loading conditions in Tables 5.14 and 5.15 correspond to different choices of interpolation for evaluating the terms of (5.8.3) which are shown underlined. For case A u_3 and $\tilde{u}_3$ are both linear polynomials, in case B u_3 is quadratic and $\tilde{u}_3$ is linear and for case C both u_3 is a quadratic polynomial and the contribution from the boundary integral is ignored. Note that case A corresponds to the geometric matrix proposed by Cook (1969).

The results show that convergence to a buckling solution is attained for each of the test cases. Unfortunately, shortage of time has not allowed study of the more fundamental aspect of reconciling the concept of mechanisms in thin shell analysis with the actual buckling pattern.

CHAPTER 6

AN ERROR ANALYSIS

6.1 Introduction

In this chapter a theoretical analysis of the numerical method is given for the triangular flat facet element approximation of circular cylindrical shells. The analysis combines the earlier work on the differential geometry of surfaces with some of the tools of finite element error analysis to provide estimates for the interpolation characteristics for the vehicle element in terms of the characteristic size of an element in a regular family of triangulations. Although the considered middle surface geometry is simple, the error analysis is very complicated. This observation suggests that as a means of validating a candidate shell element this type of analysis has limited use as a routine procedure, unlike those described earlier which demand recovery of characteristic solutions on patches of elements. The intention here is to complement the results of the above numerical experiments and give a theoretical demonstration of the convergence of the vehicle element.

It is a consequence of the complexity of the shell problem that although the literature has extensive accounts of the performance of shell elements in some simple test problems it is only recently that studies have become available which examine the convergence properties of shell finite elements. Some early work on the approximation of a circular arch subject to surface loads and satisfying clamped boundary conditions is given by Ciarlet (1975), Kikuchi (1975) and Johnson (1975) considers the case of a general arch. The extension of these works to a circular cylinder is given by Kikuchi (1984) and Bernadou et al (1988). Until recently there were no results for shells having arbitrarily curved middle surface geometry. Here

the pioneering work of Bernadou (1976, 1980, 1982, 1988) must be acknowledged. Indeed it is in this work that the present less ambitious, yet complementary, contribution is grounded.

The basic idea in the following analysis is to consider the strain energy of the smooth shell middle surface to be approximated by the sum of membrane and bending energies determined element by element on the approximate faceted middle surface. The goal is then to show that this discrete representation of the strain energy can be made to approach that of the smooth shell by refining the mesh in a regular way.

Due to the nonconformity of the vehicle element displacement field it is necessary to introduce an intermediate problem which considers an approximation over smooth curvilinear triangular patches defined on the middle surface, with patch and facet vertices coincident. Since the basis vectors for each patch are identical to those of the smooth shell middle surface, this approximation may be considered as a finite element method which is conforming for the geometry but nonconforming for the displacements.

In order to get an approximate energy from the facet model which is consistent with the energy of the smooth shell it is necessary to introduce some constraints on the functions used to describe the displacement field over the facet and patch surfaces. The required estimate in strain energies is derived by considering the difference between facet and patch, and patch and smooth shell energies.

Note that in the following the additional notation $()_h$ is used to denote quantities that are defined element by element.

6.2 The continuous problem

Consider a portion of a cylindrical shell. On the middle surface take curvilinear coordinates (ξ^1, ξ^2) where ξ^1 and ξ^2 are in the longitudinal and circumferential direction respectively, both having the

dimensions of length. The middle surface is assumed to be developed from a rectangular region, see Fig. 6.1.

The displacement and distributed force of the shell are denoted by $\underline{v} = (v_1, v_2, v_3)$ and $\underline{f} = (f_1, f_2, f_3)$ where v_i and f_i are in the ξ^i directions. The rotations of the shell are denoted by ϕ_1 and ϕ_2, and satisfy

$$\left.\begin{aligned} \phi_1 &= v_{3,1} , \\ \phi_2 &= v_{3,2} - \tfrac{1}{R} v_3 . \end{aligned}\right\} \tag{6.2.1}$$

The shell is assumed to be clamped on the middle surface boundary $\Gamma = \underline{r}(\partial\Omega)$ i.e.

$$\underline{v}|_\Gamma = 0 , \qquad \partial_\nu v_3|_\Gamma = 0 , \tag{6.2.2}$$

where ∂_ν denotes the outward normal derivative operator. The strain displacement relations are given by (3.2.16) and (3.2.23):

$$\left.\begin{aligned} \gamma_{11}(\underline{v}) &= v_{1,1} + \tfrac{1}{R} v_3 , & \rho_{11}(\underline{v}) &= v_{3,11} - \tfrac{1}{R} v_{1,1} , \\ \gamma_{22}(\underline{v}) &= v_{2,2} , & \rho_{22}(\underline{v}) &= v_{3,22} , \\ \gamma_{12}(\underline{v}) &= \tfrac{1}{2}(v_{1,2} + v_{2,1}) , & \rho_{12}(\underline{v}) &= v_{3,12} - \tfrac{1}{4R}(v_{1,2} - 3v_{2,1}) . \end{aligned}\right\} \tag{6.2.3}$$

Note that the component of twist ρ_{12} has been modified by the addition of γ_{12}/R, as is possible in first approximation theory, in preparation for the following analysis.

The total potential energy of the shell may be expressed as

$$\Pi(\underline{v}) = \int_{\Omega} \frac{Et}{1-\nu^2}\Big\{(1-\nu)\gamma^{\alpha}_{\beta}(\underline{v})\gamma^{\beta}_{\alpha}(\underline{v}) + \nu\gamma^{\alpha}_{\alpha}(\underline{v})\gamma^{\beta}_{\beta}(\underline{v}) + \frac{t^2}{12}\Big[(1-\nu)\rho^{\alpha}_{\beta}(\underline{v})\rho^{\beta}_{\alpha}(\underline{v}) + \nu\rho^{\alpha}_{\alpha}(\underline{v})\rho^{\beta}_{\beta}(\underline{v})\Big] - f^{i}v_{i}\Big\}\sqrt{a}\, d\xi^1 d\xi^2 \tag{6.2.4}$$

The actual displacement of the shell in equilibrium is characterised by minimising the total potential energy subject to the essential boundary conditions (6.2.2).

In order to formulate the above problem more precisely introduce notation for the function spaces related to Ω. Use is made of the real Sobolev spaces $H^m(\Omega)$ with norm $\|\cdot\|_m$, where m is a non negative integer. In particular the inner product and norm of $L_2(\Omega) \equiv H^0(\Omega)$ are denoted by $(\cdot,\cdot)$ and $\|\cdot\|$. The space $\underline{V}$ of admissible displacements is defined by

$$\underline{V} = \{\underline{v} = (v_1, v_2, v_3) \in \{(H^1(\Omega))^2 \times H^2(\Omega);\ \underline{v}|_{\Gamma} = \partial_{\nu} v_3|_{\Gamma} = 0\}\ , \tag{6.2.5}$$

equipped with the norm

$$\|\underline{v}\|_{\underline{V}} = \left(\|v_1\|^2_{1,\Omega} + \|v_2\|^2_{1,\Omega} + \|v_3\|^2_{2,\Omega}\right)\ . \tag{6.2.6}$$

Choosing $\underline{u}$ and $\underline{v}$ to be arbitrary functions of $\underline{V}$ and assuming the force $\underline{f}$ to be chosen from $(L_2(\Omega))^3$ provides the following statement of the shell problem:

Given $\underline{f} \in (L(\Omega)_2)^3$, find $\underline{u} \in \underline{V}$ that minimises the functional $\Pi(\underline{u})$, which may be written

$$\Pi(\underline{u}) = \tfrac{1}{2}a(\underline{u},\underline{u}) - \sum_{i=1}^{3}(f_i, u_i) \tag{6.2.7}$$

The necessary and sufficient condition for $\underline{u} \in \underline{V}$ to be the minimising function of the above functional is

$$a(\underline{u},\underline{v}) = \sum_{i=1}^{3} (f_i, v_i) \tag{6.2.8}$$

where

$$\begin{aligned} a(\underline{u},\underline{v}) = \int_{\Omega} \frac{Et}{1-\nu^2} \Big\{ & (1-\nu)\gamma^{\alpha}_{\beta}(\underline{u})\gamma^{\beta}_{\alpha}(\underline{v}) + \nu\gamma^{\alpha}_{\alpha}(\underline{u})\gamma^{\beta}_{\beta}(\underline{v}) \\ & + \frac{t^2}{12}\left[(1-\nu)\rho^{\alpha}_{\beta}(\underline{u})\rho^{\beta}_{\alpha}(\underline{v}) + \nu\rho^{\alpha}_{\alpha}(\underline{u})\rho^{\beta}_{\beta}(\underline{v})\right] \sqrt{a}\, d\xi^1 d\xi^2 \end{aligned} \tag{6.2.9}$$

With regards the existence and uniqueness of the solution to (6.2.8) the following results of Bernadou and Ciarlet (1976) are recorded.

The bilinear form $a(\cdot,\cdot)$ is $\underline{V}$-elliptic in the sense that there exists a positive constant C such that

$$a(\underline{u},\underline{u}) \geq C \, ||\underline{u}||^2_{\underline{V}} \qquad \text{for any } \underline{u} \in \underline{V} \tag{6.2.10}$$

It then follows by use of the Lax-Millgram lemma, see Ciarlet (1978), that for each $\underline{f} \in (L_2(\Omega))^3$, there exists a unique solution to (6.2.9). Furthermore

$$||\underline{u}||_{\underline{V}} \leq C\left\{\sum_{i=1}^{3} ||f_i||^2\right\} \tag{6.2.11}$$

where C is a positive constant independent of $\underline{f}$.

6.3 The patchwise defined problem

Consider a finite element shell model in which an approximation is made only of the displacement components. In effect consider a curved element approximation based on the curvilinear coordinates (ξ^1,ξ^2) .

Since $\bar{\Omega}$ is a polygon, it may be exactly covered by a regular family of curvilinear triangulations T_h and assume each subdivision satisfies the regularity conditions, see Ciarlet (1978):

(i) there exists a constant σ such that

$$\text{for each } K \in T_h \ , \ \frac{h_K}{\rho_K} < \sigma \ , \tag{6.3.1}$$

where $h_K = \text{diam}(K)$ and $\rho_K = \sup\{\text{diam}(S)\text{: } S \text{ a ball contained in } K\}$;

(ii) the quantity

$$h = \max_{K \in T_h} h_K \tag{6.3.2}$$

approaches zero.

For the vehicle finite element it is necessary to consider the nonconforming finite element space $\underline{\hat{X}}_h = \hat{X}_{h1} \times \hat{X}_{h1} \times \hat{X}_{h2}$. The functions of $\hat{X}_{h1}$ are such that

$$\left.\begin{aligned} &\text{(i) on every } K \in T_h \text{ , they belong to } P_1(K) \text{ ;} \\ &\text{(ii) on every } K \in T_h \text{ , they are determined by their} \\ &\qquad \text{values at the vertices of } K \text{ ;} \\ &\text{(iii) } \hat{X}_{h1} \in C^0(\bar{\Omega}) \ . \end{aligned}\right\} \tag{6.3.3}$$

and the functions of $\hat{X}_{h2}$ are such that

$$\left.\begin{aligned}
&\text{(i) on every triangle } K \in T_h \text{, they belong to } P_2(K) \text{ ;}\\
&\text{(ii) on every triangle } K \in T_h \text{, they are determined by their}\\
&\quad \text{values at the vertices and the value of } \phi_1, \text{ at the}\\
&\quad \text{midside nodes;}\\
&\text{(iii) } \hat{X}_{h2} \in \prod_{K \in T_h} H^2(K) \text{ .}
\end{aligned}\right\} \qquad (6.3.4)$$

Taking the boundary conditions into account provides for the definition of the space $\hat{\underline{V}}_h$ in which the patch solution is sought, where

$$\left.\begin{aligned}
\hat{V}_{h1} &= \{v \mid v \in H^1(\Omega),\ v|_\Gamma = 0\} \text{ ,}\\
\hat{V}_{h2} &= \{v \mid v \in \prod_{K \subset T_h} H^2(K) \text{ , } v|_\Gamma = \partial_\nu v|_\Gamma = 0\} \text{ ,}
\end{aligned}\right\} \qquad (6.3.5)$$

so that the nonconformity of the patch displacement field is due to the normal displacement component $\hat{v}_{h3} \in \hat{V}_{h2}$. In other words $\hat{\underline{V}}_h$ is not a subspace of $\underline{V}$ and the patchwise problem involves a nonconforming approximation.

The discrete problem for the deformation of the patch model of the shell may be expressed as:

Given $\underline{f} \in (L_2(\Omega))^3$ find $\hat{\underline{u}}_h \in \hat{\underline{V}}_h$ such that

$$\hat{a}_h(\hat{\underline{u}}_h, \hat{\underline{v}}_h) = \sum_{i=1}^{3} (f_i, \hat{v}_{hi}) \text{ , } \qquad \forall\ \hat{\underline{v}}_h \in \hat{\underline{V}}_h \text{ , } \qquad (6.3.6)$$

where the approximate bilinear form $\hat{a}_h(.,.)$ is given by

$$\begin{aligned}
\hat{a}_h(\hat{\underline{u}}_h, \hat{\underline{v}}_h) = \sum_{K \in T_h} \int_K \frac{Et}{1-\nu^2} \Big\{ &(1-\nu)\gamma_{h\beta}^{\alpha}(\hat{\underline{u}}_h)\gamma_{h\alpha}^{\beta}(\hat{\underline{v}}_h) + \nu\gamma_{h\alpha}^{\alpha}(\hat{\underline{u}}_h)\gamma_{h\beta}^{\beta}(\hat{\underline{v}}_h)\\
&+ \frac{t^2}{12}\left[(1-\nu)\rho_{h\beta}^{\alpha}(\hat{\underline{u}}_h)\rho_{h\alpha}^{\beta}(\hat{\underline{v}}_h) + \nu\rho_{h\alpha}^{\alpha}(\hat{\underline{u}}_h)\rho_{h\beta}^{\beta}(\hat{\underline{v}}_h)\right] \sqrt{a_h}\, d\xi^1 d\xi^2 \text{ ,}
\end{aligned} \qquad (6.3.7)$$

6.4 The discrete problem using the vehicle flat element

The assembly of flat finite elements gives an approximate middle surface defined by the approximate mapping $\underline{r}_h$ which is the linear interpolant of $\underline{r}$. This approximation replaces the smooth middle surface M of the real shell by a faceted middle surface M_h, see Fig. 6.1. By construction, the images of the vertices of the triangulation are in the middle surface M.

To each flat facet $k = \underline{r}_h(K)$, $K \in T_h$ it is possible to associate a local basis, fundamental forms etc. as in Chapter 5. All these quantities are constant over any given triangle $K \in T_h$ with, in general, discontinuities on interelement faces due to the discontinuity of the first derivatives of $\underline{r}_h$.

Now construct the discrete space $\tilde{\underline{V}}_h$ in which the facet solution is to be sought. To this end first introduce the space

$$\tilde{\underline{X}}_h = \tilde{X}_{h1} \times \tilde{X}_{h1} \times \tilde{X}_{h2} \,. \tag{6.4.1}$$

This is used to approximate the displacement components $\tilde{v}_{hi}$ on the local base vectors $\underline{a}_{hi}$ corresponding to a facet displacement field $\tilde{\underline{v}}_h$. Since the local base vectors are constant in any given element the functions of $\tilde{X}_{hi}$ are determined element by element without regard for the connection conditions between adjacent elements.

The functions of the space $\tilde{X}_{h1}$ are such that in any triangle $K \in T_h$ with vertices $\underline{\Sigma}_i$ the restriction $v_{h|K}$ of any function $v_h \in X_{h1}$ is such that

$$\left.\begin{aligned} &\text{(i)}\ v_{h|K} \in P_1(K)\ ; \\ &\text{(ii)}\ v_{h|K}\ \text{is completely specified by the values}\ v_{h|K}(\underline{\Sigma}_i) \\ &\qquad (i = 1,2,3)\ . \end{aligned}\right\} \tag{6.4.2}$$

The functions in the space $\tilde{\tilde{X}}_{h2}$ are such that on any triangle $K \in T_h$ with midside nodes $\underline{\Lambda}_i$ the restriction $v_{h|K}$ of any function $v_{h|K} \in \tilde{\tilde{X}}_{h2}$ is such that

$$\left.\begin{aligned} &\text{(i) } v_{h|K} \in P_2(K) \text{ ;} \\ &\text{(ii) } v_{h|K} \text{ is completely specified by the values } v_{h|K}(\underline{\Sigma}_i) \text{ , and} \\ &\quad \phi_{h1',|K}(\underline{\Lambda}_i) \ (i = 1,2,3). \end{aligned}\right\} \quad (6.4.3)$$

Next consider two facets k^+ and k^- of the approximate middle surface M_h which have a common vertex or edge. The shared vertices and midside nodes provide for the following consistency conditions.

First, a common vertex $\underline{\Sigma}$ may be associated with

(i) a point on the smooth shell middle surface M . Any displacement field $\underline{v} \in \underline{V}$ of the middle surface at the point $\underline{\sigma}$ may be expressed as

$$\underline{v}(\underline{\Sigma}) = v_i(\underline{\Sigma})\underline{a}^i(\underline{\Sigma}) \quad (6.4.4)$$

where the point $\underline{\Sigma}$ denotes the point in Ω whose image under $\underline{r}$ is the corresponding point $\underline{\sigma}$ on the middle surface;

(ii) a vertex of the facet $k^+ = \underline{r}_h(K^+)$. The displacement field $\underline{\tilde{\tilde{v}}}_h \in \underline{\tilde{\tilde{X}}}_h$ ofthe faceted surface M_h has the following displacement components at the point $\underline{\sigma}^+ \equiv \underline{\sigma}$;

$$\underline{\tilde{\tilde{v}}}_h(\underline{\Sigma}^+) = \tilde{\tilde{v}}_{hi}(\underline{\Sigma}^+)\underline{a}_h^{+i} \ , \quad (6.4.5)$$

(iii) a vertex of the facet $k^- = \underline{r}_h(K^-)$. Similarly, as in (ii) the point $\underline{\sigma}^- \equiv \underline{\sigma}$ has associated displacement components

$$\underline{\tilde{\tilde{v}}}_h(\underline{\Sigma}^-) = \tilde{\tilde{v}}_{hi}(\underline{\Sigma}^-)\underline{a}_h^{-i} \ , \quad (6.4.6)$$

Secondly, a common midside node $\underline{\Lambda}$ may be associated with

(i) a point on the smooth shell middle surface. The rotation component at the point $\underline{\Lambda}$ may be expressed as

$$\hat{\phi}_{h1'}(\underline{\Lambda}) = (h_1^{\lambda}, (\hat{v}_{h3,\lambda} + b_{\lambda}^{\mu}\hat{v}_{h\mu}))(\underline{\Lambda}) \tag{6.4.7}$$

(ii) a midside node of the facet $k^+ = \underline{r}_h(K^+)$. The rotation at the point $\underline{\Lambda}^+ \equiv \underline{\Lambda}$ may be expressed

$$\tilde{\tilde{\phi}}_{h1'}(\underline{\Lambda}^+) = h_{h1}^{\alpha}, \tilde{\tilde{v}}_{h3,\alpha}(\underline{\Lambda}_i^+) \tag{6.4.8}$$

(ii) a midside node of the facet $k^- = \underline{r}_h(K^-)$. The rotation at the point $\underline{\Lambda}^- \equiv \underline{\Lambda}$ may be expressed

$$\tilde{\tilde{\phi}}_{h1'}(\underline{\Lambda}^-) = h_{h1}^{\alpha}, \tilde{\tilde{v}}_{h3,\alpha}(\underline{\Lambda}_i^-) \tag{6.4.9}$$

The consistency conditions require the degrees of freedom of the space $\tilde{\tilde{\underline{X}}}_h$ to satisfy the following.

(i) The displacement vector $\tilde{\tilde{\underline{v}}}_h$ is continuous at the vertices $\underline{\sigma}$ of the surface so that

$$\tilde{\tilde{\underline{v}}}_h(\underline{\Sigma}^+) = \tilde{\tilde{\underline{v}}}_h(\underline{\Sigma}^-) = \hat{\underline{v}}_h(\underline{\Sigma}), \qquad \forall\ \underline{\Sigma} \in T_h \tag{6.4.10}$$

(ii) The rotations satisfy

$$\tilde{\tilde{\phi}}_{h1'}(\underline{\Lambda}^+) = \tilde{\tilde{\phi}}_{h1'}(\underline{\Lambda}^-) = \hat{\phi}_{h1'}(\underline{\Lambda}) , \qquad \forall\ \underline{\Lambda} \in T_h \tag{6.4.11}$$

Incorporating these conditions provides for the definition of the space $\tilde{\underline{X}}_h$:

$$\underset{\sim}{\tilde{X}}_h = \{\underset{\sim}{\tilde{v}}_h \in \underset{\sim}{\tilde{X}}_h : \underset{\sim}{\tilde{v}}_h \text{ satisfies (6.4.10) and (6.4.11)}\} . \qquad (6.4.12)$$

Note that a displacement $\underset{\sim}{\tilde{v}}_h \in \underset{\sim}{\tilde{X}}_h$ associates the functions $\tilde{v}_{hi}$ element by element which are such that

(i) $\tilde{v}_{h\alpha}$ form a discontinuous plane faceted surface. This follows from the fact that $\tilde{v}_{h\alpha|K} \in P_1(K)$ and the displacement components are referred to base vectors which are constant element by element and, in general, discontinuous between elements.

(ii) $\tilde{v}_{h3}$ forms a discontinuous curved faceted surface. This follows for similar reasons as in (i) but now $\tilde{v}_{h3|K} \in P_2(K)$.

(iii) the displacement field $\underset{\sim}{\tilde{v}}_h \in \underset{\sim}{\tilde{X}}_h$ associates with the approximate middle surface a discontinuous curved faceted surface which is continuous at the vertices of the corresponding triangulation and has derivatives $\partial_\nu \tilde{v}_{h3}$ continuous at midside nodes.

Thus, the space $\underset{\sim}{\tilde{X}}_h$ does not have sufficient smoothness for the inclusion $\underset{\sim}{\tilde{X}}_h \in (H^1(\Omega))^2 \times H^2(\Omega)$ to hold but only the weaker element by element condition holds

$$\underset{\sim}{\tilde{X}}_h \in \prod_{K \in T_h} H^1(K) \times H^1(K) \times H^2(K) . \qquad (6.4.13)$$

The function space $\underset{\sim}{\tilde{V}}_h$ consists of those functions of $\underset{\sim}{\tilde{X}}_h$ satisfying the essential boundary conditions of (6.2.3).

The displacement field $\underset{\sim}{\tilde{v}}_h \in \underset{\sim}{\tilde{X}}_h$ of the faceted surface provides for the definition, element by element, of the components of approximate membrane strain $\tilde{\gamma}_{h\alpha\beta}$ and curvature change $\tilde{\rho}_{h\alpha\beta}$ as follows

$$\tilde{\gamma}_{h\alpha\beta}(\underset{\sim}{\tilde{v}}_h) = \frac{1}{2}(\underset{\sim}{\tilde{v}}_{h\alpha,\beta} + \underset{\sim}{\tilde{v}}_{h\alpha,\beta}) \qquad (6.4.14)$$

$$\tilde{\rho}_{h\alpha\beta}(\underset{\sim}{\tilde{v}}_h) = \underset{\sim}{\tilde{v}}_{h3,\alpha\beta} \qquad (6.4.15)$$

and the approximate bilinear and linear forms are

$$\tilde{a}_h(\underline{\tilde{v}}_h,\underline{\tilde{w}}_h) = \sum_{K\in T_h}\int_K \frac{Et}{1-\nu^2}\Big\{(1-\nu)\tilde{\gamma}_{h\beta}^{\alpha}(\underline{\tilde{v}}_h)\tilde{\gamma}_{h\alpha}^{\beta}(\underline{\tilde{w}}_h) + \nu\tilde{\gamma}_{h\alpha}^{\alpha}(\underline{\tilde{v}}_h)\tilde{\gamma}_{h\beta}^{\beta}(\underline{\tilde{w}}_h)$$

$$+ \frac{t^2}{12}\Big[(1-\nu)\tilde{\rho}_{h\beta}^{\alpha}(\underline{\tilde{v}}_h)\tilde{\rho}_{h\alpha}^{\beta}(\underline{\tilde{w}}_h) + \nu\tilde{\rho}_{h\alpha}^{\alpha}(\underline{\tilde{v}}_h)\tilde{\rho}_{h\beta}^{\beta}(\underline{\tilde{w}}_h)\Big]\sqrt{a_h}\,d\xi^1 d\xi^2 \,, \tag{6.4.16}$$

$$\tilde{f}_h(\underline{\tilde{v}}_h) = \sum_{i=1}^{3}(f_i,\tilde{v}_{hi}) \,. \tag{6.4.17}$$

So that the strain energy of the faceted shell is approximated by the sum of the uncoupled membrane and bending energies of each element.

The discrete problem for the deformation of the facet model of the shell may be expressed as:

Find $\underline{\tilde{u}}_h \in \underline{\tilde{V}}_h$ such that

$$\tilde{a}_h(\underline{\tilde{u}}_h,\underline{\tilde{v}}_h) = \tilde{f}_h(\underline{\tilde{v}}_h) \,, \qquad \forall\ \underline{\tilde{v}}_h \in \underline{\tilde{V}}_h \,, \tag{6.4.18}$$

where $\tilde{a}_h(.,.)$ and $\tilde{f}_h(.)$ are defined by (6.4.16) and (6.4.17).

The remainder of the proof depends on some well-known and fundamental results of interpolation errors, see Ciarlet (1978), theory of nonconforming elements, see Ciarlet (1978), Stummel (1980), Lascaux and Lesaint (1975), Rannacher (1979), and error estimates of geometric approximation.

6.5 Patchwise approximation

Define the nonconforming analogue of the norm $||\cdot||_h$ by

$$||\hat{\underline{v}}_h||_h = \left\{\sum_{K\in T_h}^{3} ||\hat{v}_{h1}||_{1,K}^2 + ||\hat{v}_{h2}||_{1,K}^2 + ||\hat{v}_{h3}||_{2,K}^2\right\} \tag{6.5.1}$$

The above may be regarded as a norm over each $\underline{\hat{V}}_h$ and can be extended in a natural manner so that it is well defined for functions in $\underline{\hat{V}}_h + \underline{V}$.

Kikuchi (1984) has shown, using the techniques of Stummel (1980), that:

for sufficiently small h , the following bounds hold

$$c_1 ||\underline{\hat{v}}_h||_h^2 \geq \hat{a}_h(\underline{\hat{v}}_h, \underline{\hat{v}}_h) \geq c_1 ||\underline{\hat{v}}_h||_h^2 \qquad (6.5.2)$$

for any $\underline{\hat{v}}_h \in \underline{\hat{V}}_h$, where C_1 and C_2 are positive constants independent of h and $\underline{v}_h$.

From this it follows that the discrete analogue of (6.2.12) may be expressed:

For sufficiently small h , the solution of (6.3.6) exists uniquely in $\underline{\hat{V}}_h$ for $\underline{f} \in (L_2(\Omega))^3$. Furthermore

$$||\underline{\hat{u}}_h||_h \leq c \left(\sum_{i=1}^{3} ||f_i||^2\right)^{1/2} \qquad (6.5.5)$$

This last result ensures the uniform boundedness of the norms of the finite element solutions with respect to h . Utilising the discrete compactness properties and the convergence theorem of nonconforming methods proved by Stummell (1980) provides the route to the proof of the finite element solution in the sense

$$\lim_{h \to 0} ||\underline{u}_h - \underline{u}||_h = 0 \; . \qquad (6.5.6)$$

Consider the case where the solution $\underline{u} \in \underline{V}$ of (6.2.9) is sufficiently smooth so that

$$\underline{u} \in \underline{V} + \underline{W} \tag{6.5.7}$$

where $\underline{W} = H^2(\Omega)\times H^2(\Omega)\times H^3(\Omega)$ with norm

$$||\underline{v}||_{\underline{W}} = \left(||v_1||^2_{2,\Omega} + ||v_2||^2_{2,\Omega} + ||v_3||^2_{3,\Omega}\right)^{1/2} \tag{6.5.8}$$

In a manner parallel to the analysis of Lascaux and Lesaint (1975) and Rannacher (1979) it is possible to obtain the asymptotic estimate

$$||\hat{\underline{u}}_h - \underline{u}||_h \leq Ch||\underline{u}||_{\underline{W}} \tag{6.5.9}$$

where C is a positive constant independent of h and $\underline{u}$ for sufficiently small h .

6.6 Flat element approximations

Consider the restriction $\tilde{\underline{v}}_h|_K$ to a triangle $K \in T$ of any function $\tilde{\underline{v}}_h \in \tilde{\underline{X}}_h$. For convenience of expression this will be denoted in the following simply by $\tilde{\underline{v}}_h$. By construction $\tilde{v}_{h\alpha}$ is a linear polynomial over the element, so that for any point $\underline{\xi} = (\xi^1, \xi^2) \in K$ the following hold

$$\tilde{v}_{h\alpha}(\underline{\xi}) = \sum_{i=1}^{3} L_i \tilde{v}_{h\alpha}(\underline{\Sigma}_i) \ , \tag{6.6.1}$$

$$\tilde{v}_{h\alpha,\beta}(\underline{\xi}) = \sum_{i=1}^{3} L_{i,\beta}\, \tilde{v}_{h\alpha}(\underline{\Sigma}_i) \ , \tag{6.6.2}$$

where $\underline{\Sigma}_i = (\xi_i^1, \xi_i^2)$ $(i = 1\ ,2,3)$ are the vertices of the triangle K and L_i are the linear Lagrangian shape functions for a triangle.

The consistency conditions at the element vertices require the equality of displacement vectors of the facet and corresponding patch, i.e.

$$\tilde{\underline{v}}_h(\underline{\Sigma}_i) = \hat{\underline{v}}_h(\underline{\Sigma}_i) \ . \tag{6.6.3}$$

Resolving each displacement vector along the respective base vectors for the facet and patch and then forming scalar products with $\underline{a}_h{}^\beta$ gives

$$\tilde{v}_{h\alpha}(\underline{\Sigma}_i) = \sum_{j=1}^{3} d_{h\alpha}^{\ j} \tilde{v}_{hj}(\underline{\Sigma}_i) \ , \qquad i=1,2,3 \tag{6.6.4}$$

where the coefficients

$$d_{hk}^{j}(\underline{\xi}) = \underline{a}^j(\underline{\xi})\cdot\underline{a}_{hk} \ , \qquad \underline{\xi} \in K. \tag{6.6.5}$$

Using (6.6.4) and (6.6.5) to substitute into (6.6.2) gives

$$\tilde{v}_{h\alpha,\beta}(\underline{\xi}) = \sum_{i=1}^{3} d_{h\alpha}^{\ j}(\underline{\Sigma}_i)\ L_{i,\beta}\ \tilde{v}_{h\alpha}(\underline{\Sigma}_i) \ , \tag{6.6.6}$$

It is intended that this inequality be used to relate the derivatives of in-plane displacements on the facet to the derivatives of displacements on the corresponding patch. This is achieved by considering Taylor series expansions as follows.

Since the mapping defining the middle surface is assumed to be smooth the following expansions of the patch base vectors are valid:

$$\underline{a}^j(\underline{\Sigma}_i) = \underline{a}^j(\underline{\xi}) + (\xi_i^\lambda - \xi^\lambda)\underline{a}^j{}_{,\lambda}(\underline{\xi}) + O(h^2)\underline{c}_i^j \ , \tag{6.6.7}$$

$$\underline{a}_j(\underline{\Sigma}_i) = \underline{a}_j(\underline{\xi}) + (\xi_i^\lambda - \xi^\lambda)\underline{a}_{j,\lambda}(\underline{\xi}) + O(h^2)\underline{c}_{ji}, \tag{6.6.8}$$

where $\underline{c}_i^j$ and $\underline{c}_{ij}$ are constant vectors independent of h. So that, by making use of the Gauss and Weingarten relations, see (2.2.23) and (2.2.24), the base vectors may be written in terms of corresponding vectors at a general point $\underline{\xi} \in K$ as follows

$$\underline{a}^{\alpha}(\underline{\Sigma}_i) = \underline{a}^{\alpha}(\underline{\xi}) - \frac{1}{R}(\xi_i^{\lambda} - \xi^{\lambda})\delta_1^{\alpha}\underline{a}_3(\underline{\xi}) + O(h^2)\underline{c}_i^{\alpha} , \qquad (6.6.9)$$

$$\underline{a}_{\alpha}(\underline{\Sigma}_i) = \underline{a}_{\alpha}(\underline{\xi}) - \frac{1}{R}(\xi_i^{\lambda} - \xi^{\lambda})\delta_{\alpha}^{1}\underline{a}_3(\underline{\xi}) + O(h^2)\underline{c}_i , \qquad (6.6.10)$$

$$\underline{a}_3(\underline{\Sigma}_i) = \underline{a}_3(\underline{\xi}) + \frac{1}{R}(\xi_i^{\lambda} - \xi^{\lambda})\underline{a}_1(\underline{\xi}) + O(h^2)\underline{c}_i , \qquad (6.6.11)$$

The smoothness of the mapping $\underline{r}$ provides

$$\underline{r}(\underline{\Sigma}_i) = r(\underline{\xi}) + (\xi_i^{\lambda} - \xi^{\lambda})\underline{r}(\underline{\xi})_{,\lambda} + \frac{1}{2}(\xi_i^{\lambda} - \xi^{\lambda})(\xi_i^{\mu} - \xi^{\mu})\underline{r}_{,\lambda\mu}(\underline{\xi}) + O(h^2)\underline{c} \qquad (6.6.12)$$

Recall the following properties of the Lagrangian shape functions

$$\sum_{i=1}^{3} L_i = 1 , \quad \sum_{i=1}^{3} L_i(\xi_i^{\lambda} - \xi^{\lambda}) = 0 , \quad \sum_{i=1}^{3} L_{i,\alpha}(\xi_i^{\lambda} - \xi^{\lambda}) = \delta_{\alpha}^{\lambda} , \qquad (6.6.13)$$

and that

$$\frac{\partial L_i}{\partial \xi^{\alpha}} = O(h^{-1})c_{i\alpha} . \qquad (6.6.14)$$

So that the facet tangent base vectors may be expressed

$$\underline{a}_{h\alpha} = \underline{a}_{\alpha}(\underline{\xi}) - \frac{1}{2R}\sum_{i=1}^{3} L_{i,\alpha}(\xi_i^1 - \xi^1)^2\underline{a}_3 + O(h^2)\underline{c}_{\alpha} . \qquad (6.6.15)$$

Substituting into (6.6.5) from (6.6.9), (6.6.11) and (6.6.15) gives

$$d_{h\beta}^{\alpha}(\underline{\Sigma}_i) = \delta_{\beta}^{\alpha} + O(h^2)c_{\beta i}^{\alpha} , \qquad (6.6.16)$$

$$d_{h\alpha}^{3}(\underline{\Sigma}_i) = \frac{1}{R}\left[(\xi_i^1 - \xi^1)\delta_{\alpha}^1 - \frac{1}{2}\sum_{j=1}^{3} L_{i,\alpha}(\xi_j^1 - \xi^1)^2\right] + O(h^{\ })c_{\beta i}^{3} . \qquad (6.6.17)$$

since $\hat{v}_{h\alpha} \in P_1(K)$, $\hat{v}_{h3} \in P_3(K)$ and $\hat{v}_{hj} \in C^1(K)$ it follows by Taylor series expansion that for any $\underline{\xi} \subset K$,

$$\hat{v}_{h\alpha}(\underline{\Sigma}_i) = \hat{v}_{h\alpha}(\underline{\xi}) + (\xi_i^\lambda - \xi^\lambda)\hat{v}_{h\alpha,\lambda} , \tag{6.6.18}$$

$$\hat{v}_{h3}(\underline{\Sigma}_i) = \hat{v}_{h3}(\underline{\xi}) + (\xi_i^\lambda - \xi^\lambda)\hat{v}_{h3,\lambda}(\hat{\underline{\xi}}_i) , \tag{6.6.19}$$

where $\hat{\underline{\xi}}_i \in K$.

Combining (6.6.16), (6.6.17) with (6.6.6) and making use of the properties of the shape functions gives

$$\begin{aligned}\tilde{v}_{h\alpha,\beta}(\underline{\xi}) = \hat{v}_{h\alpha,\beta}(\underline{\xi}) + \delta_\alpha^1\delta_\beta^1 \frac{1}{R}\hat{v}_{h3}(\underline{\xi}) \\ + O(h)\left[c^j_{\alpha\beta}\hat{v}_{hj}(\underline{\xi}) + O(h)c^{\mu\omega}_{\alpha\beta}\hat{v}_{h\mu,\omega} + \sum_{i=1}^{3} c^\mu_{\alpha\beta i}\hat{v}_{h3,\mu}(\hat{\underline{\xi}}_i)\right]\end{aligned} \tag{6.6.20}$$

Thus, substituting into the definition of the facet membrane strain from (6.6.20),

$$\tilde{\gamma}_{h\alpha\beta}(\tilde{\underline{v}}_h) = \gamma_{\alpha\beta}(\hat{\underline{v}}_h) + O(h)\left[c^j_{\alpha\beta}\hat{v}_{hj}(\underline{\xi}) + O(h)c^{\mu\omega}_{\alpha\beta}\hat{v}_{h\mu,\omega} + \sum_{i=1}^{3} c^\mu_{\alpha\beta i}\hat{v}_{h3,\mu}(\hat{\underline{\xi}}_i)\right] \tag{6.6.21}$$

which is an expression relating the membrane strains in the facet element to those in the corresponding patch.

To obtain an estimate of the difference of these strain measures it is necessary to make use of the following result of interpolation theory in Sobolev space, see Ciarlet (1978),

$$|v_{hj}|_{p,\infty,K} \leq Ch^{-1}|v_{hj}|_{p,K} , \qquad p = 0,1 . \tag{6.6.22}$$

Integrating over K and taking into account the following estimate for the size of K

$$\text{meas}(K) = O(h^2) , \tag{6.6.23}$$

yields

$$|\tilde{\gamma}_{h\alpha\beta}(\tilde{\underline{v}}_h) - \gamma_{\alpha\beta}(\hat{\underline{v}}_h)|_{0,K} \leq Ch^2\left[\sum_{j=1}^{3}|\hat{v}_{hj}|^2_{0,\infty,K} + \sum_{j=1}^{3}|\hat{v}_{hj}|^2_{1,\infty,K}\right]^{1/2} \tag{6.6.24}$$

$$\leq Ch\left[||\hat{v}_{h1}||^2_{1,K} + ||\hat{v}_{h2}||^2_{1,K} + ||\hat{v}_{h3}||^2_{2,K}\right]^{1/2}$$

Attention is now focused on the expression for the facet normal displacement component in order to estimate the difference in curvature change measures in the facet and the corresponding patch. The analysis is considerably simplified by assuming the following property of the triangulations:

- the triangulations T_h are constructed so that any triangle in T has one of its edges lying on a generator of the cylinder, see Fig. 6.2. (6.6.25)

Consider again the restriction of a function $\tilde{\underline{v}}_h$ to a triangle K. By construction v_{h3} is a quadratic polynomial over K and is such that

$$\tilde{v}_{h3}(\underline{\xi}) = \sum_{i=1}^{3} M_i(\underline{\xi})\tilde{v}_{h3}(\underline{\Sigma}_i) + \sum_{i=1}^{3} N_i(\underline{\xi})\tilde{\phi}_{h1'}(\underline{\Lambda}_i) , \tag{6.6.26}$$

$$\tilde{v}_{h3,\alpha}(\underline{\xi}) = \sum_{i=1}^{3} M_{i,\alpha}(\underline{\xi})\tilde{v}_{h3}(\underline{\Sigma}_i) + \sum_{i=1}^{3} N_{i,\alpha}(\underline{\xi})\tilde{\phi}_{h1'}(\underline{\Lambda}_i) , \tag{6.6.27}$$

$$\tilde{v}_{h3,\alpha\beta}(\underline{\xi}) = \sum_{i=1}^{3} M_{i,\alpha\beta}(\underline{\xi})\tilde{v}_{h3}(\underline{\Sigma}_i) + \sum_{i=1}^{3} N_{i,\alpha\beta}(\underline{\xi})\tilde{\phi}_{h1'}(\underline{\Lambda}_i) , \tag{6.6.28}$$

where $\underline{\Lambda}_i$ (i=1,2,3) are the coordinates of the mid-side nodes of the triangle, and M_i, N_i are quadratic shape functions.

The equality of displacement vectors at the element vertices imposes the following relationship between the normal displacement component of the facet and the displacements of the patch

$$\tilde{v}_{h3}(\underline{\Sigma}_i) = d^j_{h3}(\underline{\Sigma}_i)\hat{v}_{hj}(\underline{\Sigma}_i) , \tag{6.6.29}$$

where d_{h3}^{j} are defined by (6.6.5). Expressions for these coefficients are obtained in a similar manner to the derivation of (6.6.16) and (6.6.17).

Thus by Taylor series expansion

$$\underline{a}^1(\underline{\Sigma}_i) = \underline{a}^1(\underline{\xi}) - \frac{1}{R}(\xi_i^1 - \xi^1)\underline{a}^3(\underline{\xi}) - \frac{1}{2R^2}(\xi_i^1 - \xi^1)^2\underline{a}^1(\underline{\xi}) + 0(h^{\ })\underline{c}_i^1 \ , \quad (6.6.30)$$

$$\underline{a}^2(\underline{\Sigma}_i) = \underline{a}^2(\underline{\xi}) \ , \quad (6.6.31)$$

$$\underline{a}_3(\underline{\Sigma}_i) = \underline{a}_3(\underline{\xi}) + \frac{1}{R}(\xi_i^1 - \xi^1)\underline{a}_1(\underline{\xi}) - \frac{1}{2R^2}(\xi_i^1 - \xi^1)^2\underline{a}_3(\underline{\xi}) + 0(h^3)\underline{c}_{3i} \ , \quad (6.6.32)$$

and similarly,

$$\underline{r}(\underline{\Sigma}_i) = \underline{r}(\underline{\xi}) + (\xi_i^\lambda - \xi^\lambda)\underline{a}_\lambda(\underline{\xi}) + \frac{1}{2}(\xi_i^\lambda - \xi^\lambda)(\xi_i^\mu - \xi^\mu)\underline{a}_{\lambda,\mu}(\underline{\xi}) + \frac{1}{6}(\xi_i^\lambda - \xi^\lambda)(\xi_i^\mu - \xi^\mu)(\xi_i^\omega - \xi^\omega)\underline{a}_{\lambda,\mu\omega}(\underline{\xi}) + 0(h^4)\underline{c}_i \ . \quad (6.6.33)$$

So that, as in the derivation of (6.6.15), the facet base vectors may be expressed

$$\underline{a}_{h\alpha} = \underline{a}_\alpha(\underline{\xi}) - \frac{1}{R}A_\alpha(\xi^1)\underline{a}_3(\underline{\xi}) - \frac{1}{R^2}B_\alpha(\xi^1)\underline{a}\ (\underline{\xi}) + 0(h^3)\underline{c}_\alpha \ , \quad (6.6.34)$$

where

$$A_\alpha(\xi^1) = \frac{1}{2}\sum_{i=1}^{3} L_{i,\alpha}(\xi_i^1 - \xi^1)^2 \ , \quad (6.6.35)$$

$$B_\alpha(\xi^1) = \frac{1}{2}\sum_{i=1}^{3} L_{i,\alpha}(\xi_i^1 - \xi^1)^3 \ . \quad (6.6.36)$$

The facet normal vector $\underline{a}_{h3}$ is defined by the vector product

$$\underline{a}_{h3} = \frac{1}{\sqrt{a_h}}\,\underline{a}_{h1} \times \underline{a}_{h2} \ , \quad (6.6.37)$$

see (2.1.19). Making use of (6.6.34) to substitute into the above definition gives

$$\underline{a}_{h3} = \frac{1}{\sqrt{a_h}}\left[\underline{a}_3(\underline{\xi}) + \frac{1}{R}A_\lambda(\xi^1)\underline{a}^\lambda(\underline{\xi}) - \frac{1}{R^2}B_1(\xi^1)\underline{a}_3(\underline{\xi}) + O(h^3)\underline{c}_3\right] , \quad (6.6.38)$$

where

$$a_h = 1 + \frac{1}{R^2}\left[(A_1(\xi^1))^2 + (A_2(\xi^1))^2 - 2B_1(\xi^1)\right] + O(h^3)c , \quad (6.6.39)$$

so that,

$$\underline{a}_{h3} = \underline{a}_3(\underline{\xi}) + \frac{1}{R}A_\lambda(\xi^1)\underline{a}^\lambda(\underline{\xi}) - \frac{1}{2R^2}\left[(A_1(\xi^1))^2 + (A_2(\xi^1))^2\right]\underline{a}_3(\underline{\xi}) + O(h^3)\underline{c}_3 . \quad (6.6.40)$$

With this expression it is possible to determine the quantities $d_{h3}^j(\underline{\Sigma}_i)$ by forming the appropriate scalar products defined by (6.6.5). The resulting expressions are

$$d_{h3}^1(\underline{\Sigma}_i) = \frac{1}{R}\left[A_1(\xi^1) - (\xi_i^1 - \xi^1)\right] + O(h^3)c_3^1 , \quad (6.6.41)$$

$$d_{h3}^2(\underline{\Sigma}_i) = \frac{1}{R}A_2(\xi^1) + O(h^3)c_3^2 , \quad (6.6.42)$$

$$d_{h3}^3(\underline{\Sigma}_i) = 1 + \frac{1}{R^2}A\ (\xi^1)(\xi_i^1 - \xi^1) - \frac{1}{R^2}(\xi_i^1 - \xi^1)^2 - \frac{1}{2R^2}\left[(A_1(\xi^1))^2 + (A_2(\xi^1))^2\right] + O(h^3)c_3^3 . \quad (6.6.43)$$

Combining (6.6.41)-(6.6.43) together with (6.6.29) provides the following expression for the facet normal displacement in terms of the corresponding displacements on the patch:

$$\tilde{v}_{h3}(\underline{\Sigma}_i) = \frac{1}{R}\left[A_1(\xi^1) - (\xi_i^1 - \xi^1)\right]\hat{v}_{h1}(\underline{\Sigma}_i) + \frac{1}{R}A_2(\xi^1)\hat{v}_{h2}(\underline{\Sigma}_i)$$

$$+ \left[1 + \frac{1}{R^2}A_1(\xi^1)(\xi_i^1 - \xi^1) - \frac{1}{2R^2}(\xi_i^1 - \xi^1)\right. \tag{6.6.44}$$

$$\left. - \frac{1}{2R^2}((A_1(\xi^1))^2 + (A_2(\xi^1))^2\right]\hat{v}_{h3}(\underline{\Sigma}_i) + O(h^3)c_3^j\hat{v}_{hj}(\underline{\Sigma}_i)$$

Substituting from (6.6.44) into (6.6.28) and recalling the second consistency condition of (6.4.11) provides an expression for the facet curvature change entirely in terms of quantities referred to the corresponding patch:

$$\tilde{\rho}_{h\alpha\beta}(\tilde{\underline{v}}_h) = \tilde{v}_{h3,\alpha\beta}(\underline{\xi})$$

$$= \sum_{i=1}^{3} M_{i,\alpha\beta}\left\{\frac{1}{R}\left[A_1(\xi^1) - (\xi_i^1 - \xi^1)\right]\hat{v}_{h1}(\underline{\Sigma}_i) + \frac{1}{R}A_2(\xi^1)\hat{v}_{h2}(\underline{\Sigma}_i)\right.$$

$$+ \left[1 + \frac{1}{R^2}A_1(\xi^1)(\xi_i^1 - \xi^1) - \frac{1}{2R^2}(\xi_i^1 - \xi^1)\right.$$

$$\left.\left. - \frac{1}{2R^2}((A_1(\xi^1))^2 + (A_2(\xi^1))^2\right]\hat{v}_{h3}(\underline{\Sigma}_i) + O(h^3)c_3^j\hat{v}_{hj}(\underline{\Sigma}_i)\right\}$$

$$+ \sum_{i=1}^{3} N_{i,\alpha\beta}h_1^{\lambda,}\left[\hat{v}_{h3,\lambda} - \frac{1}{R}\delta_\lambda^1\hat{v}_{h1}\right](\underline{\Lambda}_i)$$

$$= \sum_{i=1}^{3} M_{i,\alpha\beta}\hat{v}_{h3}(\underline{\Sigma}_i) + \sum_{i=1}^{3} N_{i,\alpha\beta}h_1^{\lambda,}\hat{v}_{h3,\lambda}(\underline{\Lambda}_i) \tag{6.6.45}$$

$$+ \sum_{i=1}^{3} M_{i,\alpha\beta}\left\{\frac{1}{R}\left[A_1(\xi^1) - (\xi_i^1 - \xi^1)\right]\hat{v}_{h1}(\underline{\Sigma}_i) + \frac{1}{R}A_2(\xi^1)\hat{v}_{h2}(\underline{\Sigma}_i)\right\}$$

$$+ \sum_{i=1}^{3} N_{i,\alpha\beta}(-h_1^{1,}\frac{1}{R}\hat{v}_{h1})(\underline{\Lambda}_i)$$

$$+ \sum_{i=1}^{3} M_{i,\alpha\beta}\left[\frac{1}{R^2}A_1(\xi^1)(\xi_i^1 - \xi^1) - \frac{1}{2R^2}(\xi_i^1 - \xi^1)\right.$$

$$\left. - \frac{1}{2R^2}((A_1(\xi^1))^2 + (A_2(\xi^1))^2\right]\hat{v}_{h3}(\underline{\Sigma}_i)$$

$$+ O(h)c_3^j\sum_{i=1}^{3}\hat{v}_{hj}(\hat{\underline{\xi}}_i)$$

This expression is simplified using the following results, which are a consequence of the assumption (6.6.25).

For a typical triangle in the mesh satisfying the assumption of (6.6.25), see Fig. 6.2, the quantities $A_\alpha(\xi^1)$ are such that

$$\left.\begin{aligned} A_1(\xi^1) &= \tfrac{1}{2}\left[(\xi_1^1 - \xi^1) + (\xi_2^1 - \xi^1)\right] , \\ A_2(\xi^1) &= 0 , \\ A_1(\xi^1) - (\xi_i^1 - \xi^1) &= A_1(\Sigma_i^1) , \\ A_1(\xi^1)(\xi_i^1 - \xi^1) - \tfrac{1}{2}(\xi_i^1 - \xi^1) &= \tfrac{1}{2}(\xi_1^1 - \xi^1)(\xi_2^1 - \xi^1) . \end{aligned}\right\} \qquad (6.6.46)$$

Thus, using (6.6.46)

$$\begin{aligned} &\sum_{i=1}^{3} M_{i,\alpha\beta}\left[A_1(\xi^1)(\xi_i^1 - \xi^1) - \tfrac{1}{2}(\xi_i^1 - \xi^1)\right]\hat{v}_{h3}(\underline{\Sigma}_i) \\ &= \tfrac{1}{2}(\xi_1^1 - \xi^1)(\xi_2^1 - \xi^1)\sum_{i=1}^{3} M_{i,\alpha\beta}\left[\hat{v}_{h3}(\underline{\xi}) + (\xi_i^\lambda - \xi^\lambda)\hat{v}_{h3,\lambda}(\hat{\underline{\xi}}_i)\right] \qquad (6.6.47) \\ &= \tfrac{1}{2}(\xi_1^1 - \xi^1)(\xi_2^1 - \xi^1)\sum_{i=1}^{3} M_{i,\alpha\beta}(\xi_i^\lambda - \xi^\lambda)\hat{v}_{h3,\lambda}(\hat{\underline{\xi}}_i) \\ &= O(h)c^{\lambda}_{\alpha\beta}\sum_{i=1}^{3} \hat{v}_{h3,\lambda}(\hat{\underline{\xi}}_i) , \end{aligned}$$

where use is made of the fact that a constant is invariant under the element interpolation scheme i.e.

$$\sum_{i=1}^{3} M_{i,\alpha\beta} = 0 . \qquad (6.6.48)$$

Similarly,

$$\sum_{i=1}^{3} M_{i,\alpha\beta}(A_1(\xi^1))^2\hat{v}_{h3}(\underline{\Sigma}_i)$$

$$= (A_1(\xi^1))^2 \sum_{i=1}^{3} M_{i,\alpha\beta}\left[\hat{v}_{h3}(\underline{\xi}) + (\xi_i^\lambda - \xi^\lambda)\hat{v}_{h3,\lambda}(\hat{\underline{\xi}}_i)\right] \qquad (6.6.49)$$

$$= O(h)c^{\lambda}_{\alpha\beta}\sum_{i=1}^{3} \hat{v}_{h3,\lambda}(\hat{\underline{\xi}}_i) \ .$$

Next, consider the function

$$A_1(\xi^1)\hat{v}_{h1}(\underline{\xi}) \ , \qquad (6.6.50)$$

which is a quadratic polynomial and so is invariant under the interpolation scheme of (6.6.26)-(6.6.28). Taking derivatives of this expression gives

$$(A_1(\xi^1)\hat{v}_{h1}(\underline{\xi}))_{,\alpha} = A_1(\xi^1)\hat{v}_{h1,\alpha} - \hat{v}_{h1}\delta^1_\alpha \ , \qquad (6.6.51)$$

$$(A_1(\xi^1)\hat{v}_{h1}(\underline{\xi}))_{,\alpha\beta} = -\hat{v}_{h1,\alpha}\delta^1_\beta - \hat{v}_{h1,\beta}\delta^1_\alpha \ ,$$

$$= -2\hat{v}_{h1,1}\delta^1_\alpha\delta^1_\beta - \hat{v}_{h1,2}(\delta^1_\alpha\delta^2_\beta + \delta^2_\alpha\delta^1_\beta) \ . \qquad (6.6.52)$$

Thus, by (6.6.28),

$$-2\hat{v}_{h1,1}\delta^1_\alpha\delta^1_\beta - \hat{v}_{h1,2}(\delta^1_\alpha\delta^2_\beta + \delta^2_\beta\delta^1_\alpha)$$

$$= \sum_{i=1}^{3} M_{i,\alpha\beta}A_1(\underline{\Sigma}_i)\hat{v}_{h1}(\underline{\Sigma}_i) + \sum_{i=1}^{3} N_{i,\alpha\beta}\left(h_1^\lambda, \left[A_1(\xi^1)\hat{v}_{h1,\alpha} - \hat{v}_{h1}\delta^1_\lambda\right]\right)(\underline{\Lambda}_i) \ . \qquad (6.6.53)$$

Now look at the function

$$f(\underline{\xi}) = -\frac{1}{2}\left[(\xi^1)^2 - \sum_{i=1}^{3} L_i(\underline{\xi})(\xi_i^1)^2\right] \ , \qquad (6.6.54)$$

which has the following properties

$$\left.\begin{aligned} f(\underline{\Sigma}_i) &= 0 \ , \\ f_{,1}(\underline{\xi}) &= A_1(\xi^1) \ , \\ f_{,2}(\underline{\xi}) &= 0, \\ f_{,\alpha\beta}(\underline{\xi}) &= -\delta^1_\alpha \delta^1_\beta \ . \end{aligned}\right\} \tag{6.6.55}$$

Since v_{h1} is a linear polynomial over K and $f(\underline{\xi})$ is invariant under the interpolation scheme it follows that

$$(f(\underline{\xi})\hat{v}_{h1,1})_{,\alpha\beta} = \sum_{i=1}^{3} M_{i,\alpha\beta} f(\underline{\Sigma}_i)\hat{v}_{h1,1} + \sum_{i=1}^{3} N_{i,\alpha\beta}(h_1^\lambda, f_{,\lambda})(\underline{\Lambda}_i)\hat{v}_{h1,1} \ ,$$

so that

$$-\delta^1_\alpha\delta^1_\beta\hat{v}_{h1,1} = \sum_{i=1}^{3} N_{i,\alpha\beta}(h_1^1, A_1(\xi^1))(\underline{\Lambda}_i)\hat{v}_{h1,1} \ . \tag{6.6.56}$$

Substituting into (6.6.53) using (6.6.56) gives

$$\begin{aligned} &-2\hat{v}_{h1,1}\delta^1_\alpha\delta^1_\beta - \hat{v}_{h1,2}(\delta^1_\alpha\delta^2_\beta + \delta^2_\alpha\delta^1_\beta) \\ &\quad = \sum_{i=1}^{3} M_{i,\alpha\beta} A_1(\underline{\Sigma}_i)\hat{v}_{h1}(\underline{\Sigma}_i) - \delta^1_\alpha\delta^1_\beta\hat{v}_{h1,1} + \sum_{i=1}^{3} N_{i,\alpha\beta}(h_1^\lambda, \hat{v}_{h1})(\underline{\Lambda}_i)\delta^1_\lambda \\ &\quad + \sum_{i=1}^{3} N_{i,\alpha\beta}(h_1^2, A_1(\xi^1))(\underline{\Lambda}_i)\hat{v}_{h1,2} \ . \end{aligned} \tag{6.6.57}$$

Note that the coordinates $\underline{\Lambda}_i = (\lambda_i^1, \lambda_i^2)$ of the mid-side nodes are related to the vertex coordinates by

$$\left.\begin{aligned} \lambda_1^1 = \lambda_3^1 &= \tfrac{1}{2}(\xi_1^1 + \xi_2^1) \ , \\ \lambda_2^1 &= \xi_1^1 \ . \end{aligned}\right\} \tag{6.6.58}$$

Expanding the last term on the right-hand side of (6.6.57) and substituting for λ_j^α from (6.6.58) gives

$$N_{2,\alpha\beta} h_1^2,(\underline{\Lambda}_2)(\xi_2^1 - \xi_1^1)\hat{v}_{h1,2} \ , \tag{6.6.59}$$

but for the special mesh with triangles K having side 2 parallel to the ξ^2 axis

$$h_1^2,(\underline{\Lambda}_2) = 0 \ , \tag{6.6.60}$$

so that the last term of (6.6.57) vanishes.

Substituting into (6.6.45) from (6.6.47), (6.6.49) and (6.6.56) gives

$$\tilde{\rho}_{h\alpha\beta}(\underline{\tilde{v}}_h) = \hat{v}_{h3,\alpha\beta} - \frac{1}{R}\delta_\alpha^1\delta_\beta^1\hat{v}_{h1,1} - \frac{1}{R}(\delta_\alpha^1\delta_\beta^2 + \delta_\alpha^2\delta_\beta^1)\hat{v}_{h1,2}$$

$$+ O(h)\sum_{i=1}^{3}\left[c_3^j\hat{v}_{hj}(\underline{\hat{\xi}}_i) + c_{\alpha\beta}^\lambda\hat{v}_{h3,\lambda}(\underline{\hat{\xi}}_i)\right] \tag{6.6.61}$$

$$= \rho_{\alpha\beta}(\underline{\hat{v}}_h) + O(h)\sum_{i=1}^{3}\left[c_3^j\hat{v}_{hj}(\underline{\hat{\xi}}_i) + c_{\alpha\beta}^\lambda\hat{v}_{h3,\lambda}(\underline{\hat{\xi}}_i)\right]$$

It is now possible to obtain an estimate for the difference in the curvature change measures of the facet and corresponding patch. Integrating over K and making use of (6.6.22) and (6.6.23) gives

$$\left|\tilde{\rho}_{h\alpha\beta}(\underline{\tilde{v}}_h) - \rho_{\alpha\beta}(\underline{\hat{v}}_h)\right| \le Ch^2\left[\sum_{i=1}^{3}|v_{hj}|_{0,\infty,K}^2 + \sum_{i=1}^{3}|v_{hj}|_{1,\infty,K}^2\right]^{1/2}$$

$$\le Ch\left[||v_{h1}||_{1,K}^2 + ||v_{h2}||_{1,K}^2 + ||v_{h3}||_{2,K}^2\right]^{1/2} . \tag{6.6.62}$$

6.7 Convergence and error estimate

It is necessary to estimate the consistency error

$$\left|\hat{a}_h(\underline{\hat{v}}_h, \underline{\hat{w}}_h) - \tilde{a}_h(\underline{\tilde{v}}_h, \underline{\tilde{w}}_h)\right| , \qquad \forall\ \underline{\hat{v}}_h , \underline{\hat{w}}_h \in \underline{\hat{X}}_h , \qquad \underline{\tilde{v}}_h , \underline{\tilde{w}}_h \in \underline{\tilde{X}}_h \tag{6.7.1}$$

which represents the error in the strain energies evaluated patch by patch and facet by facet. From the definitions of the bilinear forms (6.3.7) and (6.4.16) it follows that

$$|\hat{a}_h(\underline{\hat{v}}_h, \underline{\hat{w}}_h) - \tilde{a}_h(\underline{\tilde{v}}_h, \underline{\tilde{w}}_h)| \leq \sum_{K \in T_h} \sum_{i=1}^{4} |E_{Ki}| \tag{6.7.2}$$

where

$$\left.\begin{aligned} E_{K1} &= \int_K \frac{Et}{1+\nu}\left(\gamma_\beta^\alpha(\underline{\hat{v}}_h)\gamma_\alpha^\beta(\underline{\hat{w}}_h)\sqrt{a} - \tilde{\gamma}_{h\beta}^{\alpha}(\underline{\tilde{v}}_h)\tilde{\gamma}_{h\alpha}(\underline{\tilde{w}}_h)\sqrt{a_h}\right) d\xi^1 d\xi^2 , \\ E_{K2} &= \int_K \frac{Et}{1-\nu}\,\nu\left(\gamma_\beta^\alpha(\underline{\hat{v}}_h)\gamma_\alpha^\beta(\underline{\hat{w}}_h)\sqrt{a} - \tilde{\gamma}_{h\beta}^{\alpha}(\underline{\tilde{v}}_h)\tilde{\gamma}_{h\alpha}(\underline{\tilde{w}}_h)\sqrt{a_h}\right) d\xi^1 d\xi^2 , \end{aligned}\right\} \tag{6.7.3}$$

and two similar expressions involving ρ_β^α and $\rho_{h\beta}^\alpha$. Thus it is necessary to estimate the terms

$$|\gamma_{\alpha\beta}(\underline{\hat{v}}_h) - \tilde{\gamma}_{h\alpha\beta}(\underline{\tilde{v}}_h)|_{0,K}\,, \quad |\rho_{\alpha\beta}(\underline{\hat{v}}_h) - \tilde{\rho}_{h\alpha\beta}(\underline{\tilde{v}}_h)|_{0,K}\,, \quad |\sqrt{a} - \sqrt{a_h}|_{0,\infty,K}\,, \tag{6.7.4}$$

which are the differences in strain measures and determinant of the metric for the patch and associated facet.

Consider estimating $|E_{K1}|$. This may be written

$$\int_K [\gamma_\beta^\alpha(\underline{\hat{v}}_h)\gamma_\alpha^\beta(\underline{\hat{w}}_h)\sqrt{a} - \tilde{\gamma}_{h\beta}^{\alpha}(\underline{\tilde{v}}_h)\tilde{\gamma}_{h\alpha}^{\beta}(\underline{\tilde{w}}_h)\sqrt{a_h}]\, d\xi^1 d\xi^2$$

$$= \int_K (\sqrt{a} - \sqrt{a_h})\gamma_\beta^\alpha(\underline{\hat{v}})\gamma_\alpha^\beta(\underline{\hat{w}}_h)\, d\xi^1 d\xi^2 \tag{6.7.5}$$

$$+ \int_K \sqrt{a_h}[\gamma_\beta^\alpha(\underline{\hat{v}}_h)\gamma_\alpha^\beta(\underline{\hat{w}}_h) - \tilde{\gamma}_{h\beta}^{\alpha}(\underline{\tilde{v}}_h)\tilde{\gamma}_{h\alpha}^{\beta}(\underline{\tilde{w}}_h)]\, d\xi^1 d\xi^2 .$$

Recalling the estimate (6.6.39) it follows that

$$|\sqrt{a} - \sqrt{a_h}|_{0,\infty,K} \leq Ch^2 \tag{6.7.6}$$

and so

$$\left|\int_K (\sqrt{a} - \sqrt{a_h})\gamma_\beta^\alpha(\underline{\hat{v}})\gamma_\alpha^\beta(\underline{\hat{w}}_h)\, d\xi^1 d\xi^2\right| \le Ch^2 ||\underline{\hat{v}}_h||_h ||\underline{\hat{w}}_h||_h \qquad (6.7.7)$$

Similarly, using the estimate (6.6.24) it follows that

$$\left|\int_K \sqrt{a_h}[\gamma_\beta^\alpha(\underline{\hat{v}}_h)\gamma_\alpha^\beta(\underline{\hat{w}}_h) - \tilde{\gamma}_{h\beta}^{\alpha}(\underline{\tilde{v}}_h)\tilde{\gamma}_{h\alpha}^{\beta}(\underline{\tilde{w}}_h)]\, d\xi^1 d\xi^2\right|$$

$$\le \left|\int_K (\sqrt{a_h} - \sqrt{a})[\gamma_\beta^\alpha(\underline{\hat{v}}_h)\gamma_\alpha^\beta(\underline{\hat{w}}_h) - \tilde{\gamma}_{h\beta}^{\alpha}(\underline{\tilde{v}}_h)\tilde{\gamma}_{h\alpha}^{\beta}(\underline{\tilde{w}}_h)]\, d\xi^1 d\xi^2\right| \qquad (6.7.8)$$

$$+ \left|\int_K \sqrt{a}\,[\gamma_\beta^\alpha(\underline{\hat{v}}_h)\gamma_\alpha^\beta(\underline{\hat{w}}_h) - \tilde{\gamma}_{h\beta}^{\alpha}(\underline{\tilde{v}}_h)\tilde{\gamma}_{h\alpha}^{\beta}(\underline{\tilde{w}}_h)]\, d\xi^1 d\xi^2\right|$$

$$\le Ch ||\underline{\hat{v}}_h||_h ||\underline{\hat{w}}_h||_h$$

Combining (6.7.3), (6.7.5)-(6.7.8) it follows that

$$|E_{K1}(\underline{\hat{v}}_h, \underline{\hat{w}}_h)| \le Ch ||\underline{v}_h||_h ||\underline{w}_h||_h \,. \qquad (6.7.9)$$

Similar analyses show that

$$|E_{Ki}(\underline{\hat{v}}_h, \underline{\hat{w}}_h)| \le Ch ||\underline{\hat{v}}_h||_h ||\underline{\hat{w}}_h||_h \,, \qquad i = 1,2,3,4 \,. \qquad (6.7.10)$$

So that,

$$|\tilde{a}_h(\underline{\tilde{v}}_h, \underline{\tilde{w}}_h) - \hat{a}_h(\underline{\hat{v}}_h, \underline{\hat{w}}_h)| \le Ch ||\underline{v}_h||_h ||\underline{w}_h||_h \qquad (6.7.11)$$

Using this result it is possible to show the ellipticity of the bilinear form $\tilde{a}_h(\cdot,\cdot)$.

$$\tilde{a}_h(\underline{\tilde{v}}_h, \underline{\tilde{v}}_h) = \hat{a}_h(\underline{\hat{v}}_h, \underline{\hat{v}}_h) + \tilde{a}_h(\underline{\tilde{v}}_h, \underline{\tilde{v}}_h) - \hat{a}_h(\underline{\hat{v}}_h, \underline{\hat{v}}_h)$$

$$\ge \hat{\alpha} ||\underline{\hat{v}}_h||_h^2 - Ch ||\underline{\hat{v}}_h||_h^2 \,, \qquad (6.7.12)$$

i.e. there exists a constant $\tilde{\alpha} \geq 0$ such that

$$\tilde{a}_h(\underline{\tilde{v}}_h, \underline{\tilde{v}}_h) \geq \tilde{\alpha} ||\underline{\tilde{v}}_h||_h^2 \tag{6.7.13}$$

provided h is sufficiently small. Likewise, there exists a constant $\tilde{M}$ such that, for all $\underline{\hat{v}}_h, \underline{\hat{w}}_h \in \underline{\hat{V}}_h$

$$\begin{aligned} |a_h(\underline{\hat{v}}_h, \underline{\hat{w}}_h)| &= |a_h(\underline{\hat{v}}_h, \underline{\hat{w}}_h) + (a_h(\underline{\hat{v}}_h, \underline{\hat{w}}_h) - a_h(\underline{\hat{v}}_h, \underline{\hat{w}}_h))| \\ &\leq (M + Ch) ||\underline{\hat{v}}_h||_h ||\underline{\hat{w}}_h||_h \end{aligned} \tag{6.7.14}$$

which shows that $\tilde{a}(\cdot,\cdot)$ is continuous with respect to h.

It then follows by the discrete form of the Lax-Millgram lemma and standard interpolation theory estimates that

$$||\underline{\tilde{u}}_h - \underline{\hat{u}}_h||_h \leq Ch \left(\sum_{i=1}^{3} ||f_i||^2 \right)^{1/2} \tag{6.7.15}$$

Finally, by use of the triangle inequality, the following estimate is obtained:

$$\begin{aligned} ||\underline{\tilde{u}}_h - \underline{u}||_h &\leq ||\underline{\tilde{u}}_h - \underline{\hat{u}}_h||_h + ||\underline{\hat{u}}_h - \underline{u}||_h \\ &\leq Ch \left\{ \left(\sum_{i=1}^{3} ||f_i||^2 \right)^{1/2} + ||\underline{u}||_{\underline{W}} \right\} \end{aligned} \tag{6.7.15}$$

which is similar to the result obtained by Bernadou et al (1988) for the Clough-Johnson flat plate shell finite element.

CONCLUSIONS

This work presents the results of a numerical and theoretical examination of the finite element method in application to the linear theory of thin shells. It is prompted by the increasing concern regarding the responsibilities which underlie all finite element analysis. More specifically, test results published in the literature are invariably inadequate in respect of the wide spectrum of attributes demanded of shell finite elements. This situation stems from the complexity of the underlying classical theory and the consequent specialism demanded by users and developers of shell elements.

Four main avenues of thought have been followed in shell element design (see p. 57) but despite much research effort no single element emerges as the most effective based on criteria of accuracy, computational cost and simplicity of use. The fundamental difficulty to overcome in shell element design is the incorporation of adequate bending capability. Inadequacies in this respect are most apparent when the finite element model is required to recover displacements of inextensional bending.

Insight into the role of bending in finite element analysis is gained by study of the simple combined constant membrane strain and constant bending moment flat triangles. It is shown that an assembly of these elements, known as the bending model, is able to recover each of the solution types which characterise the behaviour of a thin shell. The so-called transitional model derives from the bending model by removing the element flexural rigidity and this exposes the available bending freedoms. The membrane model then derives from the transitional model by removing

mid-side rotation connectors and it is appropriate to compare its behaviour against that of the classical membrane theory.

A detailed examination of the transitional and membrane models reveals that the shell model is susceptible to a number of movements which are pure mechanisms and which extend over the whole finite element assembly. The fundamental result follows, namely, that the number of these mechanisms, which are identified as simulating the displacements of inextensional bending in the real shell, is directly related to the number of finite elements at the boundary and so do not occur in models of closed shells - just as with inextensional bending in the classical theory. In identifying with the displacements of inextensional bending advantage is taken of exact polynomial solutions available for shell middle surfaces in explicit quadratic and cubic representation where depth and Gaussian curvature are easily controlled. The example surfaces treated here refer to shells which are very deep and have strongly negative Gaussian curvature and so constitute severe test problems. It is surprising to find that there are displacement prescribed patch tests, for both the quadratic and cubic surfaces, where the principal Cartesian displacement component of inextensional bending is exactly recovered at each element vertex from the mechanism of the membrane model. The remaining displacement components are recovered approximately with accuracy dependent on mesh size. The transitional model displays these same mechanisms in addition to mechanisms of local rotation at the element sides which find their interpretation in the bending model where they accompany the curvature changes both of inextensional bending and of edge effect. Thus, two very different roles are established for bending freedoms in thin shell finite element models.

The bending model is similarly examined for inextensional bending under displacement and rotation prescribed patch tests, specifically in regard of its consistency with results of first approximation theory. It is found that surprisingly good recovery is obtained not only of displacements but also of curvature change to the effective exclusion of membrane strain. Also, a satisfactory ratio of membrane to bending strain

energy is obtained. The test results are obtained for different mesh sizes and are compared in various tables against the real shell values.

Ability to adequately recover curvature change is considered further in examining the response of the bending model to local edge effect. The vehicle finite element is used to model the behaviour of a cantilever circular cylinder under the action of a uniformly applied bending moment. The axisymmetry of the problem leads to consideration of a single longitudinal flat strip. Surprisingly good agreement is obtained with the comparison solution for the stress resultants as well as for the displacements. An important observation follows with regard to the respective merits of flat and curved elements. These results demonstrate that the absence of coupling of membrane and bending actions in a flat element do not constitute a deficiency.

In view of the subtleties of inextensional bending it is recommended that special concern be given to the testing of all candidate shell elements for their capacity to deal with this type of problem. As a first step toward a routine method of examination the investigation of bending action is concluded by giving details of a matrix procedure which is intended to identify the ability of a shell finite element model in response to inextensional bending. The matrix procedure is an elaboration of the well-known principle whereby rigid body movements are identified from eigenvalue analysis of the stiffness matrix.

Two further sets of numerical experiments demonstrate the satisfactory capability of the vehicle element to represent the effect of membrane forces. In the first set patch tests are constructed using solutions for the displacements and rotations of membrane action in shells having middle surface of quadratic parametric representation and negative Gaussian curvature. It is found that the element is able to recover 'pure' membrane action in the bending model to the effective exclusion of curvature change, in a manner consistent with first approximation theory. For the final set of results the geometric stiffness matrix is developed and used to solve the elastic stability problem for flat plates and circular cylindrical

panels. Convergence of buckling solutions is obtained in both cases for various boundary and loading conditions.

To conclude this work the results of a preliminary study of the mathematical details of convergence of the vehicle element are explored. The investigation is specific to the simple geometry of a circular cylinder and clamped boundary conditions. It is shown that, despite the highly nonconforming nature of the element, O(h) asymptotic convergence in the energy norm is achieved and in this respect is similar in behaviour with existing results for the Clough-Johnson flat plate shell finite element.

By way of final comment, it is believed that this work has revealed new insights into the behaviour and fundamental requirements of shell finite element models. The elementary considerations of mechanisms in the membrane and transitional models seem to provide a rationale for shell element design and validation as well as prompting thoughts on mathematical abstraction. The development of these ideas is suggested as possible future work.

APPENDIX

MATRIX IDENTIFICATION OF SINGLE CONNECTOR MECHANISMS

Consider a matrix [A] with linearly independent normalised columns,

$$[A] \subset R^{m\times n} , \qquad m > n , \qquad \sum_i (a_{ij})^2 = 1, \qquad \text{Rank } [A] = n , \qquad (A.1)$$

as in (5.6.4). The identification of single connector mechanisms (movements) essentially reduces to the problem of determining whether there is some vector $\underline{d}$ such that

$$[A]\underline{d} = (\delta_{1k}, \delta_{2k}, \ldots, \delta_{mk})^T , \qquad 1 \leq k \leq m , \qquad (A.2)$$

with δ_{ik} the Kronecker delta and where the index k picks out the connector which is responsible for the mechanism.

The least squares solution vector $\underline{d}$ in the overdetermined system

$$\underline{u} = [A]\underline{d} , \qquad \underline{u} \subset R^{m\times 1} , \qquad \underline{d} \subset R^{n\times 1} , \qquad (A.3)$$

is

$$\underline{d} = [A]^+\underline{u} , \qquad [A]^+ \subset R^{n\times m} , \qquad (A.4)$$

where $[A]^+$ is the pseudo-inverse,

$$[A]^+ = ([A]^T[A])^{-1}[A]^T . \qquad (A.5)$$

Use is made of uniqueness of the form

$$\underline{u} = ([A]^T[A])^{-1}[A]^T\underline{u}^* , \qquad \underline{u}^* \subset R^{m\times 1} , \tag{A.6}$$

which is demonstrated by letting

$$\underline{u} = [A][D]\underline{d}' , \quad [D] \subset R^{n\times m} , \quad \underline{d}' \subset R^{n\times 1} , \quad \text{Rank } [D] = n , \tag{A.7}$$

$$= [B]\underline{d}' , \text{ say}$$

(c.f. (A.3)), so that

$$u = [B]([B]^T[B])^{-1}[B]^T\underline{u}^* \equiv [A]([A]^T[A])^{-1}[A]^T\underline{u}^* . \tag{A.8}$$

Illustratively, suppose that [A] can be partitioned so that

$$[A] = \begin{bmatrix} A_{11} & 0 \\ A_{21} & 1 \end{bmatrix} , \tag{A.9}$$

where the scalar in the last column reveals the existence of a single connector mechanism at connector u_m in $\underline{u} = (u_1, u_2, \ldots u_m)^T$ (c.f. Eq.(A.2)). Then

$$[A]^T[A] = \begin{bmatrix} A_{11}^T A_{11} + A_{21}^T A_{21} & A_{21}^T \\ A_{21} & 1 \end{bmatrix} \tag{A.10}$$

and on writing

$$([A]^T[A])^{-1} = \begin{bmatrix} C_{11} & C_{12} \\ C_{12}^T & C_{22} \end{bmatrix} \tag{A.11}$$

it follows that

$$[C_{12}] = -[C_{11}][A_{21}]^T , \qquad [C_{22}] = 1 + [A_{21}][C_{11}][A_{21}]^T , \tag{A.12}$$

whence

$$([A]^T[A])^{-1} = \begin{bmatrix} A_{11}C_{11} & 0 \\ 0 & 1 \end{bmatrix} \qquad (A.13)$$

where the last column is identical with that in Eq.(A.9) and so reveals the presence of a single connector mechanism.

Uniqueness of the symmetric matrix $[A]([A]^T[A])^{-1}[A]^T$ (see Eq.(A.8)) therefore means that each single connector mechanism is identified by its own zero column and row with unit coefficient at the diagonal. Subsequent removal of single connector mechanisms from $[A]$ in Eq.(A.1) then permits reduction, by standard means, to linearly independent columns which describe the nonlocal mechanisms orthogonalised with respect to the single connector mechanism.

The matrix $[A]([A]^T[A])^{-1}[A]^T$ can sucessfully be used in some other circumstances where one connector is dominant in a multiple connector local mechanism or movement. Also note that each column in $[A]([A]^T[A])^{-1}[A]^T$ derives from linear combinations of the columns in $[A]$.

REFERENCES

Ahmad, S., B.M. Irons and O.C. Zienkiewicz (1968), "Curved thick shell and membrane elements with particular reference to axisymmetric problems", Proc. 2nd Conf. Matrix Meth. Struct. Mech., Wright-Patterson AFB, Ohio.

Allman, D.J. (1971), "Triangular finite elements for plate bending with constant and linearly varying bending moments", IUTAM Symp. on High-Speed Computing Elastic Structures, Univ. of Liége.

Allman, D.J. (1988a), "A quadrilateral finite element including vertex rotations for plane elasticity analysis", Int. J. Num. Meth. Eng., 26, pp. 717-730.

Allman, D.J. (1988b), "The constant strain triangle with drilling rotations: a simple prospect for shell analysis", Proc. 6th Int. Conf. Math. F. E. Appl., MAFELAP IV, (Ed. J.R. Whiteman), pp. 233-240.

Allman, D.J. (1988c), "Evaluation of the constant strain triangle with drilling rotations", Int. J. Num. Meth. Eng., 26, pp. 2645-2655.

Argyris, J.H. and D.W. Scharpf (1968), "The SHEBA family of shell elements for the matrix displacement method", J. Roy. Aero. Soc, 72, pp. 873-883.

Aron, H. (1874), "Das Gleichgewicht und die Bewegung einer unendlich dünnen beliebig gekrümmten, elastischen Schale", J. f. Reine Angew, 78.

Ashwell, P.G. and A.B. Sabir (1971), "Limitations of certain curved finite elements when applied to arches", Int. J. Mech. Sci., 13, pp. 133-139.

Batoz, J.L. and G. Dhatt (1972), "Development of two simple shell elements", AIAA J., 10, pp. 237-238.

Bazeley, G.P., Y.K. Cheung, B.M. Irons and O.C. Zienkiewicz (1965), "Triangular elements in bending - conforming and nonconforming solutions", Proc. Conf. Matrix Meth. Struct. Mech., Wright-Patterson AFB, Ohio.

Belytschko, T. J.S.J. Ong and W.K. Liu (1984), 'A consistent control of spurious singular modes in the 9-node Lagrange element for the Laplace and Mindlin plate equations', Comput. Meth. Appl. Mech. Eng., 44, pp. 269-295.

Belytschko, T., J.S.J. Ong and D. Lam (1985), 'Implementation and application of a 9-node Lagrange shell element with spurious mode control', Comput. Struct., 20, pp. 121-128.

Bernadou, M. and P.G. Ciarlet (1976), "Sur l'ellipticité du modèle lineaire de coques de W.T. Koiter", in: Lecture Notes in Economics and Mathematical Systems, 134, pp. 89-136, Berlin, Springer-Verlag.

Bernadou, M. (1980), "Convergence of conforming finite element methods for general shell problems", Int. J. Eng. Sci., 18, pp. 249-276.

Bernadou, M. and J.M. Boiserrie (1982), The Finite Element Method in Shell Theory; Application to Arch Dam Simulations, Basel, Birkhaüser.

Bernadou, M., Y. Ducatel and P. Trouvé (1988), "Approximation of circular cylindrical shell by Clough-Johnson flat plate finite elements", Numer. Math., 52, pp.187-217.

Birkhoff, C. and H. Garabedian (1960), "Smooth surface interpolation", J. Math. Phys., 39, pp. 353-368.

Bogner, F.K., R.L. Fox and L.A. Schmidt (1967), "A cylindrical shell discrete element", AIAA J., 5, pp.745-750.

Bonnes, G., G. Dhatt, A.M. Giroux and L.P.A. Robichard (1968), "Curved triangular elements for the analysis of shells", Proc. 2nd Conf. Matrix Meth. Struct. Mech., Wright-Patterson AFB, Ohio.

Budiansky, B. and J.L Sanders (1963), "On the 'best' first-order linear shell theory", in: Progress in Applied Mechanics (The Prager Vol.), pp. 129-140, Macmillan.

Cantin, G. and R.W. Clough (1968), "A curved cylindrical shell finite element", AIAA J., 6, pp. 1057-1067.

Cauchy, A. (1828), "Sur l'équilibre et le mouvement d'une plaque solide", Exercise de Mathematique, 3.

Ciarlet, P.G. (1975), "Conforming finite element methods for the shell problem", Proc. Conf. MAFELAP, Brunel University.

Ciarlet, P.G. (1978), The Finite Element Method for Elliptic Problems, North-Holland, Amsterdam.

Clough, R.W. and P. Johnson (1968), "A finite element approximation for the analysis of thin shells", Int. J. Solids Struct., 4, pp. 43-60.

Clough, R.W. and J.L. Tocher (1965), "Finite element stiffness matrices for analysis of plate bending", Proc. Conf. Matrix Meth. Struct. Mech., Wright-Patterson AFB, Ohio.

Connor, J.J. and C. Brebbia (1967), "Stiffness matrix for shallow rectangular shell element", Proc. ASCE J. Eng. Mech. Div., EM5, pp. 43-65.

Cook, R.D. (1969), "Eigenvalue problems with a mixed plate element", AIAA J., 7, pp. 982-983.

Cook, R.D. (1981), Concepts and Applications of Finite Element Analysis, Wiley, New York.

Cowper, G.R., G.M. Lindberg and M.D. Olsen (1968), "Comparison of two high precision finite elements for arbitrary deep shells", Proc. Conf. Matrix Meth. Struct. Mech., Wright-Patterson AFB, Ohio.

Cowper, G.R., G.M. Lindberg and M.D. Olsen (1970), "A shallow shell finite element of triangular shape", Int. J. Solids Struct., 6, pp.1133-1156.

Dawe, D.J. (1972), "Shell analysis using a simple facet element", J. Strain Anal., 7, pp. 266-270.

Dawe, D.J. (1974), "Curved finite elements for the analysis of shallow and deep arches", Comput. Struct., 4, pp.559-580.

Dawe, D.J. (1975), "High order triangular finite element for shell analysis", Int. J. Solids Struct., 11, pp. 1092-1110.

Dhatt, G. (1970), "An efficient triangular shell element", AIAA J., 8, pp. 2100-2102.

Dupuis, G. (1971), "Application of Ritz's method to thin elastic shells, Trans. ASME Ser E J. Appl. Mech., 38, pp. 987-996

Dupuis, G. and J.T. Goël (1970), "A curved element for thin elastic shells", Int. J. Solids Struct., 6, pp. 1413-1428.

Flügge, W. (1972), Tensor Analysis and Continuum Mechanics, Springer-Verlag, Berlin.

Flügge, W. (1973), Stresses in Shells, 2nd ed., Springer-Verlag, Berlin.

Fonder, G.A. and R.W. Clough (1973), "Explicit addition of rigid body motions in curved finite elements", AIAA J., 11, pp. 305-312.

Fried, I (1971), "Basic computational problems in the finite element analysis of shells", Int. J. Solids Struct., 7, pp. 1705-1715.

Fried, I (1975), "Finite element analysis of thin elastic shells with residual energy balancing and the role of rigid body modes", Trans. ASME J. Appl. Mech., 97, pp. 99-104.

Green, A.E. and Zerna, W. (1954), Theoretical elasticity, O.U.P., Oxford.

Grafton, P.E. and D.R. Strome (1963), "Analysis of axisymmetrical shells by the direct stiffness method", AIAA J., 1, pp. 2342-2347.

Gol'denveizer, A.L. (1961), Theory of Elastic Thin Shells(trans. G. Herrmann), Pergammon, Oxford.

Hellan, K. (1967), "Analysis of elastic plates in flexure by a simplified finite element method", Acta Polytechnica Scandinavica, Civ. Eng. Construction Ser. No. 46.

Henshell, R.D., B.K. Neal and G.B. Warburton (1971), "A new cylindrical shell finite element", J. Sound Vib., 16, pp.519-531.

Herrmann, L.R. and D.M. Campbell (1967), "A finite element analysis for thin shells", AIAA J., 6, pp. 1842-1847.

Herrmann, L.R. (1968), "Finite element bending analysis of plates", Proc. Amer. Soc. Eng., 93 (EM5), pp. 1842-1847.

Hughes, T.J.R., R.L. Taylor and W. Kanoknukulchai (1977), 'A simple and efficient finite element for plate bending', Int. J. Num. Meth. Eng., 29, pp. 1529-1547.

Hughes, T.J.R. and W.K. Liu (1981), 'Nonlinear finite element analysis of shells', Comput. Meth. Appl. Mech. Eng., 26, pp. 337-363.

Irons, B.M. (1976), "The Semiloof shell element", in: Finite Elements for Thin shells and Curved Members, eds. D.G. Ashwell and R.H. Gallagher, Wiley, New York, pp.197-227.

Johnson, C. (1975), "On finite element methods for curved shells using flat elements", in: Numerische Behandlung von Differential gleichungen, International Series of Numerical Mathematics, 27, pp. 147-154, Basel, Birkhaüser-Verlag.

Kikuchi, F. (1975), "On the validity of the finite element analysis of circular arches represented by an assemblage of beam elements", Comput. Meth. Appl. Mech. Eng., 5, pp.253-276.

Kikuchi, F. (1984), "Error analysis of flat plate element approximation of circular cylindrical shells", Theor. Appl. Mech., 32, pp. 469-484.

Kirchhoff, G. (1876), Vorlesungen über Mathematische Physik, Vol. 1, Mechanik.

Koiter, W.T. (1959), "A consistent first approximation in the general theory of thin elastic shells, Part 1, Foundations and linear theory", Report of Laboratory of Applied Mechanics, Delft.

Koiter, W.T. (1960), "A consistent first approximation in the general theory of thin elastic shells", in: Proc. IUTAM Symp. on the thecry of thin elastic shells, edited by W.T. Koiter, North-Holland, Amsterdam, pp. 12-33.

Koiter, W.T. (1961), "A systematic simplification of the general equations of the linear theory of thin shells", Proc. Kon. Ned. Ak. Wet. B64, pp. 612-619.

Koiter, W.T. (1966), "On the non-linear theory of thin elastic shells", Proc. Kon. Ned. Ak. Wet. B69, pp. 1-54.

Koiter, W.T. (1968), Summary of equations for modified, simplest possible linear theory of thin cylindrical shells, Rept. 422, Lab. of Engineering mechanics, Delft Univ. of Technology.

Koiter, W.T. (1970), "On the foundations of the linear theory of thin elastic shells", Proc. Kon. Ned. Ak. Wet. B73, pp. 169-195.

Krauss, H. (1967), Thin Elastic Shells, Wiley.

Lascaux, P. and P. Lesaint (1975), "Some non-conforming finite elements for the plate bending problem", RAIRO, 9 (R-1), pp.9-53.

Leonard, R.W. (1961), Nonlinear first approximation thin shell and membrane theory, Ph. D. dissertation, Virginia Polytechnic Institute, Blacksburg, Virginia.

Love, A.E.H. (1927), Mathematical Theory of Elasticity, 4th ed., Cambridge.

Lurie, A.I., (1961), "On the static-geometric analogue of shell theory", Problems of Continuum Mechanics, SIAM, Philadelphia.

MacNeal, R.H. (1978), "A simple quadrilateral shell element", Comp. Struct., 8, pp. 175-183.

MacNeal, R.H. and R.L. Harder (1985), "A proposed standard set of problems to test finite element accuracy", F. E. Anal. Des., 1, pp. 3-20.

Malvern, L.E. (1969), Introduction to The Mechanics of a Continuous Medium, Prentice-Hall.

McConnell, A.J. (1931), Application of the Absolute Differential Calculus, Blackie.

Mebane, P.W. and J.A. Stricklin (1971), "Implicit rigid body motion in curved finite elements", AIAA J., 9, pp. 344-345.

Melosh, R.J. (1966), "Aflat triangular element stiffness matrix", Proc. 1st Conf. MAtrix Meth. Struct. Mech., Wright-Patterson AFB, Ohio.

Morley, L.S.D. (1959), "An improvement on Donnell's approximation for thin walled circular cylinders", Q. J. Appl. Math., 12, pp. 89-99.

Morley, L.S.D. (1971), "The constant moment plate bending element", J. Strain Analysis, 6, pp. 20-24.

Morley, L.S.D. (1972), "Polynomial stress states in first approximation theory of circular cylindrical shells", Q. J. Mech. App. Math., 25, pp. 13-43.

Morley, L.S.D. (1982), "Inextensional bending of a shell triangular element in quadratic parametric representation", Int. J. Solids Struct., 18, pp. 919-935.

Morley, L.S.D. (1983a), "Fortran Computer program for inextensional bending of a doubly curved shell triangular element", Int. J. Num. Meth. Eng., 19, pp. 647-664.

Morley, L.S.D. (1983b), "Approximate displacements of exact membrane actions in a shell triangular element", Aero. Q., 34, pp. 282-302.

Morley, L.S.D. (1984), "Inextensional bending in shells of explicit cubic representation", Int. J. Solids Struct., 20, pp. 631-635.

Morley, L.S.D. (1987), "'Practical' components of vectors and tensors", Int. J. Eng. Sci., 25, pp. 37-53.

Morley, L.S.D. and A.J. Morris (1978), "Conflict between finite elements and shell theory", in: Finite Element Methods in the Commercial Environment, Robinson and Associates, Okehampton.

Morley, L.S.D. and M.P. Mould (1987), "The role of bending in the finite element analysis of thin shells", F. E. Anal. Des., 3, pp. 213-240.

Morris, A.J. (1973), "A deficiency in current finite elements for thin shell application", Int. J. Solids Struct., 9, pp. 331-346.

Morris, A.J. (1985), "Shell finite element evaluation tests", NAFEMS Rept. C4.

Mould, M.P. (1989), "Comparison solutions for assessment of inextensional bending in shells of quadratic and cubic polynomial representation", Comput. Mech., 4, pp. 31-45.

Murthy, S.S. and R.H. Gallagher (1986), "A triangular thin shell finite element based on discrete Kirchhoff theory", Comput. Meth. Appl. Mech. Eng., 54, pp. 197-222.

Naghdi, P.M. (1963), "Foundations of elastic shell theory", in: Progress on Solid Mechanics (Ed. Sneddon and Hill), Vol. IV, pp.1-90, North-Holland.

Naghdi, P.M. (1972), The theory of shells and plates. Handbuch der Physik VI a2, pp. 425-640, Springer-Verlag.

Niordson, F.I. (1985), Shell Theory, North-Holland, Amsterdam.

Novozhilov, V.V. (1959), The Theory of Thin Shells, Noordhoff.

Olsen, M. and G. Lindberg (1968), "Vibration analysis of cantilevered curved plates using a new cylindrical shell finite element", Proc. 2nd Conf. on Matrix Methods in Struct. Mech., Wright-Patterson AFB, Ohio.

O'Neill, B. (1966), Elementary Differential Geometry, Academic Press.

Parisch, H. (1979), 'A critical survey of the 9-node degenerated shell element with special emphasis on thin shell applications and reduced integration', Comput. Meth. Eng., 20, pp. 323-350.

Pawsey, S.F. and R.W. Clough (1971), 'Improved numerical integration of thick shell finite elements', Int. J. Num. Meth. Eng., 3, pp. 575-586.

Pian, T.H.H. and P. Tong (1969), "Basis of finite element methods for solid continua", Int. J. Num. Meth. Eng., 1, pp. 3-28.

Poisson, S.D. (1829), Memoire sur l'équilibre et le mouvement des corps solides, Mém. de l'Acad. Sci., Paris, 8.

Pucher, A.J. (1934), "Über die Spannungsfunktion in gekrümmten Flachen", Beton und Eisen, 33, pp. 298-305.

Pucher, A.J. (1938), "Über die Spannungsfunktion beliebig gekrümmter dünner Schalen", Proc. 5th Int. Congr. Appl. Mech., pp. 134-139.

Rannacher, R. (1979), "On nonconforming finite element methods for plate bending problems. The linear case.", RAIRO, 13, pp.369-387.

Reissner, E. (1960), "On some problems in shell theory", Proc. Symp. Nav. Struct. Mech., Pergammon, New York.

Sander, G. and S. Idelsohn (1982), "A family of conforming finite elements for deep shell analysis", Int. J. Num. Meth. Eng., 18, pp. 353-380.

Sanders, J.L. (1959), An improved first approximation theory for thin shells, NASA Rept. 24.

Sabir, A.B. and A.C. Lock (1972), "A curved cylindrical shell finite element", Int. J. Mech. Sci., 14, pp. 125-135.

Stolarski, H. and T. Belytschko (1982), "Membrane locking and reduced integration for curved elements", J. Appl. Mech., 49, pp. 172-176.

Stolarski, H. and T. Belytschko (1983), "Shear and membrane locking in curved C^0 elements", Comput. Meth. Appl. Mech. Eng., 41, pp. 279-296.

Strickland, G. and W. Loden (1968), "A doubly curved triangular shell element", Proc. 2nd Conf. Matrix Methods in Struct. Mech., Wright-Patterson AFB, Ohio.

Stummel, F. (1980), "Basic compactness properties of nonconforming and hybrid finite element spaces", RAIRO, 14, pp. 81-115.

Timenshenko, S.P. and J.M. Gere (1961), Theory of Elastic Stability, McGraw-Hill.

Truesdell, C. (1953), "The physical components of vectors and tensors", Z. Angew. Math. Mech., 33, pp.345-356.

Turner, M.J., R.W. Clough, H.C. Martin and L.J. Topp (1956), "Stiffress and deflexion of complex structures", J. Aero. Sci., 23, pp. 805-824.

Utku, S. (1967), "Stiffness matrices for thin triangular elements of non-zero Gaussian curvature", AIAA J., 5, pp. 1659-1667.

Washizu, K. (1982), Variational Methods in Elasticity and Plasticity, Pergamon Press.

Wempner, G.A. J.T. Oden and D.A. Kross (1968), "Finite element analysis of thin shells", Proc. ASCE, EM-6, pp. 1273-1294.

Zienkiewicz, O.C. (1965), "Finite element procedures in the solution of plate and shell problems", in: Stress Analysis, ed. Zienkiewicz and Hollister, Wiley.

Zienkiewicz, O.C. (1973), The Finite Element Method, McGraw-Hill.

Zienkiewicz, O.C. and Y.K Cheung (1965), "Finite element method of analysis of arch dam and shells and comparison with finite differences", Proc. Symp. Theory of Arch Dams, Pergammon Press, New York.

Zienkiewicz, O.C., C. Parekh and I.P. King (1968), "Arch dams analysed by a linear finite element shell solution program", Symp. Arch Dams, Inst. of Civil Engineers.

Zienkiewicz, O.C. R.L. Taylor and J.M. Too (1971), 'Reduced integration techniques in general analysis of plates and shells', Int. J. Num. Meth. Eng., 3, pp. 275-290.

Table 5.1 Values of h-symbols along sides 1,2,3 of the element.

Side	$h^{1}_{1'}$	$h^{2}_{1'}$	$h^{1}_{2'}$	$h^{2}_{2'}$	$h^{1'}_{1}$	$h^{1'}_{2}$	$h^{2'}_{1}$	$h^{2'}_{2}$
1	$-l_1/2A$	$l_{12}/4Al_1$	0	$-1/l_1$	$-2A/l_1$	0	$-l_{12}/2l_1$	l_1
2	$l_{12}/4Al_2$	$-l_2/2A$	$1/l_2$	0	0	$-2A/l_2$	l_2	$l_{12}/2l_2$
3	$l_{13}/4Al_3$	$l_{23}/4Al_3$	$-1/l_3$	$1/l_3$	$2A/l_3$	$2A/l_3$	$-l_{23}/2l_3$	$l_{31}/2l_3$

Table 5.2 Example values of constants $c_1, c_2, c_3 \ldots$ for inextensional bending of triangular shell models (see Fig. 5.2) of the quadratic reference surface of (5.3.7).

	q = 2	q = 3	q = 4	q = 5
c_1	0.	0.	0.	0.
c_2	0.300678×10^{-1}	0.152376×10^{-1}	-0.212234×10^{-1}	-0.322396×10^{-3}
c_3	0.347193×10^{-1}	0.460248×10^{-1}	0.277990×10^{-1}	-0.432098×10^{-1}
c_4	-0.150339×10^{-1}	-0.419051×10^{-2}	0.123448×10^{-1}	-0.198900×10^{-4}
c_5	0.	-0.670804×10^{-4}	0.735445×10^{-3}	-0.267412×10^{-7}
c_6	-0.250565×10^{-1}	-0.698419×10^{-2}	0.205747×10^{-1}	-0.331499×10^{-4}
c_7		-0.171414×10^{-2}	0.251634×10^{-2}	-0.822547×10^{-4}
c_8		-0.915157×10^{-2}	-0.103913×10^{-1}	-0.384299×10^{-2}
c_9		-0.857071×10^{-2}	0.125817×10^{-1}	-0.411274×10^{-3}
c_{10}		-0.508421×10^{-2}	-0.577294×10^{-2}	-0.213499×10^{-2}
c_{11}			-0.169145×10^{-2}	0.139820×10^{-4}
c_{12}			0.179294×10^{-4}	0.815934×10^{-4}
c_{13}			-0.169145×10^{-1}	0.139820×10^{-3}
c_{14}			0.298823×10^{-4}	0.135989×10^{-1}
c_{15}			-0.469846×10^{-2}	0.388389×10^{-4}
c_{16}				0.362087×10^{-4}
c_{17}				0.865817×10^{-4}
c_{18}				0.603478×10^{-3}
c_{19}				0.288606×10^{-3}
c_{20}				0.502899×10^{-3}
c_{21}				0.481009×10^{-4}

Table 5.3 'Inextensional' bending displacements in triangular shell model (see Fig. 5.2) of the quadratic reference surface of (5.3.7).

Number of elements	q	$U^i \times 10^2$ displacements at centroidal position in:									Most significant		
		Real shell			FE membrane model			FE bending model					
		U^1	U^2	U^3	U^1	U^2	U^3	U^1	U^2	U^3	U^1	U^2	U^3
	2	1.0023	-2.4646	2.6727							2.0045	-4.0506	2.6727
9	2				0.8909	-2.3146	2.6727	0.8907	-2.3156	2.6747			
36	2				0.9744	-2.4271	2.6727	0.9743	-2.4386	2.6950			
81	2				0.9899	-2.4480	2.6727	0.9899	-2.4526	2.6819			
144	2				0.9953	-2.4553	2.6727	0.9954	-2.4602	2.6829			
225	2				0.9978	-2.4586	2.6727	0.9979	-2.4632	2.6824			
441	2				1.0000	-2.4615	2.6727	1.0000	-2.4658	2.6818			
	3	0.6923	-1.8464	2.4420							-2.1847	-3.7384	3.1426
9	3				0.7271	-1.8286	2.4420	0.7270	-1.8289	2.4427			
36	3				0.7010	-1.8419	2.4420	0.7008	-1.8449	2.4477			
81	3				0.6961	-1.8440	2.4420	0.6956	-1.8453	2.4440			
144	3				0.6945	-1.8453	2.4420	0.6938	-1.8457	2.4433			
225	3				0.6937	-1.8457	2.4420	0.6929	-1.8458	2.4428			
441	3				0.6930	-1.8460	2.4420	0.6921	-1.8458	2.4424			
	4	-0.4499	0.4767	0.6218							-4.5190	2.2499	3.0471
9	4				-0.2533	0.1513	0.7555	-0.2532	0.1524	0.7532			
36	4				-0.4009	0.3617	0.7387	-0.4004	0.4063	0.6501			
81	4				-0.4281	0.4525	0.6238	-0.4285	0.4492	0.6286			
144	4				-0.4377	0.4648	0.6164	-0.4382	0.4603	0.6277			
225	4				-0.4421	0.3851	0.7960	-0.4427	0.4657	0.6267			
441	4				-0.4459	0.4720	0.6230	-0.4467	0.4706	0.6254			
	5	-0.1159	0.8583	-2.0355							3.9212	3.2350	-3.7752
9	5				-0.2476	1.0514	-2.0549	-0.2476	-0.1051	-2.0536			
36	5				-0.1496	0.9112	-2.0518	-0.1497	0.8972	-2.0242			
81	5				-0.1309	0.8781	2.0359	-0.1310	0.8749	-2.0294			
144	5				-0.1243	0.8692	-2.0348	-0.1245	0.8647	-2.0267			
225	5				-0.1213	0.8769	-2.0595	-0.1214	0.8602	-2.0260			
441	5				-0.1186	0.8620	-2.0357	-0.1188	0.8564	-2.0253			

Table 5.4 Example values of constants $c_1, c_2, c_3 \ldots$ for inextensional bending of triangular shell models (see Fig.5.2) of the cubic reference surface of (5.3.8).

	q = 3	q = 4	q = 5
c_1	0.	0.	0.
c_2	0.311121×10^{-1}	0.412260×10^{-1}	-0.179977×10^{-1}
c_3	0.646307×10^{-1}	-0.271618×10^{-1}	0.663029×10^{-1}
c_4	-0.155560×10^{-1}	$-0.358083\times10^{-}2$	-0.130992×10^{-2}
c_5	0.	0.	0.
c_6	-0.155560×10^{-1}	-0.358083×10^{-2}	-0.130992×10^{-2}
c_7	0.	-0.851608×10^{-2}	0.110490×10^{-2}
c_8	0.	0.322275×10^{-1}	-0.738447×10^{-2}
c_9	0.	-0.255482×10^{-1}	0.331470×10^{-2}
c_{10}	-0.155560×10^{-1}	0.716166×10^{-2}	-0.377141×10^{-2}
c_{11}		0.	0.
c_{12}		0.	-0.344896×10^{-2}
c_{13}		0.	0.
c_{14}		-0.255482×10^{-1}	-0.134255×10^{-3}
c_{15}		0.161137×10^{-1}	-0.369224×10^{-2}
c_{16}			0.
c_{17}			0.
c_{18}			0.
c_{19}			0.
c_{20}			-0.517344×10^{-2}
c_{21}			0.

Table 5.5 'Inextensional' bending displacements in triangular shell model (see Fig. 5.2) of the cubic reference surface of (5.3.8).

Number of elements	q	$U^i \times 10^2$ displacements at centroidal position in:									Most significant		
		Real shell			FE membrane model			FE bending model					
		U^1	U^2	U^3	U^1	U^2	U^3	U^1	U^2	U^3	U^1	U^2	U^3
	3	0.5185	-3.7412	4.4692							1.0371	-9.2482	4.4692
9	3				0.4609	-3.6345	4.4692	0.4609	-3.6449	4.4697			
36	3				0.5041	-3.7161	4.4692	0.5043	-3.7283	4.4849			
81	3				0.5121	-3.7230	4.4692	0.5122	-3.7412	4.4849			
144	3				0.5149	-3.7348	4.4692	0.5150	-3.7459	4.4847			
225	3				0.5162	-3.7371	4.4692	0.5162	-3.7473	4.4837			
441	3				0.5174	-3.7391	4.4692	0.5172	-3.7482	4.4826			
	4	0.8263	-2.7730	2.0596							3.3317	-3.3674	3.4927
9	4				0.6239	-2.3413	1.9218	0.6236	-2.3413	1.9235			
36	4				0.7791	-2.7228	2.0920	0.7785	-2.6992	2.0632			
81	4				0.8056	-2.7389	2.0574	0.8054	-2.7349	2.0536			
144	4				0.8147	-2.7355	2.0325	0.8145	-2.7526	2.0576			
225	4				0.8189	-2.7619	2.0604	0.8186	-2.7607	2.0594			
441	4				0.8225	-2.7650	2.0566	0.8221	-2.7680	2.0612			
	5	-0.1452	-1.8464	2.8952							-4.4234	-7.8520	5.2696
9	5				-0.0765	-1.9457	3.0740	-0.0076	-1.9969	2.9705			
36	5				-0.1350	-1.7405	2.9505	-0.0134	-1.7698	2.9872			
81	5				-0.1454	-1.7427	2.9756	-0.0145	-1.7568	2.9941			
144	5				-0.1489	-1.7500	2.9937	-0.0148	-1.7486	2.9910			
225	5				-0.1506	-1.7331	2.9735	-0.0150	-1.7442	2.9887			
441	5				-0.1518	-1.7328	2.9762	-0.1517	-1.7400	2.9863			

Table 5.6 'Inextensional' bending curvature changes κ_{ib} etc. in the triangular shell bending model (see Fig. 5.2) of the quadratic reference surface of (5.3.7).

Number of elements	q	Most significant principal value at centroidal position in:			Most significant	Strain energy			
		Real shell	FE bending model			Real shell	FE bending model		
		$\kappa_{ib}\times10$	$\kappa_{ib}\times10$	$\gamma_{ib}\times10^{5}$	$\kappa_{ib}\times10$	$U\times10^{2}$	$U_K\times10^{2}$	$U_\gamma\times10^{6}$	$U_\gamma/U_K\times10^{3}$
	2	0.3971			0.6785	0.5495			
16	2		0.3796	-0.2220			0.5279	0.8771	0.1662
49	2		0.3860	-0.1288			0.5418	2.0358	0.3758
100	2		0.3899	-0.1459			0.5454	1.7837	0.3271
256	2		0.3951	-0.1268			0.5477	1.4675	0.2681
484	2		0.3975	-0.1243			0.5483	1.4016	0.2557
625	2		0.3982	-0.1241			0.5484	1.3829	0.2521
	3	0.6603			1.0163	0.5371			
16	3		0.6251	-0.1358			0.5202	0.2626	0.0505
49	3		0.6467	0.2111			0.5297	0.5452	0.1029
100	3		0.6520	-0.7594			0.5329	0.6990	0.1312
256	3		0.6553	-0.4745			0.5351	0.8356	0.1562
484	3		0.6577	-0.3502			0.5359	0.8540	0.1593
625	3		0.6573	-0.3112			0.5361	0.8567	0.1598
	4	0.4931			1.8605	0.7863			
16	4		0.5978	-0.3551			0.6748	1.3701	0.2030
49	4		0.5500	-0.3740			0.7432	2.8601	0.3849
100	4		0.5260	-0.2502			0.7630	3.0957	0.4057
256	4		0.5137	-0.1626			0.7762	3.3193	0.4278
484	4		0.5091	-0.1880			0.7800	3.5536	0.4556
625	4		0.5078	-0.1058			0.7811	3.6221	0.4637
	5	-0.6748			-2.0905	0.9220			
16	5		-0.7490	0.0690			0.7890	0.5493	0.0696
49	5		-0.7167	-0.1392			0.8610	2.8128	0.3267
100	5		-0.6991	-0.1296			0.8869	3.4562	0.3898
256	5		-0.6800	-0.1120			0.9054	4.9179	0.5434
484	5		-0.6710	-0.1630			0.9114	5.6591	0.6209
625	5		-0.6684	-0.1850			0.9132	5.9113	0.6473

Table 5.7 'Inextensional' bending curvature changes κ_{ib} etc. in the triangular shell bending model (see Fig. 5.2) of the cubic reference surface of (5.3.8).

Number of elements	q	Most significant principal value at centroidal position in:			Most significant	Strain energy			
		Real shell	FE bending model			Real shell	FE bending model		
		$\kappa_{ib}\times10$	$\kappa_{ib}\times10$	$\gamma_{ib}\times10^{5}$	κ_{ib}	$U\times10^{2}$	$U_K\times10^{2}$	$U_\gamma\times10^{5}$	$U_\gamma/U_K\times10^{3}$
	3	0.6674			0.1347	0.9645			
16	3		0.5573	-0.4004			0.9127	0.1942	0.2128
49	3		0.5899	-0.1465			0.9451	0.1015	0.1074
100	3		0.6144	-0.1648			0.9542	0.2036	0.2134
256	3		0.6899	-0.1229			0.9601	0.1606	0.1672
484	3		0.6511	-0.1149			0.9617	0.1444	0.1507
625	3		0.6550	-0.1047			0.9622	0.1407	0.1462
	4	0.4911			0.2810	2.3395			
16	4		0.7568	4.8798			1.8213	27.1891	14.9288
49	4		0.5855	4.8198			2.1381	1.8083	0.8455
100	4		0.5372	0.2847			2.2337	0.5042	0.2257
256	4		0.5066	-0.2160			2.9545	0.5616	0.2448
484	4		0.4981	-0.2375			2.3140	0.6766	0.2924
625	4		0.4964	-0.2421			2.3191	0.7254	0.3128
	5	0.5413			0.4308	2.5867			
16	5		0.8126	-0.3935			2.0182	17.8655	8.8523
49	5		0.7073	-0.6367			2.3483	1.0763	0.4583
100	5		0.6365	-0.3711			2.4556	0.8226	0.3351
256	5		0.5573	0.1923			2.5267	1.0804	0.4275
484	5		0.5690	0.2544			2.5512	1.3491	0.5288
625	5		0.5639	0.2604			2.5576	1.4512	0.5673

Table 5.8 Results for cantilever circular cylinder under uniform edge bending moment.

	x^a	Real shell	FE bending model	
			coarse mesh[b]	fine mesh[c]
U^3	0.	0.1320	0.1189	0.1214
$N_{\theta\theta}$	0.03597	0.5771×10^4	0.5748×10^4	
	0.01798	0.6181×10^4		0.5944×10^4
M_{xx}	0.03597	0.9959×10^2	0.1000×10^3	
	0.01798	0.9989×10^2		0.1000×10^3
$M_{\theta\theta}$	0.03597	0.2999×10^2	0.2531×10^2	
	0.01798	0.3010×10^2		0.2818×10^2
U_Y	—	0.2945×10^1	0.2992×10^1	0.2988×10^1
U_K	—	0.8838×10^1	0.8489×10^1	0.8560×10^1
U_Y/U_K	—	0.3332	0.3525	0.3490
U_Y+U_K	—	0.1178×10^2	0.1148×10^2	0.1152×10^2

Cylinder modelled using 128 flat strips each subtending an angle of 2.8125 degrees.

[a] at center of leading finite element.

[b] 48 finite elements in longitudinal direction.

[c] 96 finite elements in longitudinal direction.

Table 5.9 Eigenvalues λ' of (5.6.3) and associated strain energy ratios U_Y/U_K for the hexagonal shell bending model (see Fig. 5.7) of the quadratic reference surface of (5.3.7).

Number	$\lambda' = 2U_Y$	U_Y/U_K	Number	$\lambda' = 2U_Y$	U_Y/U_K
1-12	0.	0.	19	0.7386×10^{5}	0.1106×10^{6}
13	0.9557×10^{-5}	0.1880×10^{-5}	20	0.9108×10^{5}	0.6598×10^{7}
14	0.1588×10^{-3}	0.4834×10^{-5}	21	0.1058×10^{6}	0.6894×10^{5}
15	0.2778×10^{-1}	0.6634×10^{-3}	22	0.1158×10^{6}	0.6194×10^{6}
16	0.8649×10^{4}	0.3644×10^{3}	23	0.1274×10^{6}	0.3046×10^{5}
17	0.5327×10^{5}	0.5825×10^{5}	24	0.1630×10^{6}	0.2577×10^{7}
18	0.6405×10^{5}	0.1762×10^{5}			

Table 5.10 Energy of the three 'inextensional' bending movements in the hexagonal shell bending model (see Fig. 5.7) of the quadratic reference surface of (5.3.7).

Number	U_γ	U_K	U_γ/U_K
1	0.4856×10^{-2}	0.1167×10^{2}	0.4161×10^{-3}
2	0.4945×10^{-2}	0.1017×10^{2}	0.4868×10^{-3}
3	0.1942×10^{-1}	0.3100×10^{2}	0.6267×10^{-3}

Table 5.11 Example values of constant vectors $\underline{a}$, $\underline{b}$, $\underline{c}$ for membrane action of triangular shell models of the quadratic reference surface of (5.7.3).

$\underline{a}$	$\underline{b}$	$\underline{c}$
0.	0.	0.
-0.482803×10^{-6}	-0.396777×10^{-5}	0.
0.	-0.208187×10^{-5}	0.
-0.104967×10^{-6}	0.284937×10^{-6}	-0.634674×10^{-7}
-0.531413×10^{-6}	-0.146465×10^{-6}	0.924589×10^{-7}
0.125425×10^{-6}	-0.189747×10^{-6}	0.805030×10^{-7}
-0.477228×10^{-7}	-0.233340×10^{-6}	-0.148012×10^{-7}
0.183844×10^{-6}	-0.280479×10^{-6}	-0.164282×10^{-6}
0.320697×10^{-6}	0.192828×10^{-6}	-0.301558×10^{-7}
-0.133839×10^{-6}	0.937488×10^{-7}	0.193004×10^{-7}
0.873495×10^{-8}	0.733368×10^{-8}	-0.201270×10^{-7}
0.207492×10^{-7}	0.112285×10^{-8}	0.365145×10^{-7}
0.347759×10^{-7}	-0.188341×10^{-7}	0.122107×10^{-6}
0.467554×10^{-7}	0.788306×10^{-8}	0.190071×10^{-7}
0.150173×10^{-7}	0.533595×10^{-8}	-0.564881×10^{-9}

Table 5.12 'Membrane' displacements in triangular shell model of the quadratic reference surface of (5.7.3).

Number of elements	q	$U^i \times 10^6$ displacements at centroidal position in:									Most significant		
		Real shell			FE membrane model			FE bending model					
		U^1	U^2	U^3	U^1	U^2	U^3	U^1	U^2	U^3	U^1	U^2	U^3
	2	-0.2042	-2.0306	0.00706							-0.6268	-3.9089	0.0992
9	2				-0.2041	-2.0290	-0.00327	-0.2041	-2.0294	-0.00088			
36	2				-0.2041	-2.0303	0.00512	-0.2042	-2.0304	0.00558			
81	2				-0.2043	-2.0303	0.00653	-0.2042	-2.0305	0.00643			

Table 5.13 'Membrane' strains γ_m etc. in the triangular shell bending model of the quadratic reference surface of (5.7.3).

Number of elements	q	Most significant principal value at centroidal position in:				Most significant		Strain energy			
		Real shell		FE bending model				Real shell	FE bending model		
		$\gamma_m \times 10^5$	$\kappa_m \times 10^8$	$\gamma_m \times 10^5$	$\kappa_m \times 10^6$	$\gamma_m \times 10^5$	$\kappa_m \times 10^7$	$U \times 10^6$	$U_\gamma \times 10^6$	$U_\kappa \times 10^{11}$	$U_\kappa / U_\gamma \times 10^5$
	2	-0.1127	0.5633			-0.1164	0.1571	0.6166			
16	2			-0.1121	-0.1583				0.6148	0.2748	0.4410
49	2			-0.1123	-0.1080				0.6160	0.2703	0.4387
100	2			-0.1125	-0.0842				0.6163	0.2696	0.4375

Table 5.14 Buckling coefficients for a flat plate under uniform plane stress.

	Clamped boundary, biaxial compression[a]			Simply supported boundary, uniaxial compression[a]			Simply supported boundary, shear[b]		
	A	B	C	A	B	C	A	B	C
2x2	1.766	2.484	3.357	2.330	2.243	2.669	1.927	1.692	2.174
4x4	3.570	3.699	4.582	3.428	3.343	3.636	4.589	4.187	5.250
6x6	4.350	4.322	4.939	3.762	3.666	3.837	6.094	5.768	6.333
8x8	4.716[c]	4.666[c]	5.087[c]	3.842[c]	3.801[c]	3.908[c]	6.763	6.528	6.863
12x12	5.022[c]	4.983[c]	5.203[c]	3.928[c]	3.908[c]	3.959[c]	—	—	—
16x16	5.141[c]	5.115[c]	5.246[c]	3.959[c]	3.947[c]	3.977[c]	—	—	—
Exact[d]		5.315			4.000			7.710	

[a] aspect ratio = 1

[b] aspect ratio = 1.25

[c] result from quarter mesh and symmetry.

[d] Timoshenko and Gere (1961)

Table 5.15 Buckling stresses for a cylindrical panel under uniform plane stress.

	Clamped boundary, uniaxial compression			Simply supported boundary, uniaxial compression			Simply supported boundary, shear		
	A	B	C	A	B	C	A	B	C
2×2	29.932	31.779	40.153	26.672	20.996	30.557	14.563	13.307	20.015
4×4	69.676	66.409	75.111	40.582	39.561	41.862	23.789	22.722	25.074
6×6	82.676	80.559	86.904	41.885	41.203	42.668	25.997	25.393	26.414
8×8	89.378	87.720	92.835	42.443	41.992	42.930	26.771	26.400	26.936
12×12	95.313[a]	94.319[a]	96.881[a]	42.878[a]	42.658[a]	43.110[a]	—	—	—
16×16	97.689[a]	97.060[a]	98.633[a]	43.038[a]	42.905[a]	43.171[a]	—	—	—

Radius of panel = 10

Angle subtended = 0.1 rad

Length of panel = 1

[a] result from quarter mesh and symmetry.

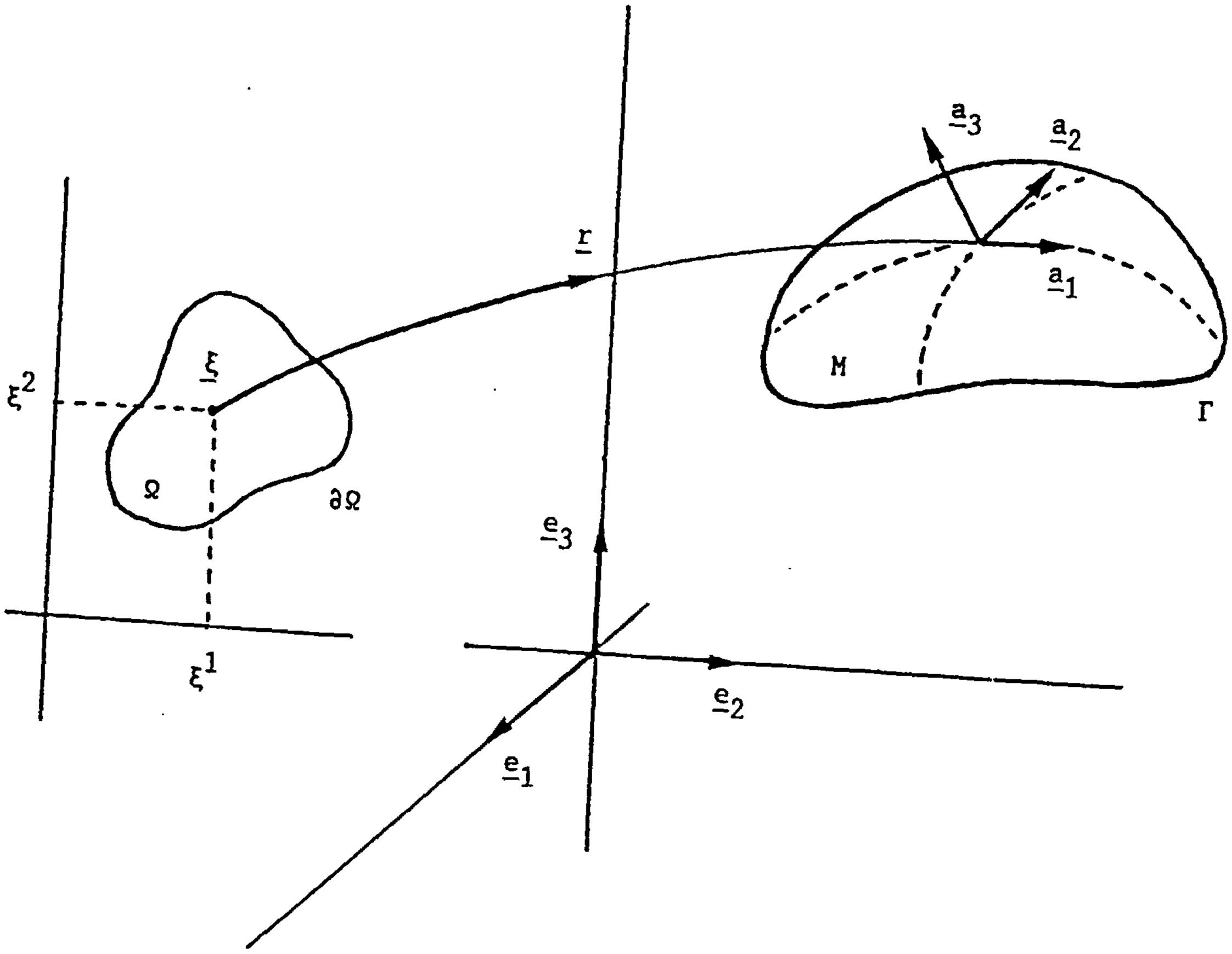

Fig. 2.1 Geometry of a shell.

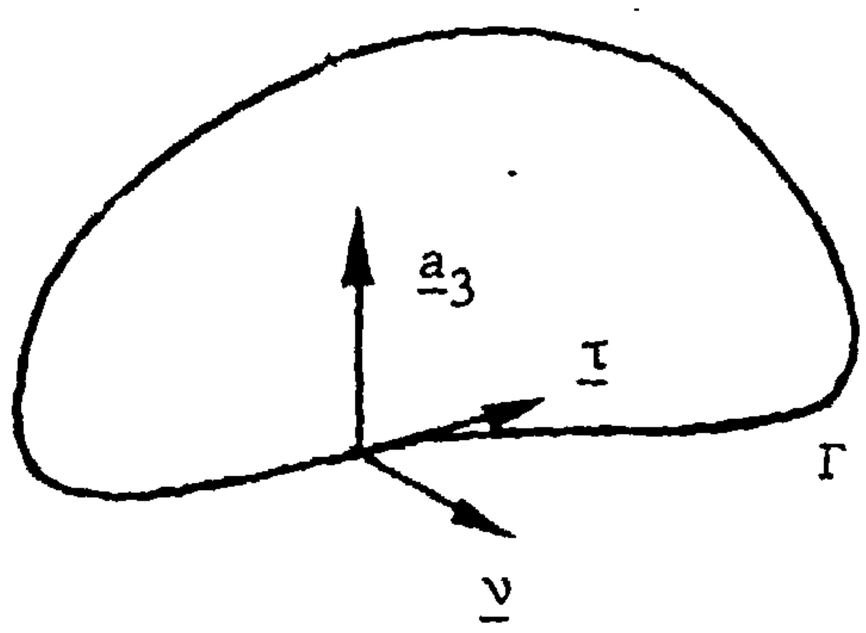

Fig. 2.2 Unit vectors defining boundary curve coordinate system.

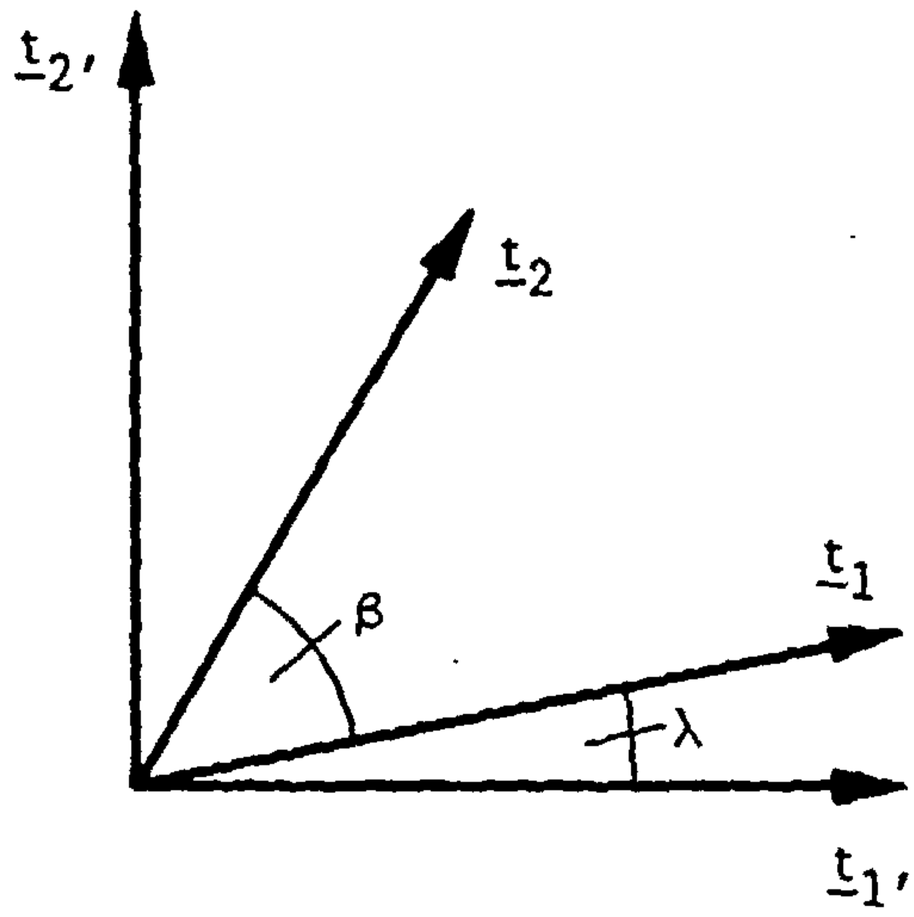

Fig. 2.3 Unit vectors at a point on the middle surface.

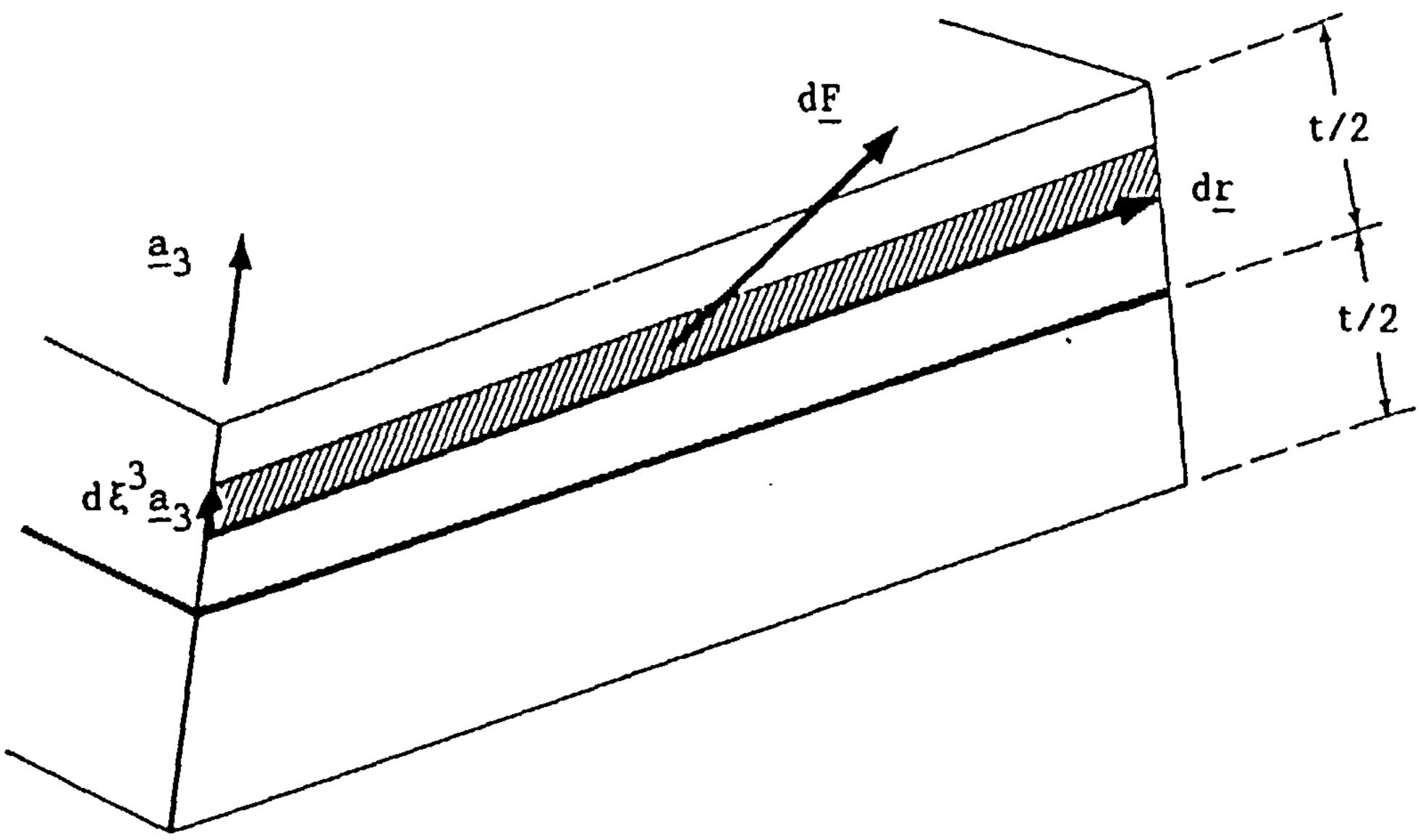

Fig. 3.1 Section through a shell.

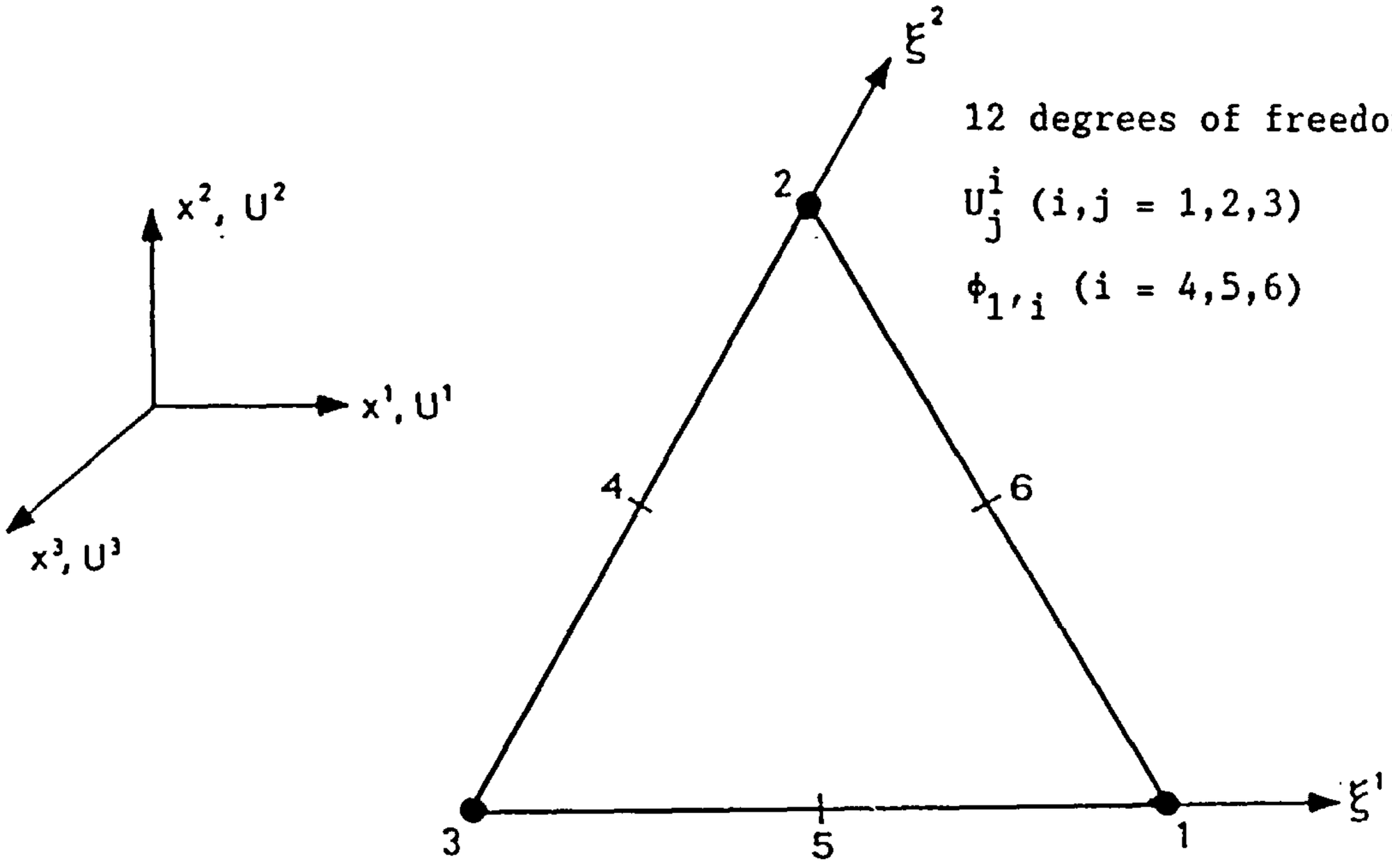

Fig. 5.1 Flat triangular finite element.

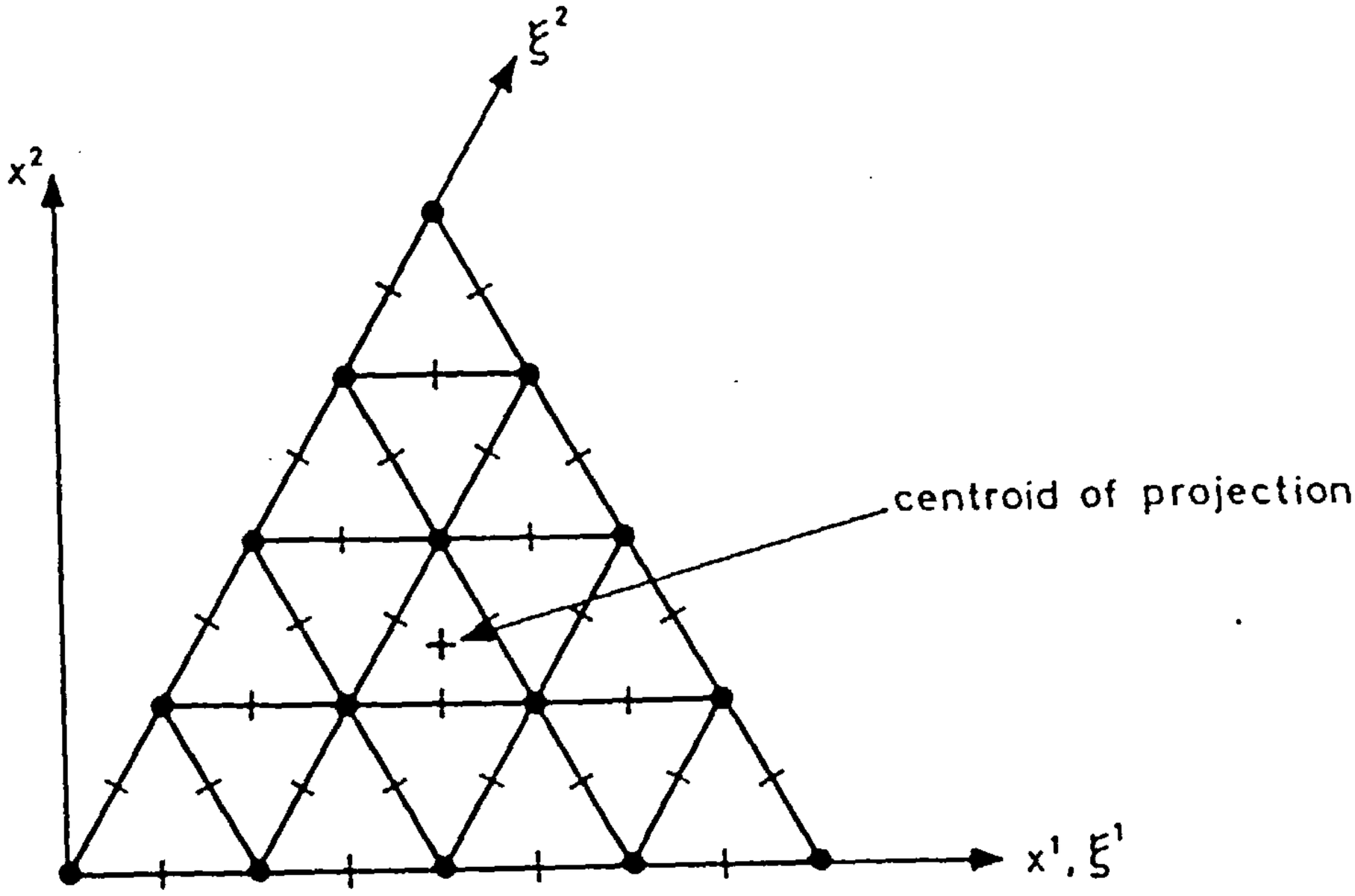

Fig. 5.2 Equilateral triangular projection of example real shell and its typical finite element model onto the x^{α}-plane.

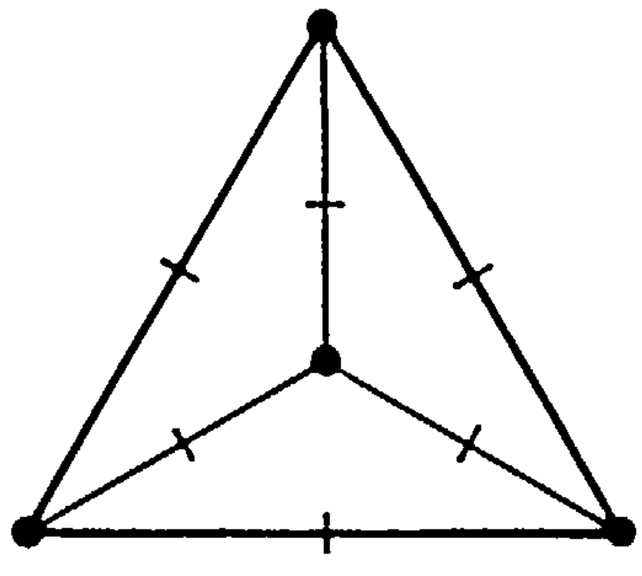

Fig. 5.3 Example of compounded element which makes no additional contribution to the nonlocal mechanisms.

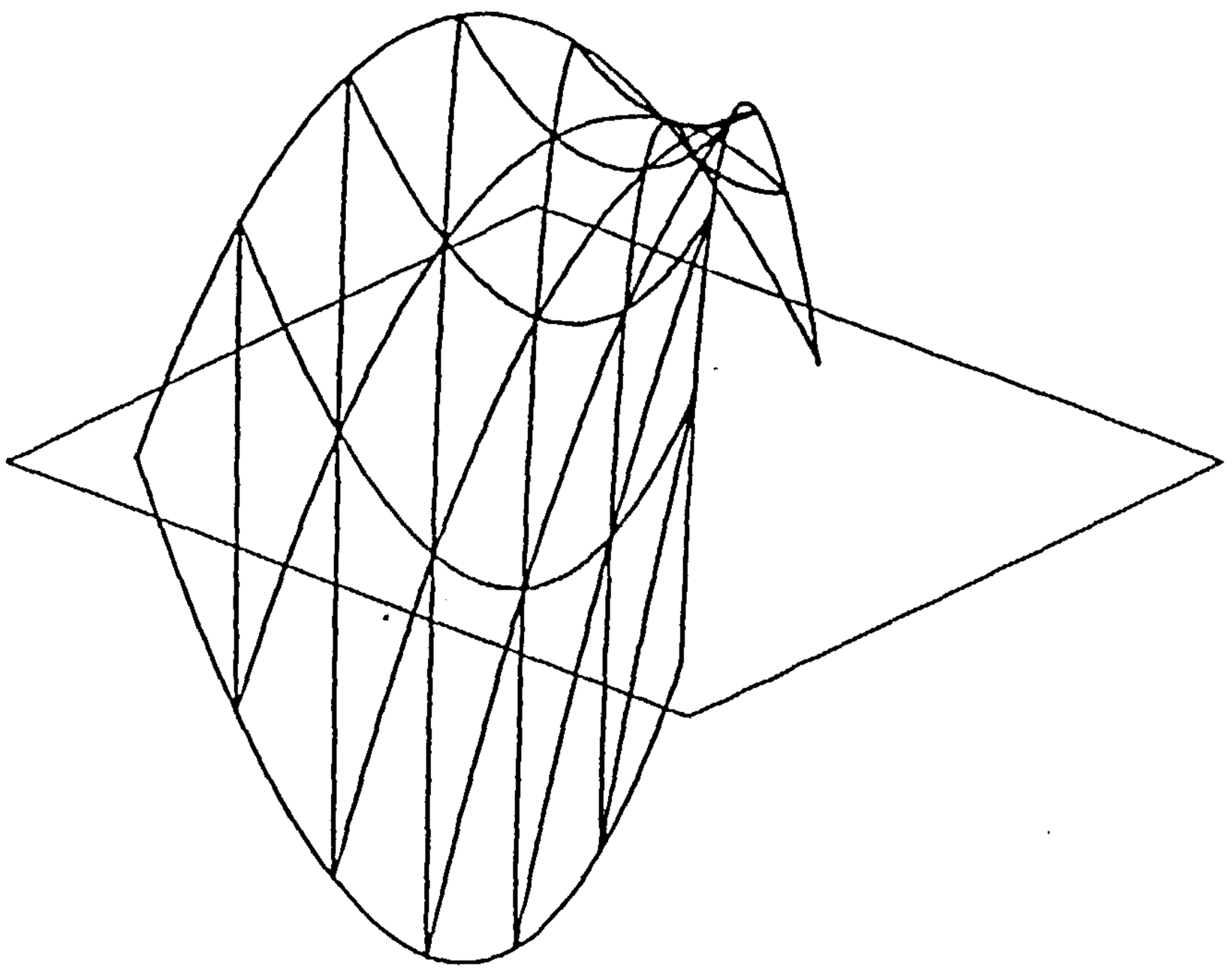

Fig. 5.4 Perspective view of the negative Gaussian curvature surface defined by (5.3.7).

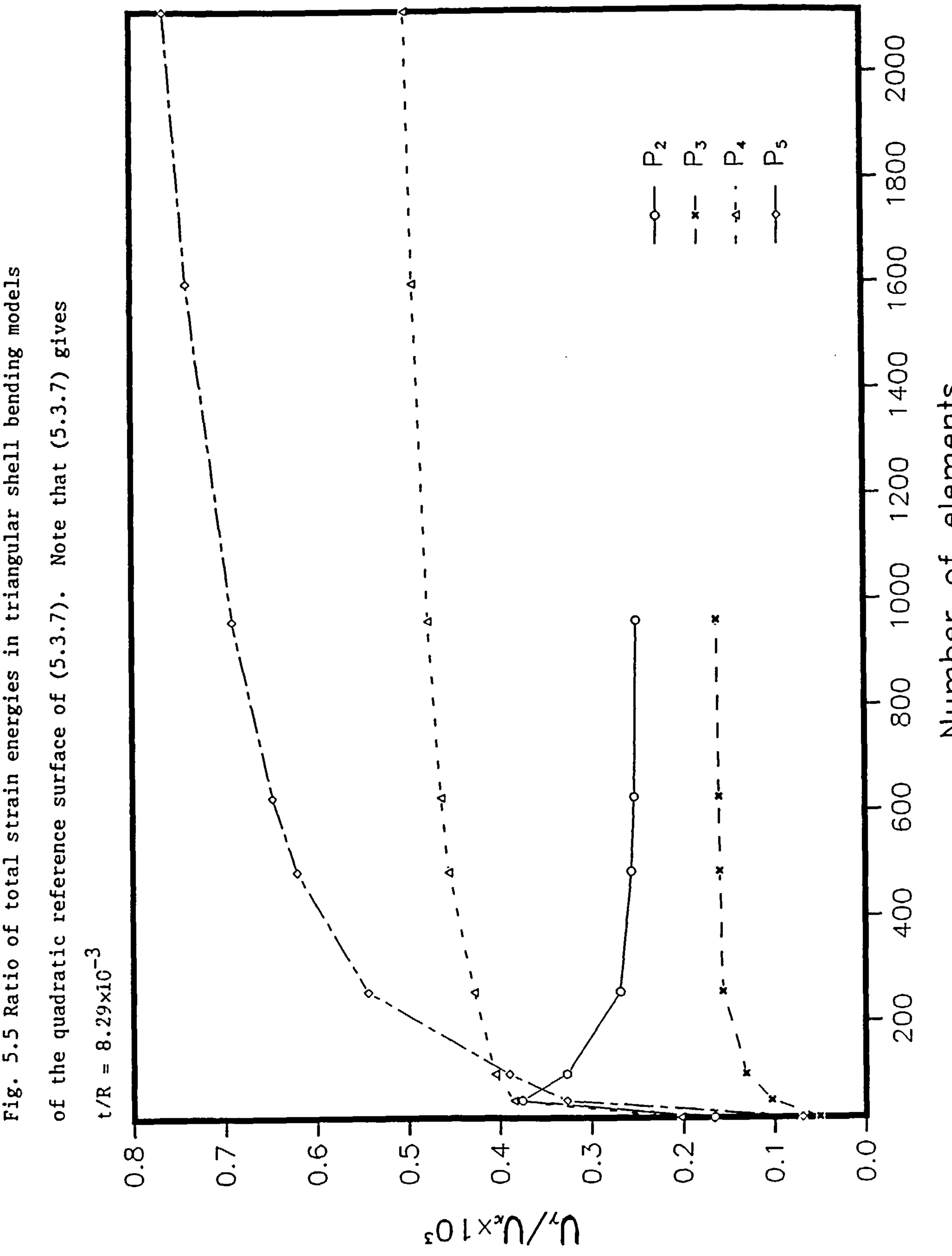

Fig. 5.5 Ratio of total strain energies in triangular shell bending models of the quadratic reference surface of (5.3.7). Note that (5.3.7) gives

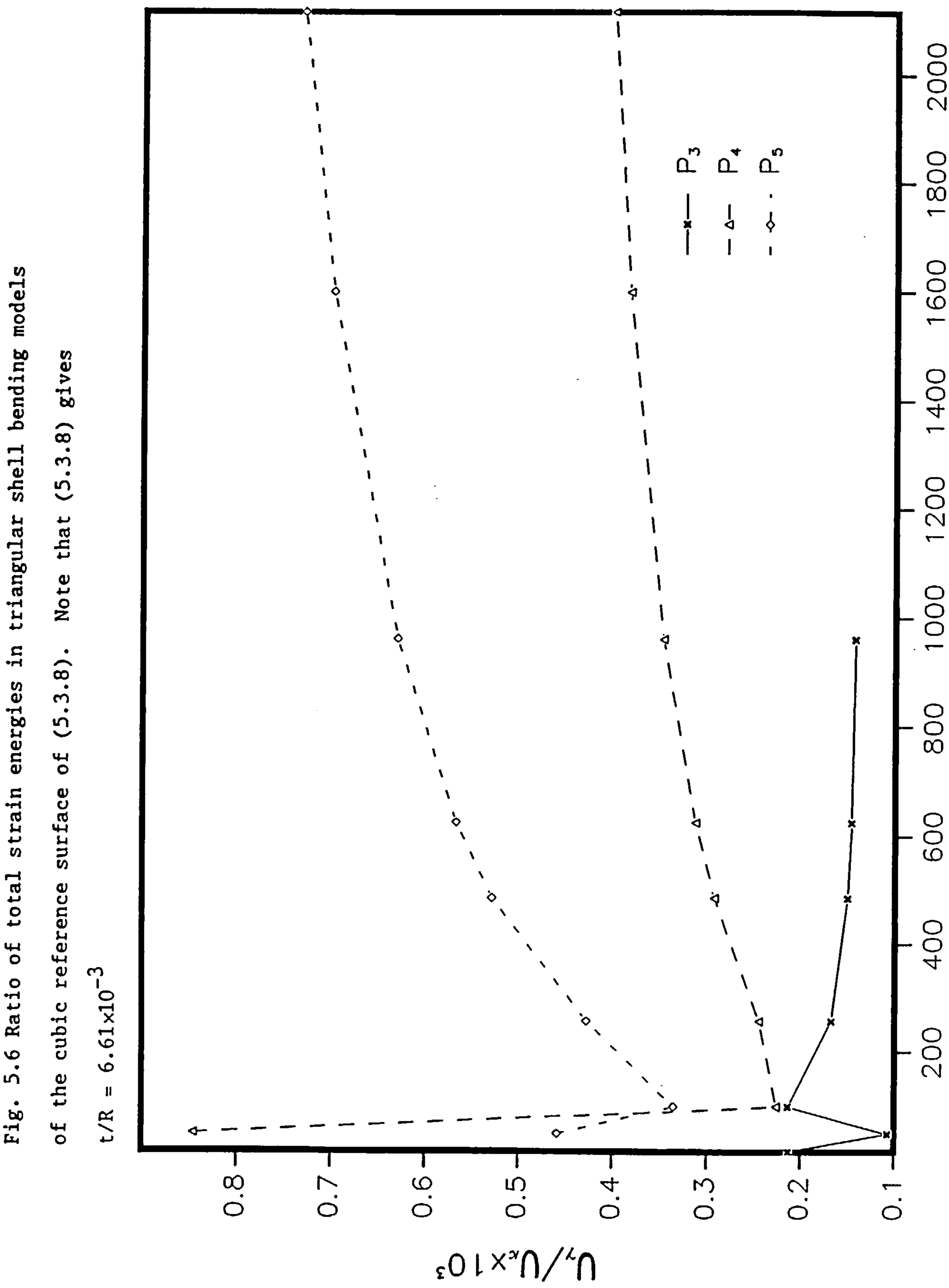

Fig. 5.6 Ratio of total strain energies in triangular shell bending models of the cubic reference surface of (5.3.8). Note that (5.3.8) gives $t/R = 6.61 \times 10^{-3}$

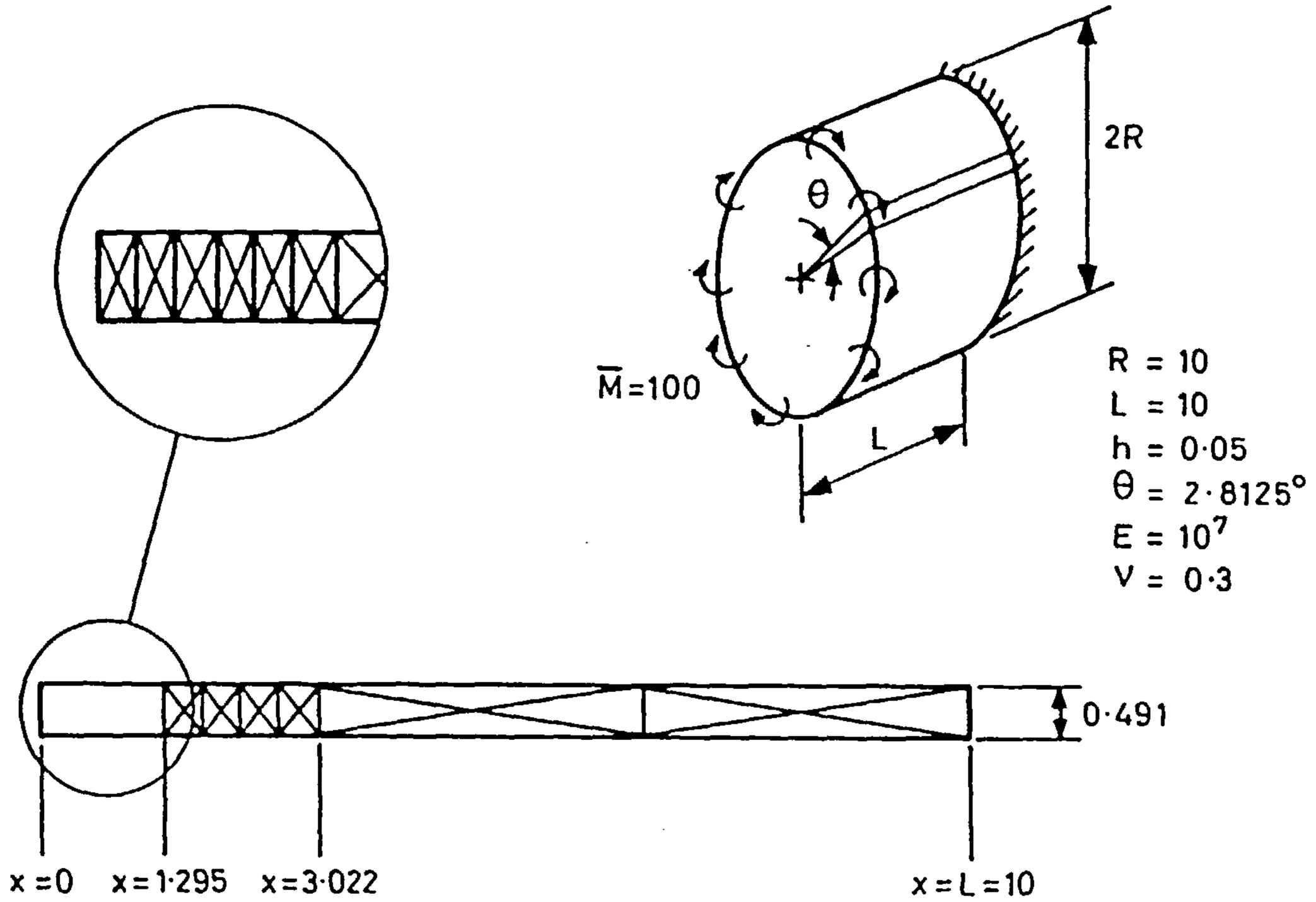

Fig. 5.7 Cantilever circular cylinder under uniform edge moment.

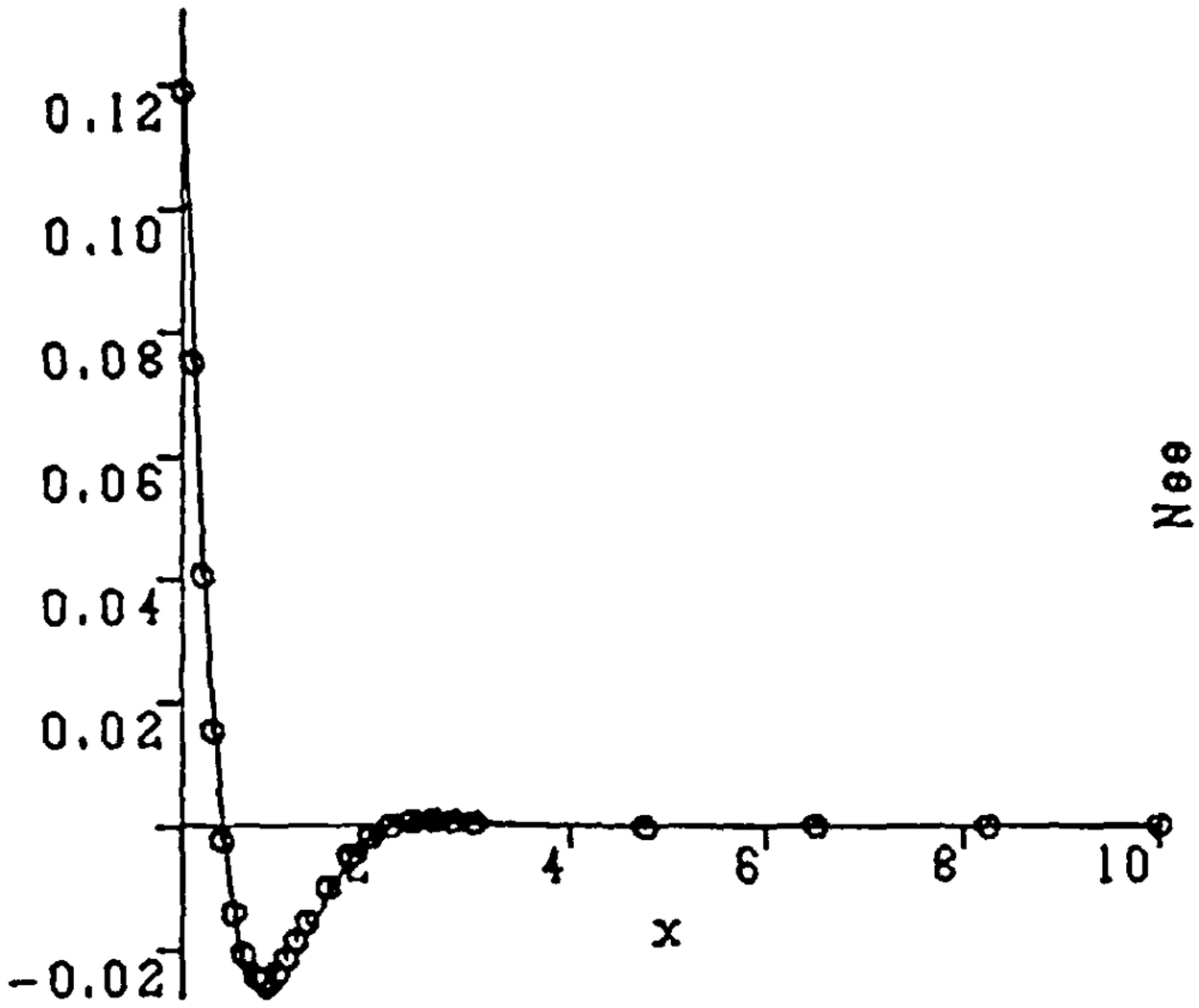

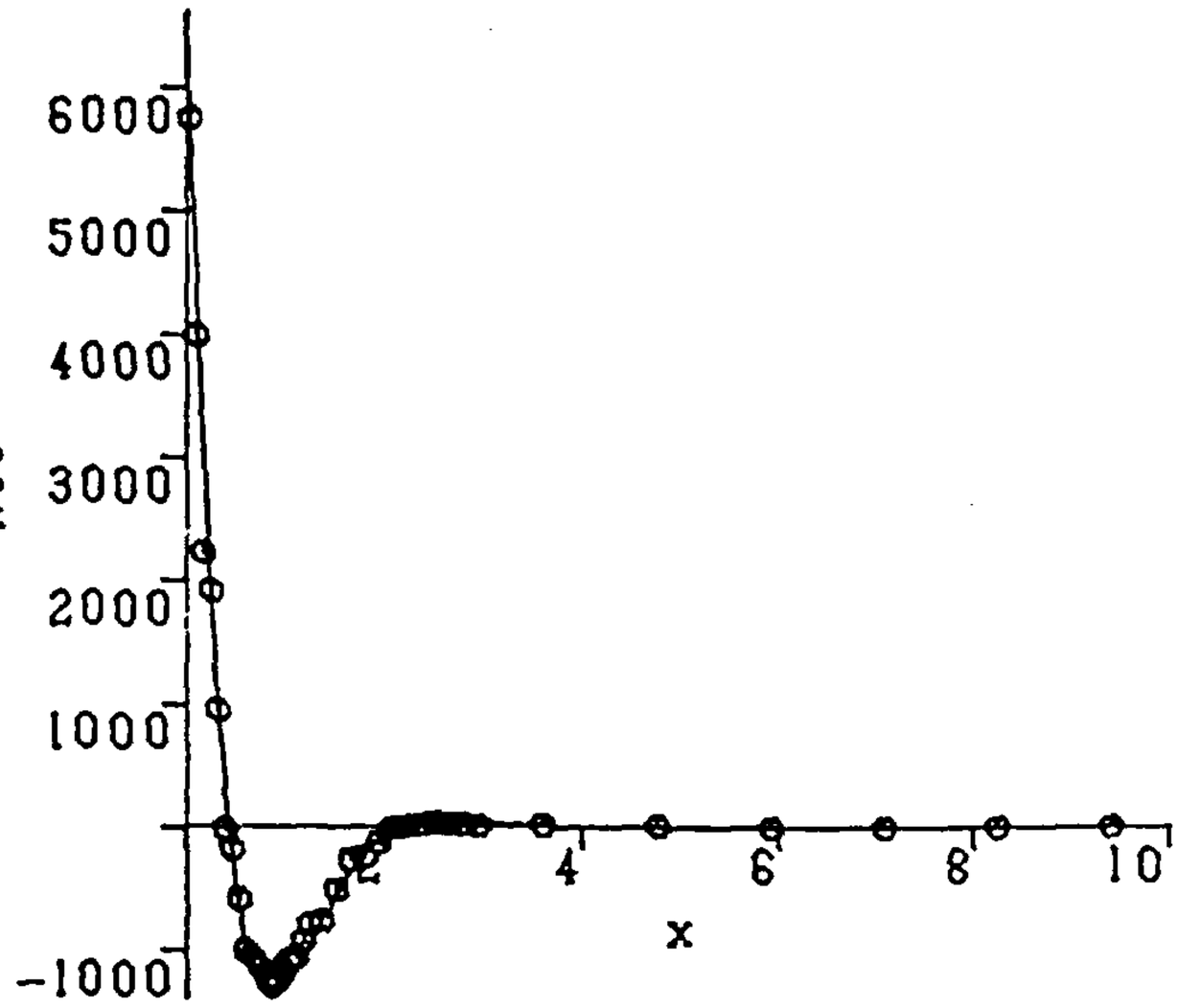

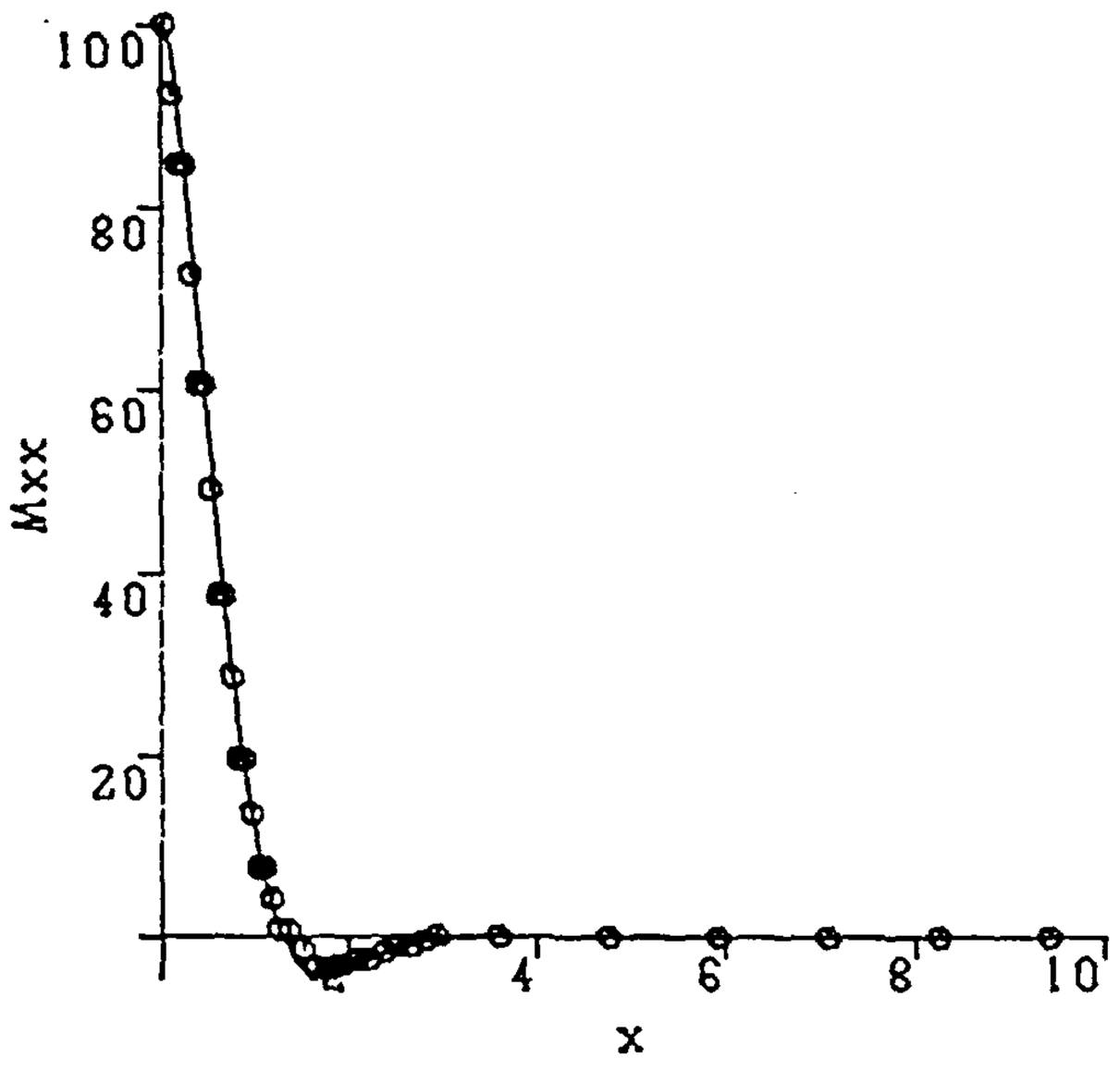

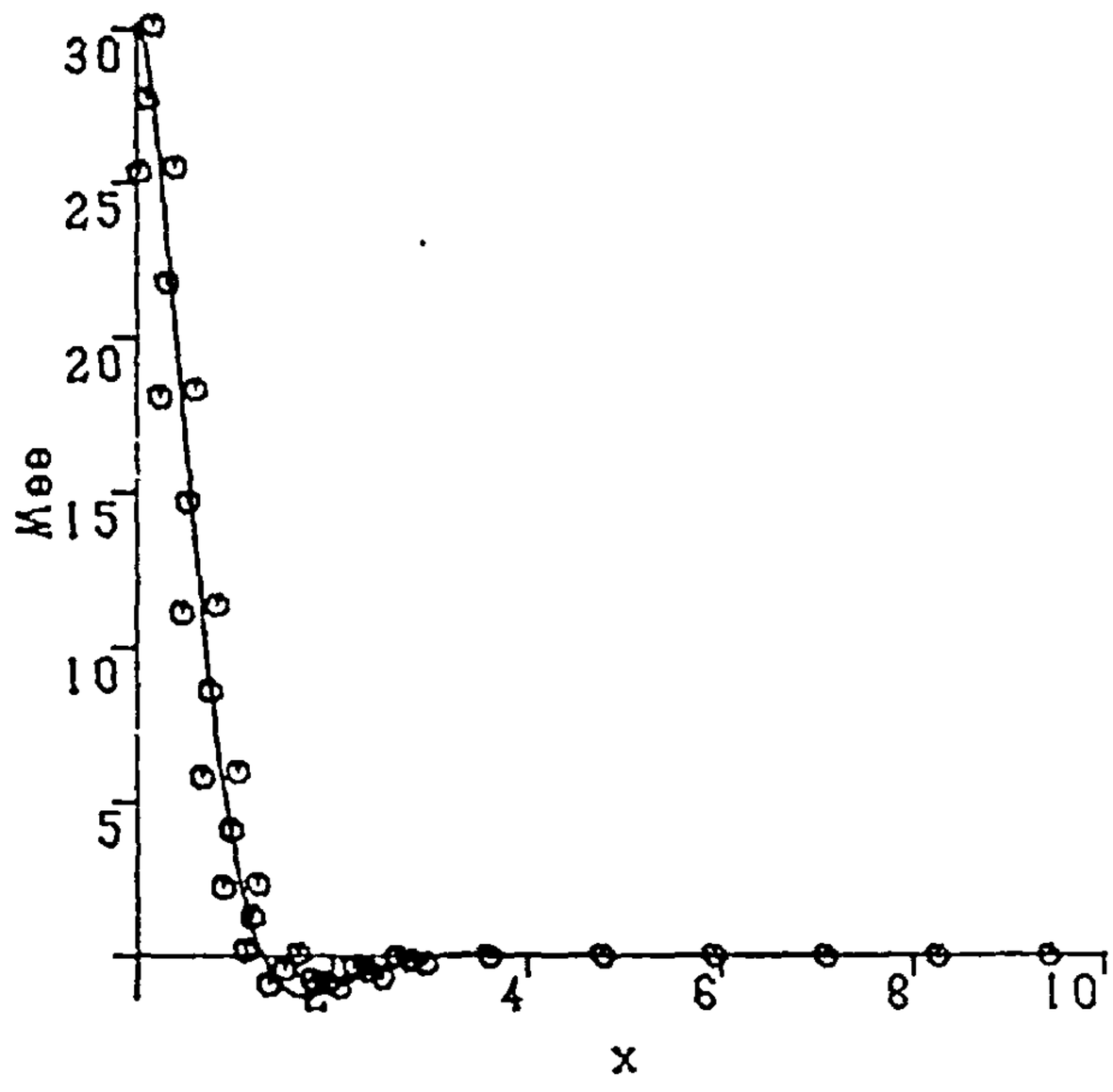

——————Classical solution

⊙ Finite element bending model

Fig. 5.8 Results for cantilever circular cylinder under uniform edge moment.

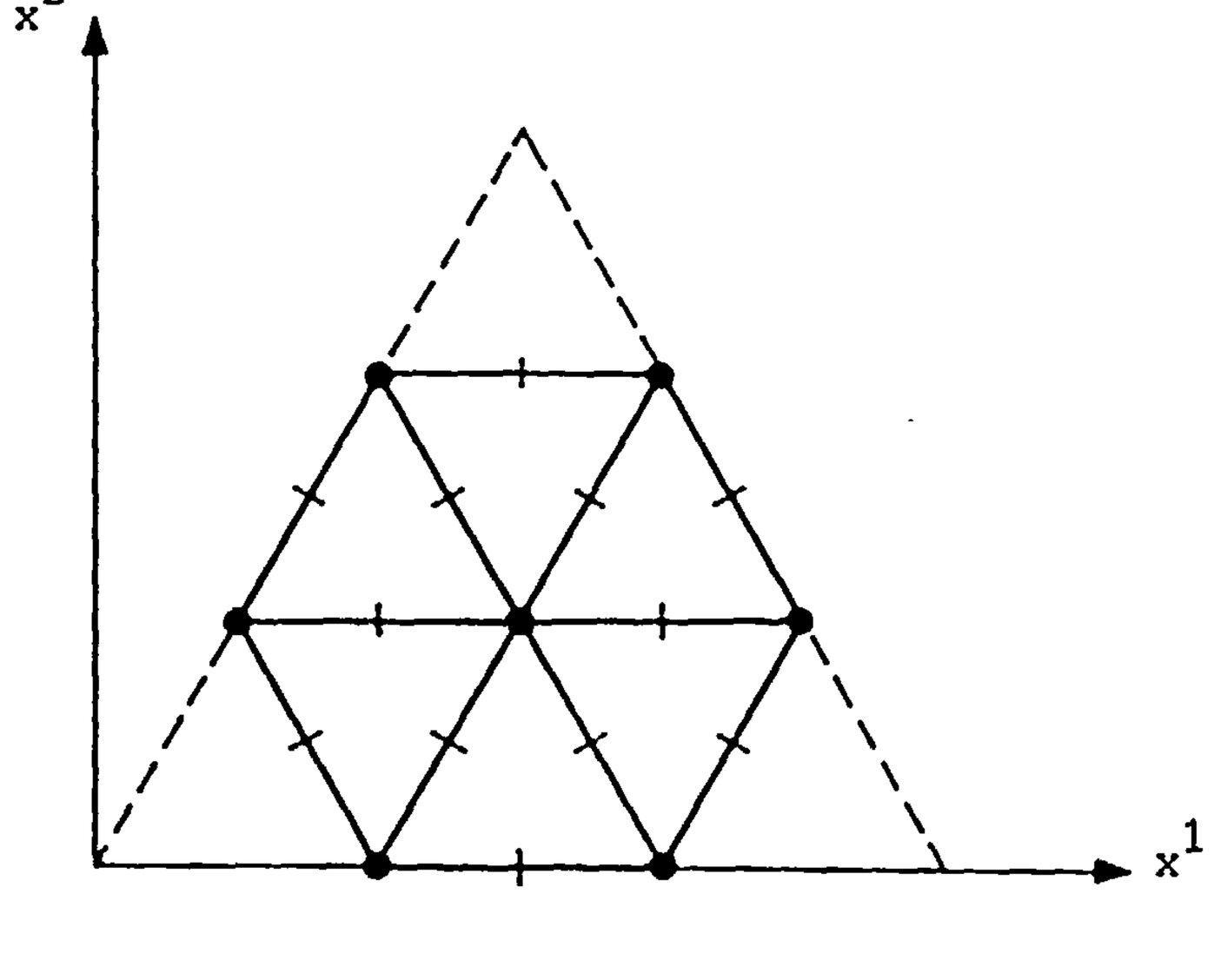

Fig. 5.9 Equilateral hexagonal projection onto the x^{α}-plane of an example 6 finite element shell model.

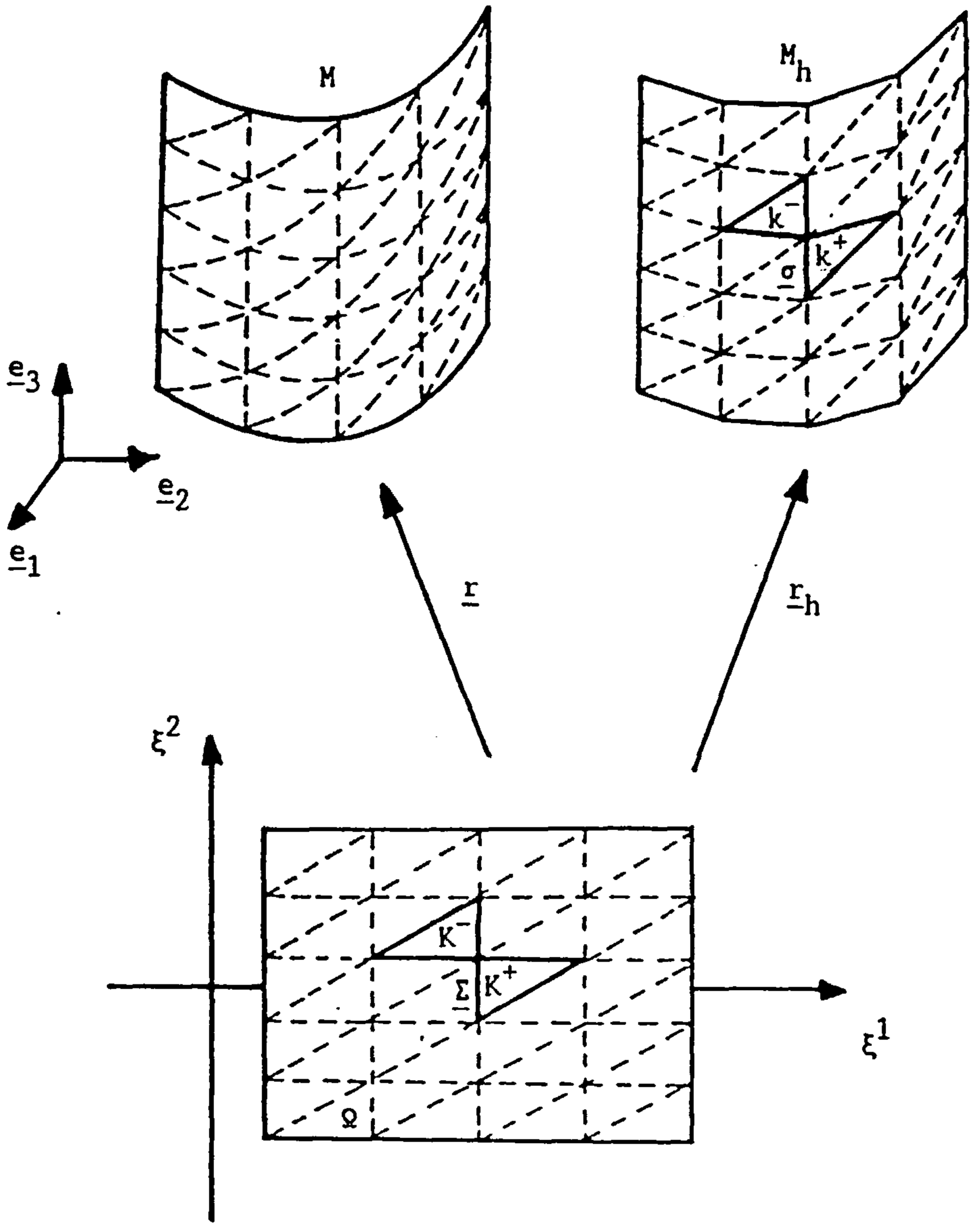

Fig. 6.1 The mappings $\underline{r}$ and $\underline{r}_h$ defining the smooth shell middle surface M and approximate facet middle surface M_h.

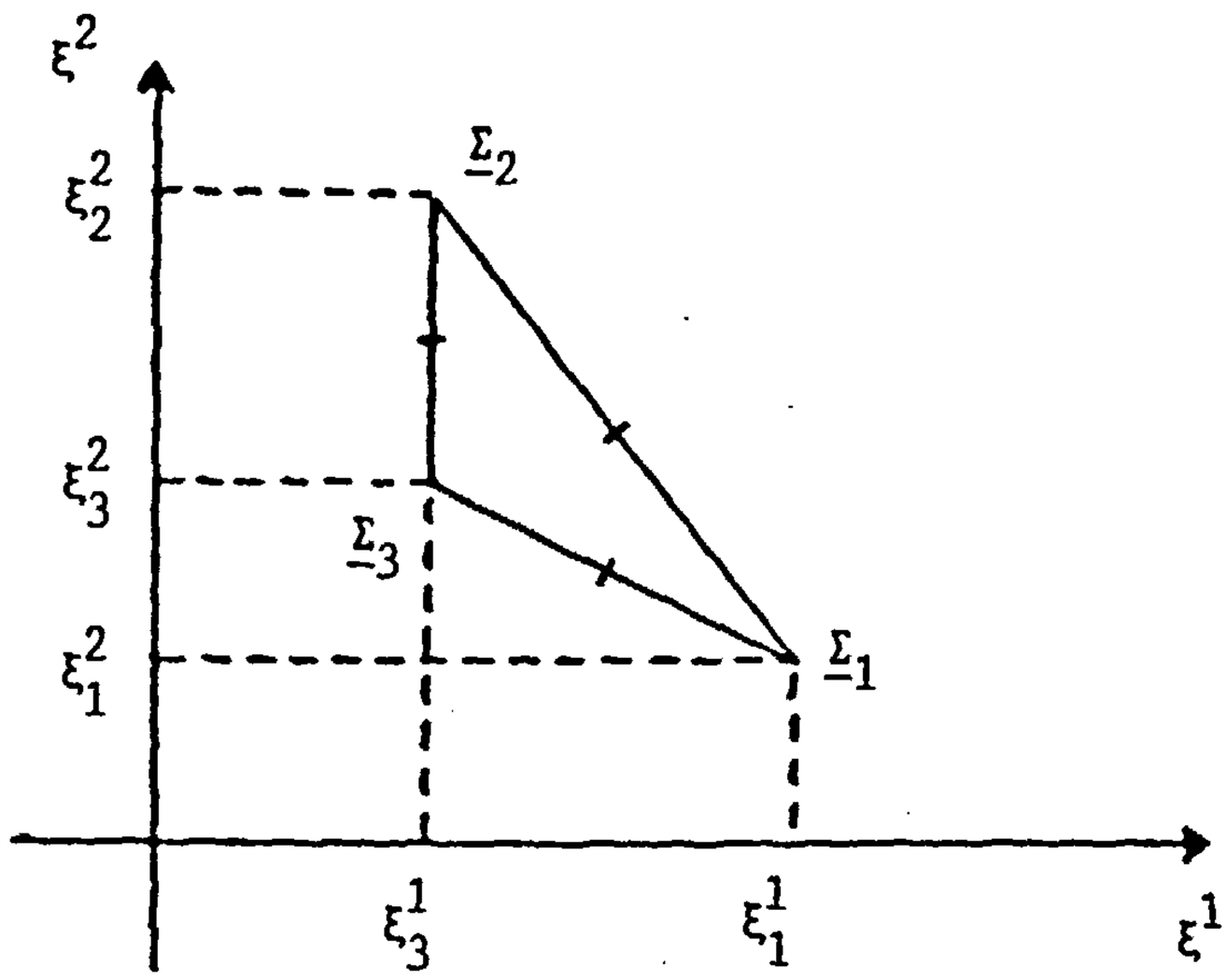

Fig. 6.2 Example of a triangle satisfying the assumption of (6.6.25).